I declare that this thesis was composed by myself and the work contained within, unless otherwise stated, is my own.

Edinburgh, 24/3/95

To My Parents

Still: ***Frustration is the fertiliser of success***

Prior

ACKNOWLEDGEMENTS

I would like to thank:

firstly, my parents for all the support and being the best parents I ever had;

Nick D. Read for giving me the opportunity to do this work and for his support;

Anthony Trewavas for his help (however, I still ponder about the similarities between conidia and coconuts);

especially, the two Richards: Richard M. P. for his help, co-operation and discussions in all (!) situations of life from fly-fishing to love matters and Richard W. (1813-1886) for providing entertainment in the dark hours of microscopy;

Helen Page, for having made some of the data gathering an enjoyable task, being always a support and having introduced me to the world of vocal classical music;

Amanda Collis, for her shoulder when times where rough, and shared opinions on the hassles in this world;

Tony Collins, for his help with the computers;

Jim Deacon for significant ($P < 0.01$) help on the statistical front;

Isobel Black and Graham Simpson for bruuvreading;

Robert the Redgwell, for being a friend;

Pascal L. and "Le Tigre" for the good times ("lets have more of it !");

Birgit, Ulli and Jaana for not forgetting me;

all the people who were always putting milk in the fridge downstairs;

and Rui, Sabine, Billy, John, John, Babs, Rita, Graham, Ian, and many more for all the help which made life easier.

ABBREVIATIONS

Standard SI (*International System of Units*) units used throughout the thesis. Non-SI units are as follows:

AM ester	Acetoxymethyl ester
ATP	Adenosine-5′-triphosphate
β_{ic}	Buffer capacity
cAMP	Adenosine-3′,5′-cyclic monophosphate
cGMP	Guanosine-3′,5′-cyclic monophosphate
DIC	Differential interference contrast
DMSO	Dimethyl sulphoxide
Eq	Equivalent
GTP	Guanosine-5′-triphosphate
h	Hour
HEPES	N-[2-Hydroxyethyl]piperazine-N′-[2-ethanesulphonic acid]
kDa	Kilodalton
LSCM	Laser scanning confocal microscope
LSD	Least significant difference
min	Minute
Mw	Molecular weight
MES	2-[N-Morpholino]ethanesulphonic acid
n	Number of replicates
N.A.	Not applicable
pH_c	Negative logarithm of the cytosolic proton concentration
pH_e	Negative logarithm of the extracellular proton concentration
pK_a	Negative logarithm of the equilibrium constant of an acid
RGD	Arginine-Glycine-Aspartic acid
sec	Second
SEM	Standard error of the mean
SNARF-1	5(6)-carboxyseminaphthorhodafluor-1
UV	Ultraviolet
w/v	Weight per volume
v/v	Volume per volume

TABLE OF CONTENTS

ABSTRACT

The role of external signals (particularly the substratum surface, light and nutrients) in regulating the pre-penetration phase of *Magnaporthe grisea* (Herbert) Barr [anamorph, *Pyricularia grisea* Sacc.] was analysed on rice leaves, artificial substrata and in liquid suspension. Surface contact was found to be essential for appressorium induction but not conidium germination. Both a high surface hydrophobicity and light favoured the formation of short differentiated germ tubes and large numbers of appressoria, but neither factor was essential for their induction. Light intensity had a graded effect on the lengths of differentiated germ tubes but not on the number of appressoria formed. No single sugar or nitrogen source was found to have a marked influence on appressorium formation. However, a high concentration of a complete nutrient source prevented differentiation in the dark but not in the light. Higher numbers of appressoria differentiated on rice leaves than on artificial substrata suggesting that the host provides additional factors, and thus a more conducive environment, for promoting appressorium formation. Overall, the results indicated that the pre-penetration phase of rice blast infection involves a programme of growth and differentiation triggered at conidium germination and regulated by multiple signals from the host and environment.

The role of cytosolic pH (pH_c) in growing germ tubes during conidium germination, germ tube growth and appressorium formation was analysed by confocal ratio imaging of the pH-sensitive fluorescent dye 5(6)-carboxyseminaphthorhodafluor-1 (SNARF-1). The cytosol of these cells was successfully loaded with the AM-ester of the dye and pH_c visualised and quantified in living cells by simultaneous, dual emission confocal ratio imaging. *In vitro* calibrations of the free acid and *in vivo* calibrations produced similar results in the pH 6.0-8.0 range. The pH_c in growing germ tubes was consistently pH 7.2 $\pm$ 0.1 during all developmental stages analysed. Only slight changes in pH_c (< 0.1 pH unit) were found in response to alkaline external pH (pH 8.0). No changes in pH_c occurred in response to an acidic extracellular pH (pH 6.0) or to the presence of nutrients. Neither pronounced gradients nor changes in pH_c in growing germ tubes accompanying conidium germination, germ tube growth or appressorium formation, were observed.

1. INTRODUCTION

Rice blast is the most destructive fungal disease of rice worldwide. The causative organism, *Magnaporthe grisea*, has been the subject of intensive study for more than a century. However, rice blast infection can still only be controlled rather than prevented. Fungal pathogens are particularly susceptible to anti-microbial agents during their pre-penetration phase of infection. Targeting novel anti-microbial compounds at *M. grisea* should thus be facilitated by a detailed understanding of the growth and developmental processes involved during this critical phase of infection. In *M. grisea*, this pre-penetration phase involves conidium attachment, conidium germination, germ tube growth, and the differentiation of an appressorium from which the host surface can be breached. Although the morphological events which take place during the pre-penetration phase of *M. grisea* have been well described (Howard, 1994), the role of environmental factors in regulating this process has been little studied (Uchiyama & Okuyama, 1990; Lee & Dean, 1993; Xiao *et al.*, 1994a). In particular, the significance of light, nutrients, temperature and pH as external signals during the pre-penetration phase of *M. grisea* has been poorly investigated. In the present study, the influence of these factors on conidium germination, germ tube growth and appressorium formation has been analysed in detail, both *in vitro* and *in vivo*. The primary focus of the first part of the study was to determine whether single or multiple signals are important in regulating different events during the pre-penetration phase.

Temporal and spatial changes in cytosolic pH (pH_c) have been implicated in cell signalling, polarised cell growth and cell differentiation in a range of plant and fungal cells (see Heath, 1990; Gadd, 1995; Gow 1995a,b). Critical to a rigorous analysis of the role of pH_c in fungal morphogenesis is the ability to measure pH_c within living cells. Most of the established techniques used to measure pH_c have limited spatial resolution and are therefore unsuitable for studies requiring an understanding of the significance of pH_c at the cellular level. Fluorescence microscopy provides an experimental tool with high spatial and temporal resolution for the analysis of pH_c. Recently, this technique has provided evidence for the existence of pronounced gradients in pH_c in tip growing cells (Roncal *et al.*, 1993; Gibbon & Kropf, 1994). The second part of this study aimed to assess the suitability of

confocal ratio imaging of the pH-sensitive fluorescence dye 5(6)-carboxyseminaphthorhodafluor-1 (SNARF-1) as a tool to image and quantify pH_c during fungal growth and morphogenesis. The method was then to be used to analyse the pH_c in growing and differentiating germ tubes of *M. grisea in vitro*.

2. REVIEW OF THE LITERATURE

2.1 GENERAL INTRODUCTION TO RICE BLAST

Rice blast is the most severe disease of rice (*Oryza sativa*) plants and is caused by the heterothallic, filamentous ascomycete *Magnaporthe grisea* (Herbert) Barr [anamorph, *Pyricularia grisea* Sacc.], formerly called *Pyricularia oryzae* Cavara (Rossman *et al.*, 1990). Yield loss from light infections can be > 5%, whilst epidemics cause much greater losses (Ou, 1980). Rice blast occurs in all of the major rice growing regions of the world. The high levels of virulence from polymorphism in pathogen populations usually allow the fungus to overcome the resistance of new rice cultivars within 2-4 years (Leung & Taga, 1988). Hundreds of races are distinguished among rice infecting strains according to their ability to infect particular cultivars of rice (Crawford *et al.*, 1986). Besides rice, *M. grisea* also infects > 50 different species of the Gramineae, including rye (*Secale cereale*) and wheat (*Triticum aestivium)* (Ou, 1985; Moss & Trevathan, 1987; Valent, 1990).

M. grisea attacks all aerial parts of the rice plant. Leaf spots are the most conspicuous symptoms. The initial stages of infection by *M. grisea* usually require wind dispersal of asexual conidia which each contain three cells. Attachment involves the immediate and persistent adhesion of a conidium to the rice leaf by means of a glue (the *spore tip mucilage*) released from the spore apex (Hamer *et al.*, 1988).

Germination can occur from one or more of the conidial cells and each germ tube has the potential to differentiate a single, terminal pigmented appressorium. The appressorium acts as a holdfast to allow the *penetration peg* to pierce the host surface and invade the plant. Once within the epidermis, the infection peg develops into larger infection hyphae which, in compatible reactions, colonise the rest of the host tissue (Peng & Shishiyama, 1988; Bourett & Howard, 1990; Howard *et al.*, 1991a; Howard, 1994) (Fig. 1).

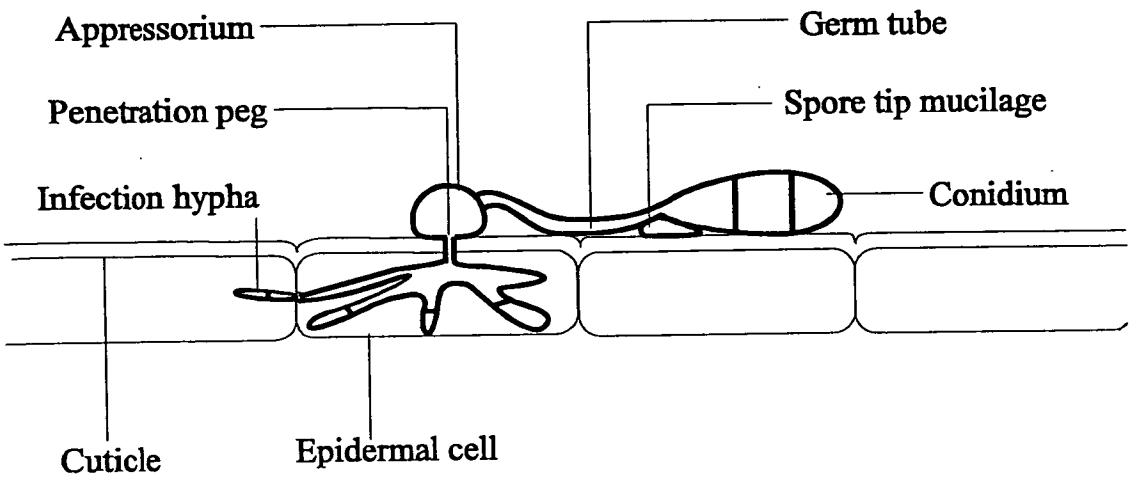

Fig. 1. Early infection structures of *M. grisea* on a rice leaf.

Conidia are produced in lesions on the rice plant about 6 days after inoculation and are released in high humidity (Ou, 1985). *M. grisea* is a hemibiotrophic pathogen, meaning that it is initially biotrophic, obtaining its nutrients from living host cells, and then becomes necrotrophic when it obtains its nutrients from killed host cells (Luttrell, 1974). The lesions caused by rice blast infection and the necrotic reactions of the rice host often destroy enough photosynthetically active tissue to eventually cause the death of the whole plant.

Under natural conditions, only the asexual life cycle described above has been found. The sexual cycle of *M. grisea* can be readily induced under laboratory conditions, and the degree of fertility is highly dependent on host origin with isolates from non-rice hosts such as finger millet (*Eleucine coracana*), goosegrass (*E. indica*) and weeping lovegrass (*Eragrostis curvula*) being more fertile than isolates from rice hosts (Leung & Taga, 1988).

M. grisea offers an excellent experimental system in which to address many of the most significant questions in plant pathology (Valent, 1990). In recent years, studies of the cell biology and molecular genetics of this fungus have permitted a number of critical elements of host-pathogen interactions to be analysed (Valent, 1990; Valent & Chumley, 1991). One important aspect studied has been the pre-penetration phase of infection.

2.2 PRE-PENETRATION PHASE OF INFECTION BY THE RICE BLAST FUNGUS

The pre-penetration phase of *M. grisea* has been studied *in vivo* on the rice leaf (Peng & Shishiyama, 1988) and *in vitro* on different substrata (see section 2.3). The time course of events occurring during the pre-penetration phase *in vitro* is shown in Table 1.

Table 1. Sequence of events during the pre-penetration phase of *M. grisea* grown on Cellophane (adapted from Bourett & Howard, 1990)

Time after inoculation (h)	Event
0.2-1.5	Germination of conidia.
	Germ tube elongation.
1.6-4.0	Cessation of germ tube elongation.
	Hook formation/apical expansion of germ tube.
	Mitosis of nucleus in germinated conidium cell.
	One daughter nucleus migrates into incipient appressorium.
	Formation of a septum at base of incipient appressorium.
	Membrane cisternae and vesicles abundant.
	Cell wall on underside of appressorium thins.
	Formation of new outer wall layer over appressorium.
4.1-12.0	Melanisation of appressorium begins.
	Membrane cisternae and vesicles absent.
	Formation of appressorium pore.
12.1-24.0	Accumulation of granular substance (possibly an adhesive) at appressorium-substratum interface.
	Glycogen rosettes abundant in appressorium.
	Development of pore ring.
24.1-31.0	Formation of pore wall overlay.
	Glycogen rosettes disappear.
	Penetration peg emerges.
31.1-70.0	Formation of infection hyphae.

Conidia of *M. grisea* are usually pyriform and hyaline to pale olive in colour. During maturation, the apical cell of the conidium releases spore tip mucilage into a periplasmic compartment at the conidium apex (Hamer *et al.*, 1988). This material serves to attach the conidium to virtually any surface, even under water. Spore tip mucilage binds the plant lectin concanavalin A, indicating that it contains glucose and/or mannose residues (Hamer *et al.*, 1988; Bourett *et al.*, 1993).

Conidia begin to germinate typically within 3 h of attachment to the rice leaf surface. Germination of the conidium can occur from any of its three cells and usually produces 1-3 germ tubes. The 2 μm wide germ tube grows to a variable length until the tip begins to swell and forms a *hook*. An appressorium is formed from the swelling 3 h after germination (Peng & Shishiyama, 1988). In germlings grown on Cellophane, it has been shown that the nucleus of the germinated conidium cell divides and one daughter nucleus remains in the conidium cell whilst the other migrates into the incipient appressorium (Bourett & Howard, 1990). The germ tubes and appressoria of *M. grisea* secrete an adhesive material which mediates firm contact with the substratum (Hamer *et al.*, 1988). The appressorium is even more tenaciously adherent to the host surface than are conidia and, when mature, generates a hydrostatic pressure (> 80 bar) of unprecedented magnitude in living eukaryotic cells. The appressoria appear darkly pigmented due to a discrete cell wall layer of melanin (Howard & Ferrari, 1989). It has been suggested that the melanin layer blocks the efflux of some glycogen metabolites and thus creates an osmotic potential inside the appressorium which causes the influx of water and build up of the large turgor pressure. This pressure provides a mechanical force which seems to be the primary mechanism by which an emergent penetration peg pushes through the rice leaf cuticle. However, the involvement of enzymatic processes cannot be excluded and *in vivo* this may enhance the penetration process (Howard & Ferrari, 1989; Howard *et al.*, 1991a; Howard, 1994).

During most of the period of appressorium development, the underside of the appressorium possesses a wall-less region (the *appressorium pore*, Howard & Ferrari, 1989). To seal this pore against pressure leakage, a strong glue and an *O-ring* of unknown constitution are built (Howard *et al.*, 1991a; Bourett & Howard, 1992). Shortly before substratum penetration, the appressorium pore becomes blanketed by the deposition of new

cell wall material, the *pore wall overlay.* A penetration peg (< 1μm in width) grows through the overlay and is surrounded by a cell wall, continuous with the overlay (Bourett & Howard, 1992) (Fig. 2). The cytoplasm of the penetration peg, as well as adjacent cytoplasm in the appressorium, contains few organelles but numerous actin filaments have been immunolocalised in this region (Bourett & Howard, 1992). Once within a host epidermal cell, the penetration peg differentiates into wider infection hyphae (2 μm in width).

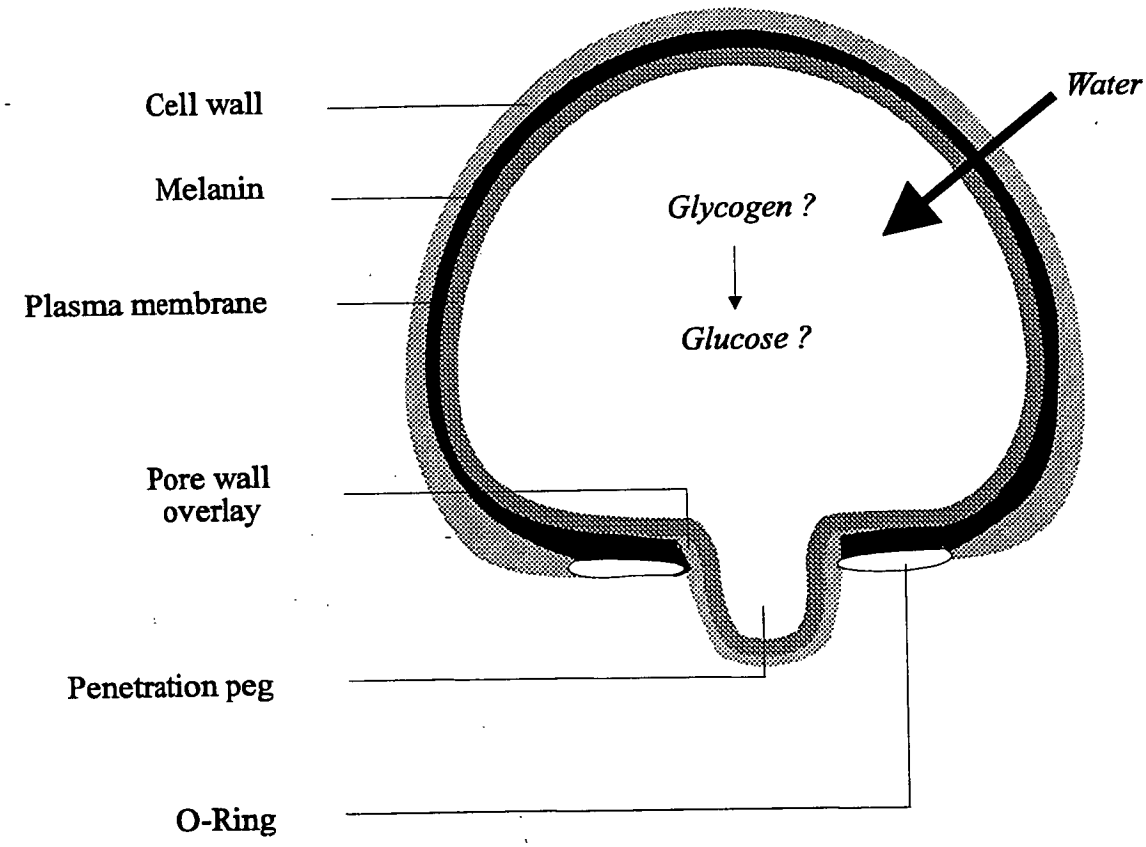

Fig. 2. Schematic representation of an appressorium of *M. grisea* (adapted from Howard *et al.*, 1991a).

The pre-penetration events of *M. grisea* described above usually occur during the 31 h following conidium attachment (Table 1). During this short period the growth pattern of the pathogen changes repeatedly. Polarised germination of a conidium cell and polarised germ tube elongation are followed by unpolarised expansion of an appressorium. After appressorium maturation, a thin penetration peg again exhibits polarised growth and subsequently differentiates into wider polarised infection hyphae. This sequence of switching between polarised and non-polarised growth is typical of all appressorium-forming fungi regardless of their mode of penetration.

Direct penetration through the cuticle, as exhibited by *M. grisea*, is the most common strategy for appressorium-forming fungi breaching the host surface. In this respect, *M. grisea* shares features in common with other important pathogens including *Colletotrichum* (Bailey *et al.*, 1992) and *Erysiphe* (Mount & Slesinski, 1971). Direct penetration into the host epidermis as an invasion strategy contrasts with the method used by rust fungi. The uredospore germlings of these fungi differentiate appressoria over stomata through which they invade the host tissue (Hoch & Staples, 1991; Read *et al.*, 1992a).

2.3 EXTERNAL SIGNALS INFLUENCING EARLY INFECTION PROCESSES OF FUNGAL PLANT PATHOGENS

The period between spore release and successful invasion of host tissue is the most critical phase in the life cycle of a pathogenic fungus. The pathogen not only lives on limited endogenous nutrients but is also exposed to a hostile environment. Therefore the pathogen relies on strategies to respond actively to external signals to facilitate swift and successful invasion of the host. The importance of external factors in regulating the early development of plant pathogenic fungi has been well documented. However, most studies have focused on rust fungi (Emmett & Parbery, 1975; Lucas & Knights, 1987; Hoch & Staples, 1991; Read *et al.*, 1992a). For direct-penetrating fungi, similar work has mainly concentrated on *Colletotrichum* species (Bailey *et al.*, 1992). Table 2 summarises key studies on the responses of plant pathogenic fungi to external signals.

Table 2. Studies on the responses of plant pathogenic fungi to external signals

Signal	Specific treatment	Response	Species	Reference
Temperature	Increase from 20°C to 30°C (heat shock)	Infection structure formation	Numerous rust species	Read *et al.*, 1992a
	Interaction between temperature and light	Infection structure formation	*Puccinia graminis*	Emge, 1958
Light	High intensity	Inhibition of germination	*P. graminis*	Dillon-Weston, 1931; Sharp *et al.*, 1958, Knights & Lucas, 1980
			Hemileia vastatrix	Nutman & Roberts, 1963;
	High intensity	Reduced germination; increased appressorium formation	*Colletotrichum falcatum*	Singh, 1973
	Low intensity	Stimulation of infection structure formation	*Colletotrichum gloeosporioides*	Purkayastha & Gupta, 1973
	Unidirectional light	Germ tube phototropism	Numerous rust species	Chang & Calpouzos, 1973
	Sunlight	Stimulation of germination and development	Powdery mildews	Yarwood, 1932; Sharp *et al.*, 1958
Water	Water gradients	Hydrotropism of germ tube growth	*Cercospora beticola;* *Dothistroma pini*	Rathaiah, 1977; Peterson & Walla, 1978
	Free water	Germination	*Magnaporthe grisea*	Ou, 1985
	High humidity	Infection	*M. grisea*	Ou, 1985
Nutrients	Sucrose, glucose, complete media	Infection structure formation	Numerous rust species	Kaminskyj & Day, 1984
	Glucose and amino acids	Stimulation of infection structure formation	*Colletotrichum gloeosporioides*	Purkayastha & Gupta, 1973
	Amino acids	Germination	*Pythium aphanidermatum*	Donaldson & Deacon, 1992
	Long chain fatty acids	Germination and infection structure formation	*Colletotrichum gloeosporioides*	Podila *et al.*, 1993
	Complete media	Inhibition of infection structure formation	*Colletotrichum lindemuthianum*	Mercer *et al.*, 1971
Chemicals	Acrolein	Infection structure formation	*P. graminis*	Allen & Dunkel, 1970; Macko *et al.*, 1978
	Pelargonaldehyde	Germination	*P. graminis*	French & Weintraub, 1957
	Hexenol	Infection structure formation	*P. graminis*	Grambow, 1977
	Ethylene	Germination and infection structure formation	*Colletotrichum musae;* *Colletotrichum gloeosporioides*	Flaishman & Kolattukudy, 1994

- continued -

Table 2 continued

Signal	Specific treatment	Response	Species	Reference
Ions	Potassium	Infection structure formation	*Uromyces phaseoli* (=*U. appendiculatus*)	Staples *et al.*, 1983
	Iron	Germination and infection structure formation	*Colletotrichum musae*	Swinburne, 1986
pH	Gradients	pH-taxis	*Phytophthora palmivora*	Cameron & Carlile, 1980
	Gradients	pH-tropism	*Uromyces viciae-fabae*	Edwards & Bowling, 1986;
			Uromyces appendiculatus	Stumpf *et al.*, 1991
Substratum	Topography	Directional germ tube growth	Numerous rust species	Hoch & Staples, 1991, Read *et al.*, 1992a
	Topography	Appressorium formation	Numerous rust species	Hoch & Staples, 1991, Read *et al.*, 1992a
	Hardness	Appressorium formation	*Uromyces ssp.*	Freytag *et al.*, 1988
		Appressorium formation	*M. grisea*	Xiao *et al.*, 1994a
	Hydrophobicity	Appressorium formation	*M. grisea*	Uchiyama & Okuyama, 1990

The differentiation of appressoria in rust fungi has been shown to be primarily the response to a single external signal provided by topographical features of the host surface (Hoch *et al.*, 1987). In direct-penetrating fungi, Emmett & Parbery (1975) proposed that multiple environmental signals provide a *conducive environment* which allows the systematic execution of a pre-programmed sequence of events terminating in appressorium formation and subsequent penetration.

In *M. grisea*, most attention has focused on the influence of temperature and humidity during the pre-penetration phase. The optimal temperature for conidium germination was found to be 26-28°C (Ou, 1985). Free water is required for germination and high relative humidity near saturation is necessary for infection (Ou, 1985). The roles of other factors, such as light, substratum and nutrients, have not been rigorously analysed during the pre-penetration phase. It is well established that successful infection of rice plants can take place in either the light or the dark (Ou, 1985). But it also has been reported that germ tube elongation is inhibited by light (Abe, 1931). Furthermore, appressoria have been shown to differentiate on a wide range of artificial substrata with marked differences in their hydrophobicity, hardness and other surface properties. Appressoria have thus been induced to form on Cellophane (Hashioka, 1972; Araki & Miyagi, 1977; Uchiyama *et al.*, 1979; Hirooka *et al.*, 1982; Bourett & Howard, 1990; Xiao *et al.*, 1994a), Teflon (polytetrafluoroethylene) and polyethylene (Howard *et al.*, 1991b; Xiao *et al.*, 1994a), on Mylar (polyester), Lucite (polymethylmathacrylate), Surylan (polyethylenmethacrylic acid), Kevlar (*p*-phenyleneterephtalamide) (Howard *et al.*, 1991b), on polycarbonate, Parafilm, polypropylene, alkylbenzenestyrene and Nylon (Xiao *et al.*, 1994a), and on wax paper, polystyrene and gel bond (Lee & Dean, 1993). There is an interesting discrepancy in the literature regarding appressorium formation on glass. In several studies it has been shown that appressoria of *M. grisea* can develop on this substratum (Uchiyama *et al.*, 1979; Yaegashi *et al.*, 1987; Uchiyama & Okuyama, 1990; Xiao *et al.*, 1994a) whilst other workers have reported that they do not (Hamer *et al.*, 1988, 1989; Howard *et al.*, 1991b; Lee & Dean, 1993). The reason for this inconsistency is not clear.

The availability of exogenous nutrients has been reported to cause a deviation from the normal germination pattern of *M. grisea* in which only one germ tube typically emerges from either the apical or the basal cell of the conidium (Howard, 1994). An acceleration of conidium germination can be stimulated by guttation fluid from rice leaves (Weintraub *et al.*, 1958). Fatty alcohols promote appressorium formation by *M. grisea* on Cellophane and glass (Uchiyama & Okuyama, 1990). Glucose has been shown to have no influence on appressorium formation (Lee & Dean, 1993). Cyclic AMP, which is elevated in response to starvation in some eukaryotes (e.g. in *Dictyostelium*, Gerisch, 1987), also seems to be involved in appressorium induction in *M. grisea* (Lee & Dean, 1993).

2.4 INTRACELLULAR SIGNALLING DURING THE PRE-PENETRATION PHASE OF FUNGAL PLANT PATHOGENS

There is growing evidence for a multiplicity of signal transduction components and processes operating during the pre-penetration phase of plant pathogens. It has been shown that several components of well-defined signal-transduction pathways in animal and plant cells (Trewavas & Gilroy, 1991; Alberts *et al.*, 1994) can induce infection structure differentiation in rust fungi when added externally. These components include adenosine-3′,5′-cyclic monophosphate (cAMP), guanosine-3′,5′-cyclic monophosphate (cGMP), guanosine-5′-triphosphate (GTP), calcium ions (Ca^{2+}), and diacyglycerol (reviewed by Read *et al.*, 1992a).

The addition of cAMP, cAMP analogues or inhibitors of phosphodiesterase, which naturally hydrolyses cAMP, has been shown to induce appressorium formation in *M. grisea* (Lee & Dean, 1993), and septum formation and mitosis in germ tubes of *Uromyces phaseoli* (= *U. appendiculatus*) (Hoch & Staples, 1984; Epstein *et al.*, 1989). An elevation of the intracellular cAMP concentration has also been observed during the dimorphic transition from yeast-like to hyphal growth which occurs during infection by the Dutch elm disease fungus, *Ophiostoma ulmi* (= *Ceratocystis ulmi*) (Brunton & Gadd, 1989).

Although the external addition of Ca^{2+} did not induce appressorium formation on non-inductive surfaces in *M. grisea* (Lee & Dean, 1993), there is indirect evidence for Ca^{2+} having a signalling role during the early infection phase of other plant pathogenic fungi. Calmodulin, a Ca^{2+}-binding protein and activator of Ca^{2+}-dependent cyclic nucleotide phosphodiesterase, has been isolated from uredospores of *U. appendiculatus* (Laccetti *et al.*, 1987). Furthermore, it has been shown that calmodulin functioning is important in spore germination, regulation of the cell cycle and dimorphism in *O. ulmi* (Muthukumar & Nickerson, 1984; Muthukumar *et al.*, 1985).

Preliminary evidence suggests that phosphatidylinositol signalling may play a role during the early infection phases of plant pathogenic fungi. In *O. ulmi* this evidence comes from inhibitor studies on dimorphism (Brunton & Gadd, 1991). All important components and intermediates of the phosphatidylinositol signal system have been identified in *Fusarium graminearum* (Prior *et al.*, 1993)

The high concentration of microtubules and actin microfilaments next to the plasma membrane at the fungus-substratum interface, and their reorganisation during appressorium differentiation in rust fungi, suggests a role for the cytoskeleton during contact sensing of these fungi (Staples & Hoch, 1988; Kwon *et al.*, 1991)

Although the importance of pH_c in regulating various cell activities in animal and plant cells is well established (Madshus, 1988; Guern *et al.*, 1991), its role in regulating different growth and differentiation processes during the pre-penetration phase of plant pathogenic fungi is little understood.

2.5 CYTOSOLIC PH

2.5.1 Importance of cytosolic pH

The cytosolic concentration of free protons (pH_c) is a crucial factor in co-ordinating the activities of enzyme-catalysed pathways, membrane transport, protein folding, second messengers and other regulators (e.g. hormones). Furthermore, protons act as both substrates and products in many metabolic reactions (Guern *et al.*, 1991).

The importance of pH_c in influencing cellular activities and the fact that water in the aqueous, intracellular milieu spontaneously ionises, make it essential for a cell to regulate its cytosolic H^+ concentration. The regulation of pH_c involves a balance between intracellular H^+ production, H^+ consumption by metabolic processes, and H^+ transfer across membranes.

2.5.2 Regulation of cytosolic pH

Two major ways of regulating cytosolic H^+ concentration are known: the *biochemical* (internal production or consumption of protons) and the *biophysical* (net flux of H^+ or OH^- across membranes) mechanisms.

The internal production or consumption of protons is directly linked to the concentration of organic acids in the cell. In plant cells malic acid concentration in particular has been shown to respond to artificial changes in pH_c. It has therefore been suggested that malic acid has a key role in regulating pH_c (Marre, 1979; Mathieu *et al.*, 1986). Further evidence for malic acid being involved in the control of pH_c comes from studies which show a strong pH dependence of key enzymes responsible for the production of malic acid (phosphoenolpyruvate carboxylase and phosphofructokinase) (Trivedi & Danforth, 1966; Davies, 1986).

The net flux of H^+ or OH^- across membranes is mainly achieved by H^+ pumps. Proton pumps are likely to have a key role in the control of pH_c (Guern *et al.*, 1991). However, pH_c cannot be simply regulated by H^+-pumping alone (Kurkdjian & Guern, 1989). Transmembrane H^+ fluxes driven by primary H^+ pumps, such as H^+-ATPases, have to be associated with fluxes of cations in the opposite direction or of anions in the same direction. Lack of coupling H^+ fluxes with the fluxes of other ions would produce extensive changes in the membrane potential which, in many cases, would be incompatible with the physiology of the cell (Mellman *et al.*, 1986).

Proton pumps, driven by ATP-hydrolysis, are present in animal and plant cells (Madshus, 1988; Guern *et al.*, 1991) and H^+-ATPases have been clearly identified and characterised in *Neurospora crassa* (Scarborough, 1980; Slayman, 1987) and yeasts (Dufour *et al.*, 1982). Plasma membrane H^+-ATPases are considered to play a major role in regulating pH_c (Sze, 1984) although the regulation does not depend on the action of the pump *per se* (Sanders & Slayman, 1982). Studies on fungal and plant cells indicated that firstly, a deactivation of the H^+ pump does not alter significantly the pH_c and, secondly, that an artificial acidification of the cytoplasm can be corrected, even with deactivated proton-ATPase. These results suggest that the H^+-ATPase is only one element of the complex system involved in pH_c homeostasis (Sanders & Slayman, 1982; Mathieu *et al.*, 1986; Frachisse *et al.*, 1988). A recent development to elucidate the role of the plasma membrane H^+-ATPase in the regulation of pH_c has involved the use of yeast mutants with impaired H^+-ATPase activity. Expression of the mutant phenotype led to an acidification of the cytosol which was correlated with a reduced growth rate (Portillo & Serrano, 1989).

A further H^+-ATPase is located in the vacuolar membrane of plant cells and has also been reported in the same location in *N. crassa* and yeast (Bowman *et al.*, 1992; Stevens, 1992). The low sensitivity of this H^+-ATPase to pH_c changes suggests that the protein is primarily involved in solute accumulation in the vacuole through the pH gradient and electrical potential differences it generates across the vacuolar membrane (Guern *et al.*, 1991). In addition to this H^+-ATPase, the vacuolar membrane of higher plants also contains a H^+-pumping pyrophosphatase, the existence of which is still uncertain in fungi (Garrill, 1995).

Several other ion-coupled H^+ transport systems across the plasma membrane are known (Fig. 3). Whereas the Na^+/H^+ antiport is considered to have a major function in regulating pH_c in animal cells (Madshus, 1988), its function in plant cells is less clear (Guern *et al.*, 1991). The exchange of H^+ against K^+ is more likely to be involved in the regulation of pH_c in plant cells than a Na^+/H^+ antiport system (Felle, 1989). However, in higher plants and fungi the relationships between H^+ and K^+ transport at the plasma membrane appear rather complex since various different transport systems, namely K^+ channels, K^+/H^+-symport and antiport, are involved (Gustin *et al.*, 1986; Rodriguez-Navarro *et al.*, 1986; Hedrich & Schroeder, 1989; Bertl & Slayman, 1992). In animal cells, the role of Cl^- and HCO^- exchanges in regulating pH_c is well established (Madshus, 1988). Cl^- uptake has been shown in *Chlorella* and *Chara* (Doblinger & Tromballa, 1982; Sanders *et al.*, 1985) and HCO^- exchange has been demonstrated in *Acer pseudoplatanus* and rose cells (Murphy *et al.*, 1983; Mathieu *et al.*, 1986) and thus could be part of the processes involved in the control of pH_c in fungal cells.

Transport of a wide range of solutes across the plasma membrane in plant cells is energised via the coupling of the electrochemical gradient of protons built up and maintained by the H^+-ATPase (Reid & Walker, 1984; Felle & Johannes, 1990; Bush, 1993). The symport with protons seems in fact to be the predominant mechanism for accumulative uptake of most nutrients, including sugars, amino acids, inorganic ions and nucleotide precursors, in plants and fungi (Slayman *et al.*, 1994). Several of the genes involved in this proton-coupled symport have been cloned and sequenced (Quagliariello & Palmieri, 1992; Reuss *et al.*, 1993). In *N. crassa* detailed functional studies of these transport systems have been performed by measuring currents associated with the nutrient fluxes (Hansen & Slayman, 1978; Sanders *et al.*, 1983; Rodriguez-Navarro *et al.*, 1986).

Mechanosensitive ion channels which are permeable to cations have been identified in the plasma membrane of several fungi. The influence of these channels on the pH_c has so far not been addressed in any detail.

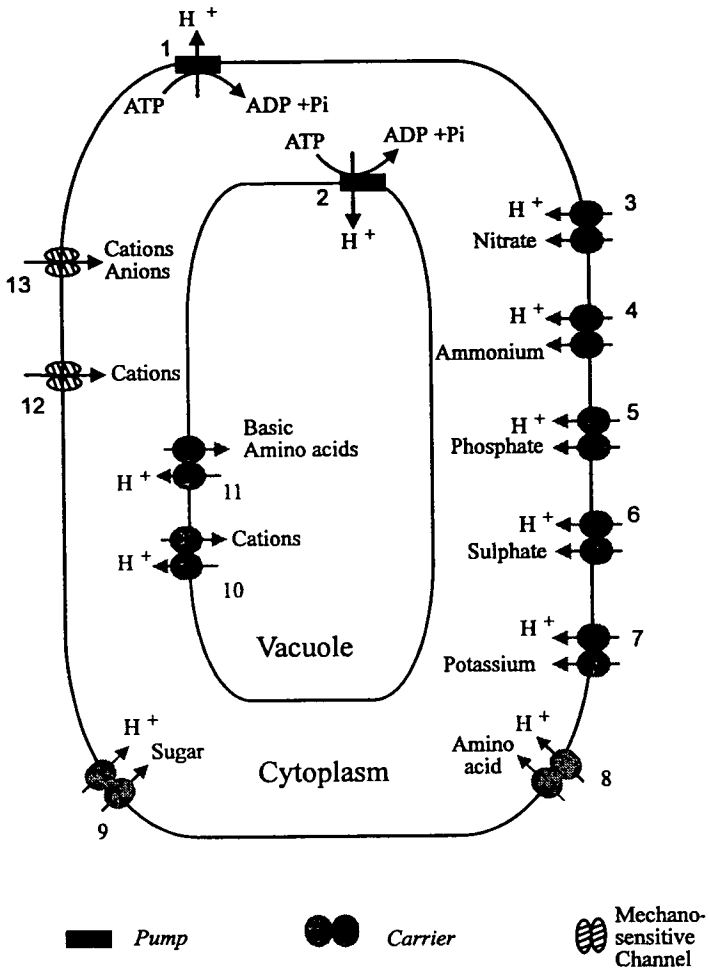

Fig. 3. Representation of H^+-coupled transport processes identified in the fungal plasma membrane and vacuolar membrane (adapted from Garrill, 1995).

1) Plasma membrane H^+-ATPase (*Neurospora crassa*, reviewed in Slayman, 1987; *Saccharomyces cerevisiae*, Serrano *et al.*, 1986; *Schizosaccharomyces pombe*, Ghislain *et al.*, 1987; *Candida albicans*, Monk *et al.*, 1991)
2) Vacuolar H^+-ATPase (*N. crassa*, Bowman & Bowman, 1986)
3) H^+/Nitrate symporter (*C. utilis*, Eddy & Hopkins, 1985)
4) High affinity ammonium transporter (*S. cerevisiae*, Dubois & Grenson, 1979)
5) H^+/Phosphate symporter (*N. crassa*, Lowendorf *et al.*, 1975)
6) H^+/Sulphate symporter (*N. crassa*, Marzluf, 1970)
7) H^+/ Potassium symporter (*N. crassa*, Rodriguez-Navarro *et al.*, 1986)
8) H^+/amino acid symporter (*N. crassa*, *Penicillium chrysogenum* and others, reviewed by Horak, 1986)
9) H^+/sugar symporter (*N. crassa*, Slayman & Slayman, 1975)
10) H^+/cation antiporter (*S. cerevisiae*, Gadd, 1993)
11) H^+/amino acid antiporter (*S. cerevisiae*, Sato *et al.*, 1984)
12) Cation selective stretch-activated channels (*S. pombe*, Zhou & Kung, 1992; *Uromyces appendiculatus*, Zhou *et al.*, 1991; *Saprolegnia ferax*, Garrill *et al.*, 1992, 1993)
13) Unselective stretch-activated channels (*S. cerevisiae*, Gustin *et al.*, 1988)

The cytosolic buffer capacity (β_{ic}) has been estimated in numerous plant and fungal cells (reviewed in Guern *et al.*, 1991). In general β_{ic} was found to be between 20 and 100 μEq $H^+ \cdot ml^{-1} \cdot$pH unit. However, the importance of β_{ic} for the regulation of pH_c is not well understood. Whereas Guern *et al.* (1991) discussed a role of β_{ic} especially in the regulation of sudden shifts in pH_c, Sanders & Slayman (1982) found no significant role for β_{ic} in the regulation of pH_c in hyphae of *Neurospora crassa*, other than very small shifts in pH_c.

2.5.3 Methods for cytosolic pH measurement

Various methods are available for direct measurements of pH_c. The most widely used of these techniques are summarised in Table 3.

In addition to these direct methods to quantify pH_c, indirect information on pH_c can be obtained from:

a) membrane potential measurements using microelectrodes (e.g. Slayman, 1965a,b; Slayman & Slayman, 1974);

b) measurements of extracellular pH (pH_e) with a pH-sensitive microelectrode close to the cell surface (e.g. Gow *et al.*, 1984; Takeuchi *et al.*, 1988);

c) measurements of electrical fields around cells using a vibrating microprobe (e.g. Gow *et al.*, 1984; Kropf *et al.*, 1984) and

d) perturbation of components of the pH_c regulatory system (e.g. H^+-ATPase) using inhibitors (e.g. Stewart *et al.*, 1988) or mutants (Portillo & Serrano, 1989).

Table 3. Direct methods for measurements of cytosolic pH

Method	Principle	Advantages	Disadvantages	References
^{31}P Nuclear Magnetic Resonance (NMR) Spectroscopy	Detection of the transition between energy levels associated with the nuclear magnetic moment of the ^{31}P atom. The characteristics of these transitions depend on the molecular environment, including pH.	Non-invasive.	Low temporal resolution. Non-linear sensitivity. Unsuitable for single-cell measurement. Measurements made under non-physiological conditions.	Gillies *et al.*, 1981 Cassone *et al.*, 1983 Stewart *et al.*, 1988
Microelectrodes	A sensor resin in the electrode acts as a H^+ selective membrane causing the build up of an H^+ diffusion potential which, in conjunction with a reference electrode, allows pH measurements.	High temporal resolution (msec). Suitable for single-cell measurements. Continuous recording possible. Membrane potential simultaneously measured.	Invasive technique. Measurement limited to small area at the site of microelectrode impalement.	Sanders & Slayman, 1982
Dyes	Fluorescence of the dye is pH-dependent and is measured in a fluorometer or with a fluorescence microscope	High temporal resolution (msec). High spatial resolution. Suitable for single-cell measurements.	Invasive technique. Dye sequestration within organelles common.	Davies *et al.*, 1990 Haworth & Fliegel, 1993 Roncal *et al.*, 1993 Slayman *et al.*, 1994
Weak acids/bases	The uncharged form of a radioactively labelled or fluorescent weak acid/base is membrane permeable. The distribution of the dissociated form is directly dependent on the cytosolic pH, extracellular pH and the dissociation constant of the probe. The distribution of the dissociated probe can then be measured in a scintillation counter or fluorometer	Technically simple.	Low temporal resolution. Invasive technique. Unsuitable for single-cell measurement. Metabolism or binding of the probe to cellular constituents. Dissociated probe form can sometimes diffuse across the plasma membrane.	Stewart *et al.*, 1989 Gresik *et al.*, 1991 Kaur & Mishra, 1994

2.5.4 Role of cytosolic pH in fungal morphogenesis

In section 2.2 it was indicated that cellular morphogenesis during the pre-penetration phase of a fungal pathogen involves switches between polarised and non-polarised growth. Evidence from several systems indicates that pH_c plays a role in both growth patterns.

In *Candida albicans* cytoplasmic alkalinisation accompanies germ tube formation from yeast cells (Kaur *et al.*, 1988; Stewart *et al.*, 1988). Inhibition of the plasma membrane H^+-ATPase inhibited both the dimorphic switch and cytoplasmic alkalinisation (Stewart *et al.*, 1988). However, studies on the regulation of the H^+-ATPase questioned the role of changes of the cytosolic H^+ concentration as the primary determinant in the morphogenesis of this fungus (Monk *et al.*, 1993).

Indirect evidence for the involvement of pH_c in fungal morphogenesis was obtained from studies on the electrical fields associated with developing cells, and especially from tip growing cells around which these electrical fields were found to be very prominent (reviewed by Gow, 1989). Fungal hyphae, as well as fertilised zygotes of the brown algae *Pelvetia*, pollen tubes of *Lilium*, and internode cells of the characean algae, were used to study transcellular currents in detail. In most of these organisms, positive charge entered cells at their apices. The transcellular currents were suggested to influence cell activity by processes such as those involving electrophoresis of vesicles and/or membrane proteins, by gating of voltage sensitive ion channels, or by influencing polymerisation and depolymerisation of the cytoskeleton. Later results contested the hypothesis that ionic gradients play a significant role in controlling polarity (Gow, 1989; Harold & Caldwell, 1990). In *Achlya bisexualis* and *N. crassa*, transiently reversed currents were found in growing hyphae (Kropf *et al.*, 1983; McGillviray & Gow, 1987), and in hyphae of *Allomyces macrogynus* the inward current revealed sites of H^+-driven nutrient transport (De Silva *et al.*, 1992). In addition, the current in *Allomyces macrogynus* was always found to be directed outwards even when hyphae exhibited 'reverse growth' (Youatt *et al.*, 1988). The latter is an active growth process in which the hypha first widens at its apex then widens backwards towards its base.

A gradient of protons in growing hyphae of *N. crassa* was postulated by Slayman, (1965a,b) and Slayman & Slayman (1974) on the basis of membrane potential measurements. This gradient is thought to be established by an exclusion of proton pumping ATPase activity from the apical plasma membrane so that protons are pumped out subapically from the hypha and are replenished by protons that flow into the hyphal apex, probably in conjunction with other ions and/or nutrients (Slayman, 1987). This hypothesis is supported by the following evidence from numerous systems:

a) Measurements of electrical fields around hyphae in experiments, in which different ions were substituted in the surrounding medium, established firstly, that protons were the main ions carrying the electrical current in hyphae and secondly, that the current usually entered the tips of growing hyphae and exited subapically (Gow, 1989).

b) Analysis of pH_e, using pH-sensitive microelectrodes, showed that there was a depletion of protons around the tips of growing hyphae of *Achlya bisexualis* (Gow, 1984) and *N. crassa* (Takeuchi *et al.*, 1988).

c) Measurements of pH_c using non-fluorescent and fluorescent pH indicator dyes (Turian *et al.*, 1985; McGillviray & Gow, 1987; Roncal *et al.*, 1993) suggested that a cytoplasmic acidification takes place in hyphal apices. However, these measurements cannot be regarded as conclusive because they are very prone to artefacts (see section 5.1). More reliable data have been obtained from the combined use of fluorescent dyes (SNARF-1 imaged by confocal microscopy) and pH-sensitive microelectrodes to measure pH_c in rhizoids of the marine algae *Pelvetia* (Gibbon & Kropf, 1994). This study reported the presence of a gradient in pH_c, with a ΔpH of 0.5 pH units, over the first 50 μm of growing rhizoids. Although, as indicated, there is preliminary evidence for pH gradients occurring in growing fungal hyphae, convincing direct evidence of their existence is still lacking.

3. MATERIALS AND METHODS

3.1 QUANTITATIVE ANALYSIS OF THE EFFECTS OF EXTERNAL SIGNALS

3.1.1 Organism and growth conditions

M. grisea, strain 0-42 (kindly supplied by Dr. Barbara Valent, Du Pont Co., Wilmington, Del., USA) was bulked up and stored as described by Valent *et al.* (1991). For experimentation, oatmeal agar plates (1.5% agar containing 50 g per litre of Scotch porridge oat flakes) were inoculated with small pieces of filter paper bearing the fungus (Valent *et al.*, 1991) and incubated at 25°C for 18-24 days under continuous fluorescent light at 45 μmol photons·m^{-2}·s^{-1} in a cooled incubator. Conidia were isolated from 14- to 24-day-old cultures, using a scalpel and suspended in sterile, double-distilled water. The suspension was filtered through two layers of sterile cheesecloth and centrifuged at 1000 x g for 5 min. The concentration of conidia in suspension was adjusted to 1-2 x 10^4 ml^{-1} in sterile, double-distilled water. At conidial concentrations higher than this, it was not possible to determine accurately the percentage conidium germination and appressorium formation. Illumination was minimised during conidial isolation by wrapping the centrifuge tubes containing conidia in aluminium foil. All conidia produced by this isolation procedure lacked spore tip mucilage.

3.1.2 *In vitro* system on solid substrata

For all *in vitro* experiments, unused glass slides (Blue Star, Chance Propper, Warley, UK) were washed in Fairy Liquid detergent (Procter and Gamble, Newcastle upon Tyne, UK) and rinsed thoroughly with double-distilled water. Three silicon gaskets (Swinnex-13, Millipore, Bedford, Mass., USA), covered in melted dental wax (Anutex, Associated Dental Products Ltd, Swindon, UK), were applied to the slides to which they adhered once the wax cooled. The gasket rings prevented run off of the inoculum drop during subsequent manipulations. To minimise microbial contamination during experimentation, the slides with gaskets were treated with UV-A irradiation for at least 4 h prior to inoculation. For experiments on Cellophane (gauge 525, uncoated 'rayophane' from A.A. Packaging, Walmer Bridge, Lancs., UK) or Teflon (polytetrafluoroethylene from Du Pont Co., Wilmington, Del., USA), 10 mm diameter circles of the substrata were cut using a

cork borer. After autoclaving, the circles were placed within the silicon gaskets. Experiments on glass were performed directly on the slides. A 20 µl conidium suspension was applied to the substratum and the slides placed in sterile, 12 x 12 cm square Petri dishes. To maintain high humidity, sterile tissue paper, saturated with sterile water, was placed in each dish which was then sealed with Parafilm. Except where stated, the fungal samples were grown for 24 h and incubated at 25°C under continuous light from fluorescent tubes at 45 µmol photons·m^{-2}·s^{-1} in a cooled incubator. Dark-grown samples were covered in light-tight bags normally used to store photographic paper. To determine the effects of different light intensities, Petri dishes were wrapped in polyester neutral density filters (Lee Lighting Ltd., Glasgow, UK) of different grades (50%, 25% and 15% transmission). Temperature measurements with a digital thermometer showed that the temperatures within sealed Petri dishes grown in the light and in the dark, and within the incubator, were the same (± 0.5°C).

For the quantitation of germination and appressorium formation under different pH conditions a *universal buffer* with the following composition was used: 28.6 mM citric acid; 28.6 mM KH_2PO_4; 28.6 mM boric acid and 28.6 mM diethylbarbituric acid (Perrin & Dempsey, 1974). To titrate the buffer to the appropriate pH 200 mM NaOH was added to 100 ml of the buffer stock solution followed by dilution to 200 ml (Table 4).

Table 4. Amount of NaOH added to universal buffer for titration to defined pH value

pH	ml 200 mM NaOH	pH	ml 200 mM NaOH
2.6	0	7.0	50
3.0	6	8.0	62
4.0	16	9.0	72
5.0	28	10.0	82
6.0	40	-	-

All nutrients were obtained from Sigma, Poole, UK. The complete nutrient medium used contained 1% sucrose, 0.6% yeast extract and 0.6% casein hydrolysate.

3.1.3 *In vitro* system in liquid suspension

In order to analyse conidium germination in liquid suspension, hanging drop cultures were prepared. This involved adding 20 µl drops of conidium suspension to glass slides, immediately inverting the slides, and then incubating them on a support over damp tissue paper in Petri dishes (as described in section 3.1.2). Conidium germination and appressorium formation in the hanging drops were assessed after 24 h using a Nikon Diaphot inverted microscope.

3.1.4 Fixation and quantitative analysis

After 24 h (48 h for the temperature experiments), the silicon gaskets were removed and each sample immobilised and fixed by applying a molten drop of 20 µl 2% agarose (Type VIII, Sigma, Poole, UK) containing 5% glutaraldehyde (Sigma) at 50°C. For the time-course experiments, samples were immobilised and fixed at the times indicated. Percentage conidium germination, germination patterns and appressorium formation were assessed using a Reichert-Jung Polyvar Photomicroscope with a x 10 plan apo objective and a total magnification of x 125. Germ tube lengths were measured using a Bio-Rad MRC-600 laser scanning confocal system (Bio-Rad Microscience Ltd., Hemel Hempstead, UK) mounted on a Nikon Diaphot inverted microscope and the images analysed with CoMOS (Bio-Rad) software. Unless stated otherwise, 6 replicates were performed for each experiment which was done at least twice. All conidia (100-300) were counted in each replicate. Percentage appressorium differentiation was taken as the percentage of germinated conidia (sporelings) that were differentiated. An appressorium was regarded as a rounded, pigmented, terminal swelling of a germ tube (Fig. 5). Statistical analyses were performed using either Fig P for Windows v. 1.0 (Biosoft, Cambridge, UK) or Microsoft Excel v. 4.0. Statistical tests (t-test and analysis of variance) were done after arcsine transformation.

3.1.5 Plant growth conditions and infection

Rice plants (M-201, California Cooperative Rice Research Foundation Inc.) were grown in standard soil (Fisons, Type M3) and watered with Hoagland's nutrient solution (Hoagland & Arnon, 1950). Plants were grown under a 14 h photoperiod at 27°C in the light (300 μmol photons·m^{-2}·s^{-1}) and 21°C in the dark. Plants were transferred to a cooled incubator 14-18 days after seed germination. The third or fourth leaf of each plant was placed in a Petri dish (50 mm diameter) by guiding it through small openings cut in the dishes. Care was taken not to damage the leaf or touch the leaf surface to be studied. Damp filter paper was placed in the base of the Petri dish to maintain a high humidity. Prior to inoculation, the leaves were left for at least 8 h in open Petri dishes, after which 8 μl drops of conidial suspension were pipetted on to the upper surfaces of leaves. The Petri dish lids were then replaced. For dark samples, the Petri dishes were wrapped in black photographic bags in such a way that they were light-tight. Incubation conditions were as described for the *in vitro* system (section 3.1.2)

3.1.6 Staining of infected leaves

Leaves were removed and sprayed with 0.05% Calcofluor M2R (Sigma, Poole, UK) 24 h after inoculation. Quantitation of germination patterns and appressorium formation was performed immediately afterwards by fluorescence microscopy, using the U1 filter block (containing a 330-380 nm excitation filter, 420 nm dichroic mirror, and 418 nm long path barrier filter) of the Reichert-Jung Polyvar microscope. Germ tube lengths were measured using CoMOS image analysis software.

3.2. Imaging And Analysis of Cytosolic pH

3.2.1 *In vitro* system

For all experiments unused glass coverslips (20 x 50 mm, N° 1½, Chance Propper, Warley, UK) were used. One silicon gasket, covered in dental wax, was applied to each coverslip to which it adhered once the wax cooled. Eighty µl conidium suspension was then applied to each glass slip which was immediately inverted, and then incubated on a support over damp tissue paper in Petri dishes (for further details see section 3.1). For dye loading hanging drops were transferred on to similarly prepared coverslips. The samples were then kept for at least 30 min in a humid chamber to allow the germinated conidia to recover from any physical stress experienced during transfer and to adhere tightly to the glass surface. For dye loading and imaging the sample was placed on the microscope stage where water from the sample was carefully removed with filter paper and replaced by 50 µl of 2.5 µM dye. After 5-10 min the dye was removed and the sample washed once with double-distilled water. Images were captured in the first 15 min following dye loading because thereafter the signal became too weak due to dye sequestration and leakage. To assess the effects of higher concentrations of SNARF-1 and extended loading times, germlings were incubated in 50 µM of dye. After removing the dye, germlings were incubated as described in section 3.1.2. To assess the effects of external buffers on cytosolic pH (pH_c), germinated conidia were loaded with dye dissolved in 50 mM MES-HEPES buffer adjusted with KOH to pH 6.0, 7.0 or 8.0. Imaging was then performed in the same buffer in the absence of dye. To investigate the effects of nutrients on pH_c, conidia were hydrated and incubated in a complete nutrient medium (see section 3.1.2). Dye was then applied directly to the complete medium. Images were captured during continuous loading of germlings for 15 min after dye application.

3.2.2 Dyes

The free acid form, the acetoxymethyl (AM)-ester and the 70 KDa dextran conjugate of the pH-indicator dye SNARF-1 [5(6)-carboxyseminaphthorhodafluor-1] and Pluronic F-127 were obtained from Molecular Probes Inc. (Eugene, OR, USA). The pH-sensitive dye SNARF-1 exhibits a pH-dependent shift in its emission spectrum. When excited at 514 nm, it exhibits two peaks in its emission spectrum: one at 588 nm (the acid form) and one at 643 nm (the basic form) (Fig. 4). As a result of its marked pH-dependent shift in its emission spectrum, SNARF-1 is ideally suited to ratio imaging of pH.

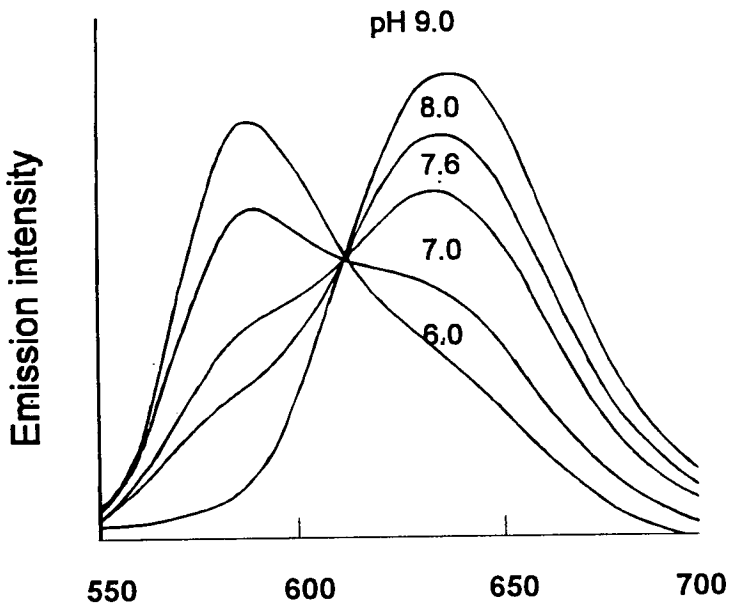

Fig. 4. pH-dependent emission spectrum of SNARF-1 excited at 514 nm (adapted from Haugland, 1992).

In order to solubilise the SNARF-1 ester the detergent Pluronic F-127 was used. Pluronic was diluted in dimethyl sulphoxide (DMSO) to give 25% w/v stock and then further diluted to 2% in double-distilled water. The dilutions of SNARF-1 used are shown in Table 5.

Table 5. SNARF-1 preparation used in the present study

	SNARF-1 free acid	SNARF-1-AM	SNARF-1 dextran
Stock	2 mM in water (adjusted to pH 6.0 with KCl)	20 mM in anhydrous DMSO	2 mM in water
Storage	4°C	-70°C	4°C
Substock	100 µM in water	200 µM in 0.05% Pluronic	500 µM in water
Storage	4°C	-20°C	4°C
Final concentration	20 µM in buffer	2.5 µM in buffer or water Pluronic: < 0.01% DMSO: < 0.1%	100 µM in buffer
Experiments	*in vitro* calibrations	measurements of cytosolic pH, and *in vivo* and *in situ* calibration	*in vitro* calibrations

Carboxyfluorescein-diacetate (Sigma, Poole, UK) was first dissolved in 50°C hot ethanol (1 mg/150 µl) and then diluted to a final concentration of 20 µg/ml in water. The concentration of ethanol in the final solution was 0.3% (v/v).

3.2.3 Dye loading

Dye loading of living cells was performed with the membrane-permeant ester of SNARF-1 and carboxyfluorescein. For loading with SNARF-1 germinated conidia were incubated for 10 min in 50-100 µl of dye solution which was then removed with filter paper and the cells immediately imaged in double-distilled water. For experiments which required the application of a buffer, germinated conidia were first washed with 50 µl buffer and then imaged in fresh buffer. For loading with carboxyfluorescein, germinated conidia were

incubated for 15 min in the dye-ester and then washed twice with double-distilled water. Before imaging, the dye was allowed to accumulate within the vacuolar system for 30 min.

3.2.4 Imaging

Confocal fluorescence imaging was performed with the Bio-Rad MRC-600 LSCM (Laser Scanning Confocal Microscope) controlled from the CoMOS (Version 6.03), TCSM (Version 1.1C) and MPL (Version 1.01) software. The confocal system was interfaced with a Nikon Diaphot inverted microscope.

The set-up procedures were followed as described in the manufacturer's operating manual. Briefly, the excitation laser beam and then the emission signal beams were aligned after the excitation filter block (514 nm excitation filter, 540 nm dichroic mirror and 550 nm long pass filter) and a custom-built SNARF-1 filter block had been inserted. The required settings for imaging were then set up. Optimal settings used are shown in Table 12 (section 5.2.1.2).

Bright field images were collected via a transmission device which gathered transmitted laser light and delivered it, via a fibre-optic cable, direct to the second photomultiplier detector. Collection of sequential optical sections in the z-plane was made with the CoMOS *z-series* command using the focus motor to step the focus up or down through the specimen.

Simultaneous dual-emission ratio imaging was performed by simultaneous collection of two fluorescence images, at different wavelengths, with two photomultipliers. To get the best alignment of the two images for calculating the ratio of the individual pixels, the initial emission signal beam alignment was found to be critical. It was also important to use the exact setting for the correction rings on the objectives to correct for coverslip thickness and have the same confocal aperture settings for both channels. The emission of SNARF-1 was collected simultaneously at 580 ± 15 nm (Channel 2) and 640 ± 18 nm (Channel 1) via a Nikon x 40 plan apo objective. Black levels were set to give a background

current signal of 10 pixel intensity. All settings were kept at exactly the same values for all experiments. Special care was taken to keep the individual electronic amplification of either emission signal, and the aperture settings for each channel, at virtually the same settings during all experiments as changes in these settings would significantly alter the ratio values.

3.2.5 Image processing and analysis

Image processing was kept to a minimum, and continual reference made during image processing to the original images captured to reduce or avoid the creation of imaging artefacts. The only enhancement used was the *3 x 3 rank filter* command of the TCSM software.

To measure growth rates, the lengths of individual germ tubes in successive images were measured using the CoMOS *length* command.

The ratio values were calculated pixel-by-pixel using the TCSM software. If not stated otherwise, ratio values for whole germ tubes were extracted by measuring the pixel intensity of the first 30 µm of the growing germ tube by using the *Histogram* command in CoMOS. Care was taken not to include areas close to the edge of the germ tube since low fluorescence intensity and image enhancement caused artefacts in this region (see section 5.2). Ratio values were converted to pH values after suitable calibration (see next section)

Pixel-by-pixel intensity measurements in transects along the lengths of germ tubes were done using the *line* command in MPL.

Hard copies of coloured images were produced with a Mitsubishi CP 200B video copy processor (Mitsubishi Electrical Corporation, Japan). Black-and-white images were recorded on Kodak TMax 100 film using a Polaroid VI-350 Quick print (Polaroid Corporation, Mass., USA).

3.2.6 Calibration

The *in vitro* calibrations of SNARF-1 free acid and SNARF-1 dextran were done in 10 mM MES-HEPES buffer titrated with KOH to the appropriate pH. SNARF-1 free acid was additionally calibrated in a buffer designed to mimic conditions in the cytoplasm (Fricker, M.D., personal communication). This pseudocytoplasmic buffer consisted of: 100 mM KCl, 20 mM NaCl, 1 mM $MgSO_4$, 10 mM MES, 10 mM HEPES. Viscosity was increased by adding 60% (w/v) sucrose and the hydrophobicity altered by inclusion of 25% (v/v) ethanol. For each pH value two samples of 25 µl of dye, at the final concentration as indicated in Table 5, were then imaged on a cover slip (20 x 50 mm, N^{o} 1«, Chance Propper, Warley, UK). The dye concentration was chosen so that at pH 7.0 the signal intensity gave a pixel intensity of approximately 100 at each wavelength. The electronic amplification of the signals was adjusted so that at pH 7.0 both channels gave a similar signal and which after diversion gave a ratio = 1. In each case, dye closest to the cover slip was measured as it gave the brightest signal. Each calibration was done three times.

For the *in situ* calibration, germinated conidia were incubated for 5 min in 50 µM solubilised amphotericin B (Sigma, Poole, UK). The ionophore solution was then replaced by 2.5 µM SNARF-1-AM in 50 mM MES-HEPES buffer plus 100 mM KCl titrated to the appropriate pH with KOH. Imaging was performed in the first 5 min after dye loading to avoid interference from dye leakage/sequestration and increasing vacuolation. Experiments demonstrated that the change in the pH_c, caused by this treatment, was completed within 2 min of buffer application (data not shown).

For the *in vivo* calibration, the pH_c in growing germ tubes was clamped with either a weak acid or a weak base. Thirty mM propionic acid Na-salt was titrated with the free acid form to pH 6.0 and 30 mM NH_4Cl was adjusted to pH 7.0 and 8.0 with NH_4OH. The acid or base was then applied to dye-loaded samples. Images were captured 10 min after the application of buffer. Preliminary experiments in which germ tubes were incubated for 1 h and repeatedly loaded with dye revealed that complete equilibration of the pH_c with the external pH under these conditions was achieved within 10 min (data not shown).

4. THE ROLE OF EXTERNAL SIGNALS IN REGULATING THE PRE-PENETRATION PHASE OF INFECTION

4.1 INTRODUCTION

As explained in section 2.3 very little is known about the role of external factors in regulating the pre-penetration phase of *M. grisea*. The aim of the work covered in this chapter is to provide a detailed analysis of the influence of the substratum, light, temperature, nutrients and pH on conidium germination, germ tube growth and appressorium differentiation. These analyses were carried out on both artificial substrata (Cellophane, glass and Teflon) and rice leaves.

4.2 RESULTS

The pre-penetration phase of *M. grisea* starts with the attachment of a hydrated conidium to a surface, such as a rice leaf. Soon after attachment up to three germ tubes can emerge from the conidial cells. One of the germ tubes will commonly swell at its tip and form a melanised appressorium. Fig. 5 shows the appearance of the conidium, germ tube and appressorium on Cellophane, glass, Teflon and the rice leaf. With the exception of the lengths of germ tubes (see below), the general appearance of germinated conidia bearing appressoria was similar on rice leaves and artificial substrata. Mature appressoria were pigmented and typically circular in profile. Sometimes, however, the appressoria on rice leaves were irregular in outline (not shown) because they tend to mould themselves around the protrusions (papillae) found on the rice leaf surface (Hirooka *et al.* 1982; Talbot, 1995).

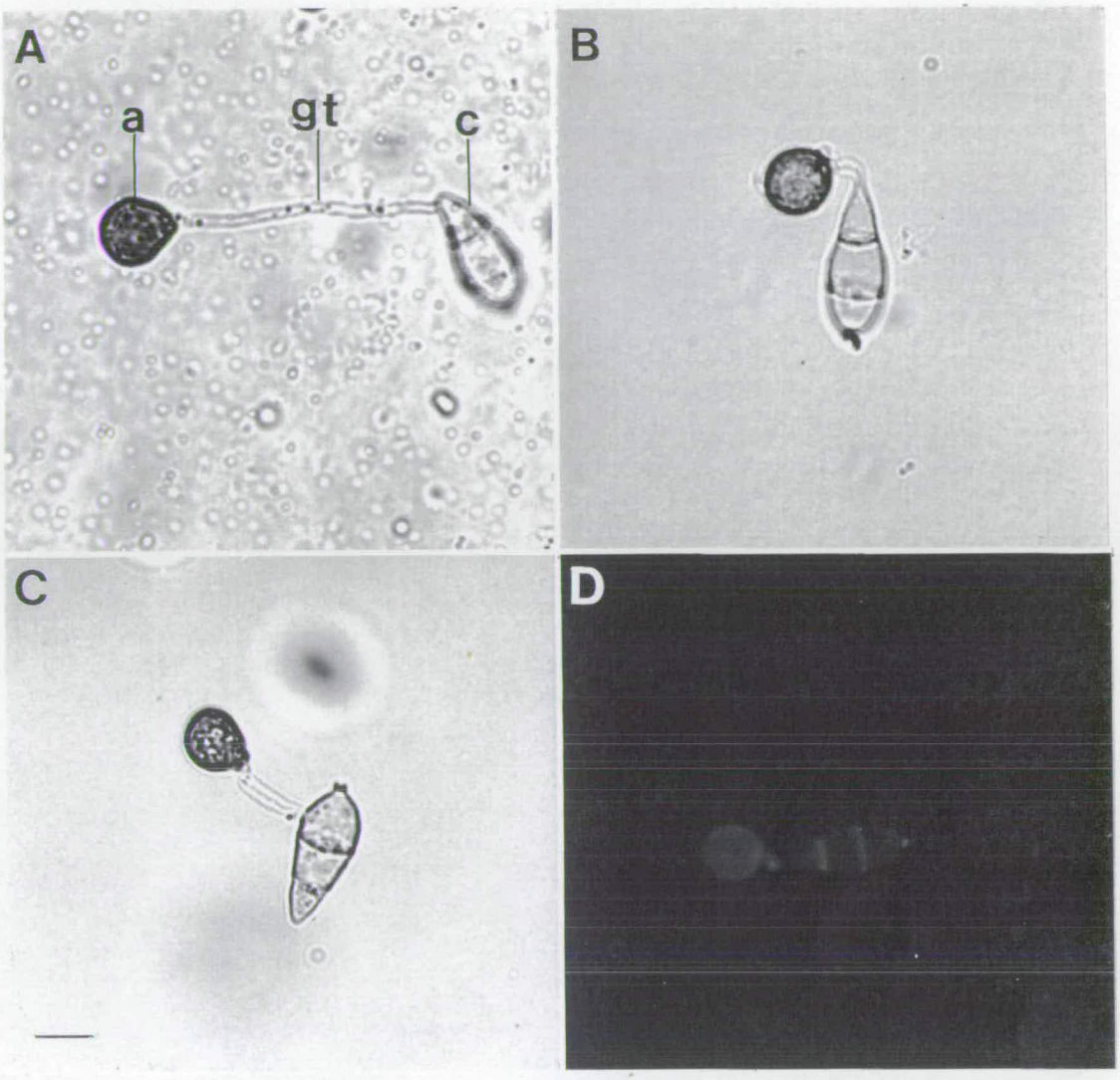

Fig. 5. Brightfield light micrographs of a germinated conidium (c) of *M. grisea* from which a germ tube (gt) has differentiated an appressorium (a) on Cellophane (**A**), Teflon (**B**) or glass (**C**). In (**D**) a fluorescence light micrograph is shown of a germinated conidium from which a germ tube has differentiated an appressorium on a rice leaf. The germinated and differentiated sporeling was loaded with calcofluor. Bar represents 10 μm.

4.2.1 Conidium germination

4.2.1.1 Light and substratum

To investigate the influence of surface contact and the influence of different substrata on the germination of hydrated conidia, germination was quantified in hanging drops and on various substrata. Furthermore, the influence of light on germination was evaluated. The mean percentage of conidium germination, on the different substrata and in hanging drops, ranged from 92.8 ± 3.5 (SEM) to 98.3 ± 1.3 (SEM) in the light and in the dark (Table 6). No significant difference between the light and dark treatments was found for any of the substrata.

Table 6. Percentage germination (± SEM) of *M. grisea* conidia on rice leaves, Cellophane, Teflon and glass in the light and in the dark after 24 h

	% Germination	
	Light	Dark
Rice leaf	98.3 ± 1.3	98.1 ± 2.7
Cellophane	98.0 ± 0.9	97.8 ± 2.2
Teflon	95.0 ± 1.6	96.5 ± 1.3
Glass	94.9 ± 2.2	95.2 ± 1.8
Hanging drop	94.0 ± 0.6	92.8 ± 3.5

Four patterns of germination were representative of > 90% of all patterns exhibited by differentiated sporelings (Fig. 6). The relative proportion of sporelings within each of these four classes did not differ significantly ($P < 0.05$) on all substrata. Conidia germinated from one or more of their three cells although < 2% germinated from their middle cells. Greater than 70% of sporelings possessed one germ tube only; the most common type had one differentiated germ tube which had emerged from the apical cell of the conidium.

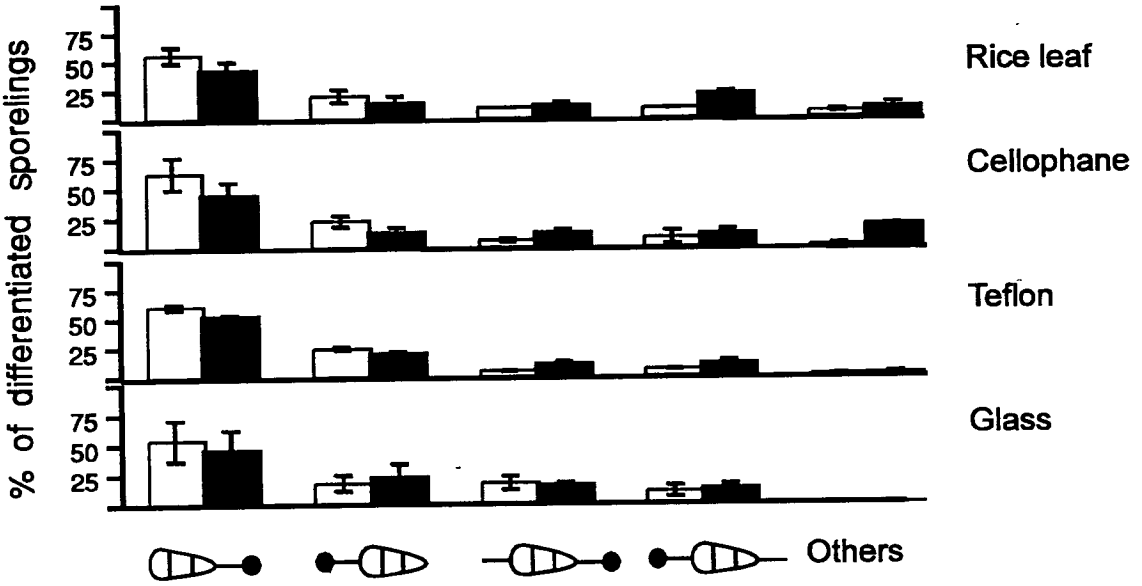

Fig. 6. Germination and differentiation patterns of *M. grisea* conidia on rice leaves, Cellophane, Teflon and glass in the light (□) and in the dark (■) after 24 h. Bars represent SEMs. Graphics on the x-axis symbolise germinated conidia. Open ended lines symbolise undifferentiated germ tubes whereas lines ending in black circles indicate differentiated germ tubes bearing appressoria. (The measurements made to obtain the results for Teflon and glass were done in collaboration with H. A. Page.)

To determine if light influenced the rate of germination, the percentage germination was quantified at different times after hydration in the light and in the dark on Cellophane. More than 65% of the conidia had germinated within 4 h after hydration (Fig. 7). Between 4 and 6 h after hydration the rate of germination was greater in the dark than in the light. In both treatments, germination was completed within 8 h.

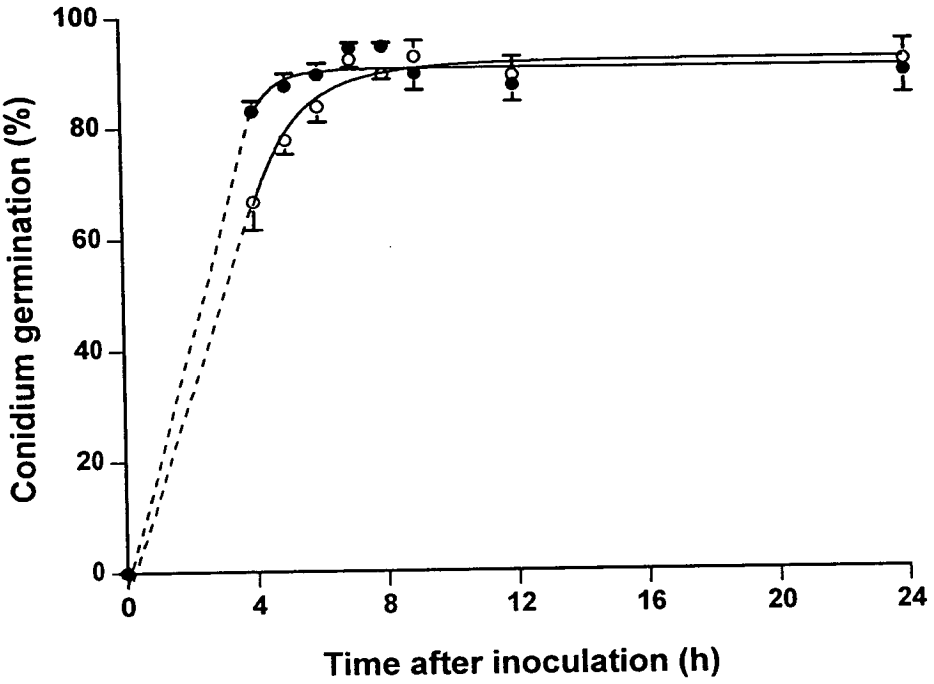

Fig. 7. Time course of germination of *M. grisea* conidia on Cellophane in the light (O) and in the dark (●). Bars represent SEMs.

4.2.1.2 pH

The influence of pH on germination in the light and in the dark on Cellophane was quantified using a *universal buffer* (see section 3.1.2) to control external pH. Comparison between germination in double-distilled water (pH 6.5-7.0 in the laboratory) and in the buffer at pH 7.0 indicated that there was little if any inhibition of germination in the buffer used (Table 7). Between 80.3% and 98.1% of conidia germinated over the pH-range of 2.6 to 8.0 on Cellophane in the light and in the dark. At more alkaline pH values the percentage of germination was significantly lower ($P < 0.01$).

Table 7. Influence of external pH on percentage germination (± SEM) of *M. grisea* conidia after 24 h incubation on Cellophane in the light and in the dark

External buffered pH	2.6	3.0	4.0	5.0	6.0	7.0	8.0	9.0	10.0	Water
Germination Light (%)	80.7 ± 16.0	90.8 ± 3.1	95.6 ± 0.5	96.6 ± 2.3	96.8 ± 1.9	98.1 ± 1.0	95.5 ± 2.8	27.2 ± 11.8	6.0 ± 6.0	98.4 ± 0.8
Germination Dark (%)	80.3 ±14.4	92.1 ± 2.0	93.5 ± 2.1	96.9 ± 1.2	94.6 ± 2.4	93.1 ± 0.7	82.6 ± 5.1	30.1 ± 7.0	1.8 ± 1.0	96.7 ± 0.7

4.2.1.3. Nutrients and temperature

Percentage germination was > 80% in all of the nutrient solutions (glucose, 3-o-methyl-glucose, fructose, sucrose, NH_4NO_3 or complete medium) tested. Greater than 80% of conidia also germinated over the 15-30° C temperature range investigated (data not shown).

4.2.2 Germ tubes

The lengths of differentiated germ tubes were assessed in the light and in the dark on different substrata, in various solutions of nutrients and at different external pH values. The lengths of undifferentiated germ tubes were also measured at different external pH values.

4.2.2.1 Light and substratum

The lengths of differentiated germ tubes were measured to investigate the effects of light and the substratum on germ tube differentiation. On the rice leaf, germ tubes with appressoria showed a marked tendency to be shorter in the light than in the dark: 97% and 77% of the germ tubes were < 60 μm long in the light and in the dark, respectively (Fig. 8). Of the artificial substrata, only differentiated germ tubes on Cellophane were significantly shorter in the light (80% < 60 μm long) than in the dark (51% < 60 μm long). On Teflon, 100% and 97% of germ tubes were < 60 μm in the light and in the dark, respectively; on glass, 93% and 90% were < 60 μm in the light and in the dark, respectively.

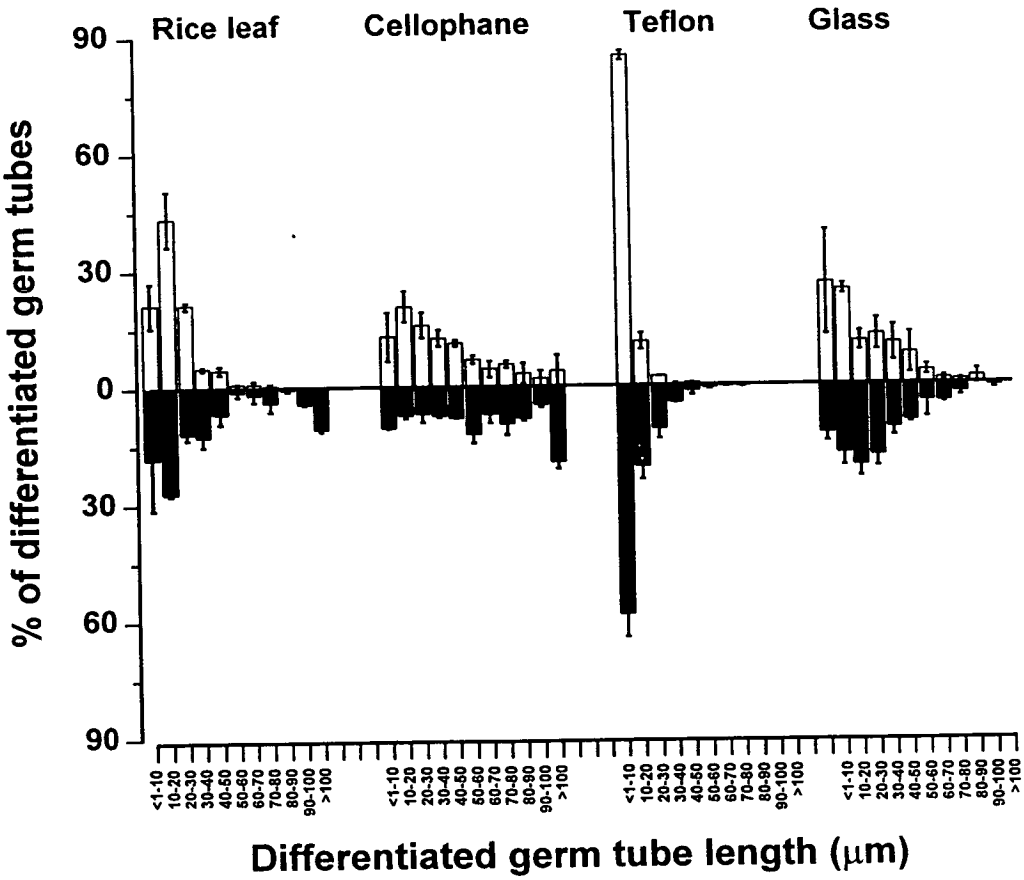

Fig. 8. Percentage of differentiated *M. grisea* germ tubes in defined length classes on rice leaves, Cellophane, Teflon, and glass in the light (□) and in the dark (■) after 24 h. Bars represent SEMs.

Of the three artificial substrata tested, only Cellophane resembled rice leaves by inducing the fungus to produce shorter differentiated germ tubes in the light than in the dark (Fig. 8). It was, therefore, chosen as a substratum to investigate further effects of light, nutrients, temperature and pH on germ tube lengths and/or appressorium formation.

To investigate the effect of irradiance on the length of differentiated germ tubes, germinating conidia were exposed to light of different intensities (photon flux densities). It was found that light intensity had a marked effect on the lengths of differentiated germ tubes and this was a graded response: the higher the light intensity, the lower the number of long (> 100 μm) differentiated germ tubes (Fig. 9).

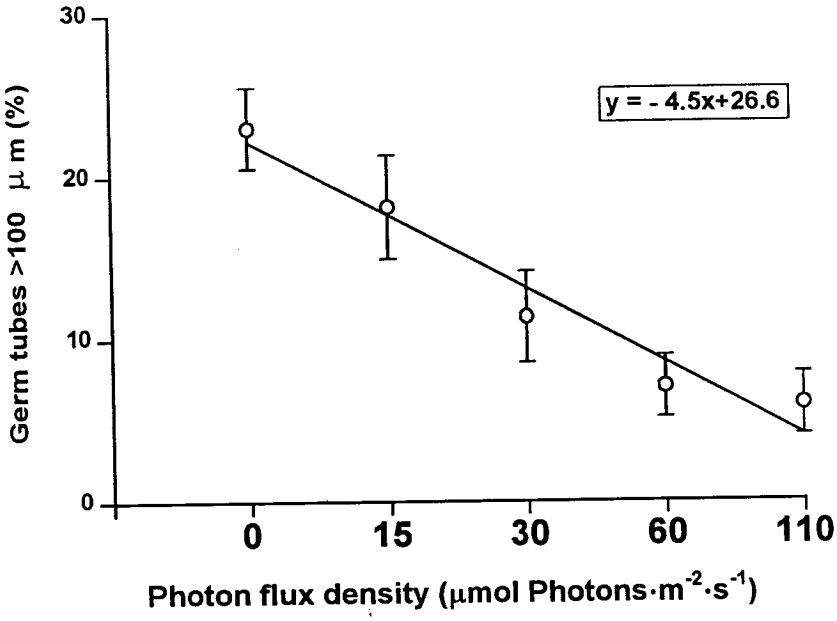

Fig. 9. Influence of photon flux density on the percentage of differentiated germ tubes of *M. grisea* > 100 μm long after 24 h incubation on Cellophane. Bars represent SEMs of nine replicates per treatment. The line was fitted by regression analysis ($r = 0.98$; $P < 0.01$).

4.2.2.2 Nutrients

The influence of different sugars, ammonium nitrate and a complete medium (yeast extract plus casein hydrolysate plus sucrose) on the lengths of differentiated germ tubes on Cellophane was evaluated to investigate the effects of nutrients on germ tube growth. Glucose had a marked effect on the length of differentiated germ tubes in the dark but not in the light (Fig. 10). The proportion of germ tubes > 60 μm in length increased from 47% with 1 mM glucose to almost 70% with 250 mM glucose in the dark. No such effect was caused with glucose in the light or with 3-o-methyl-glucose, a non-metabolisable analogue of glucose, in either the light or the dark. Strong effects were not observed on the lengths of differentiated germ tubes when germ tubes were grown in the presence of fructose, sucrose or ammonium nitrate at any of the concentrations examined. Growth in complete medium increased the proportion of germ tubes > 60 μm in length by between 15 and 33% compared with the control incubated in water.

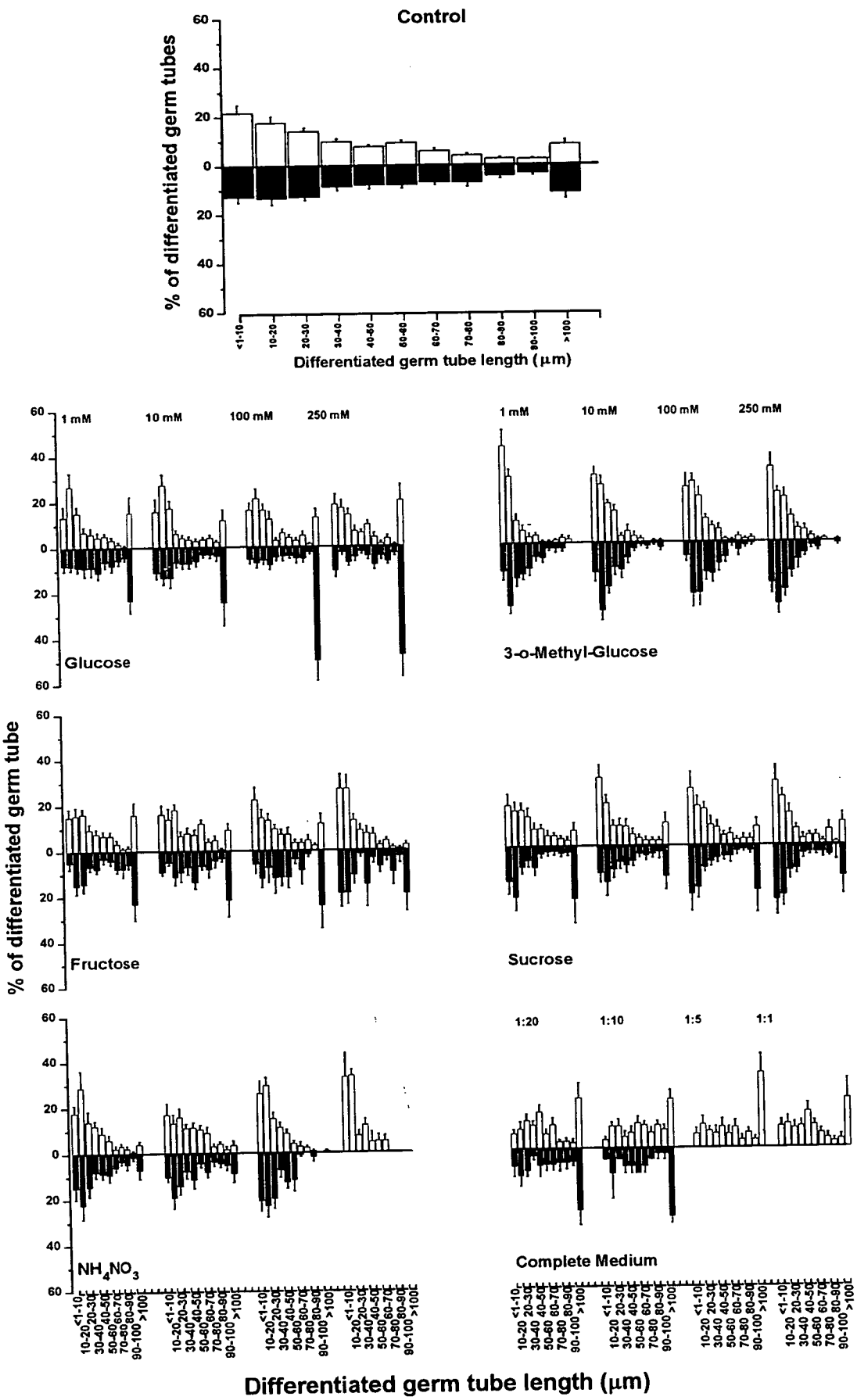

Fig. 10. Percentage of differentiated *M. grisea* germ tubes in defined length classes, in water (control) and in solutions containing various nutrients on Cellophane in the light (□) and in the dark (■) after 24 h. Note that no germ tube differentiated in some of the treatments with ammonium nitrate or complete medium. Bars represent SEMs.

4.2.2.3 pH

To assess the effects of external pH on growth of germ tubes, the lengths of differentiated and undifferentiated germ tubes were measured on Cellophane in buffers with different pH values. Over the pH range 3.0 to 7.0, the mean length of differentiated germ tubes was between 38.5 μm at pH 3.0 and 90.0 μm at pH 6.0 in the light (Table 8). The average length of differentiated germ tubes in water was 81.5 μm. Undifferentiated germ tubes were consistently longer than differentiated germ tubes over the whole pH range tested. The longest undifferentiated germ tubes grew at pH 4.0 where the average length was 168.2 μm.

Table 8. Lengths of differentiated and undifferentiated germ tubes (± SEM) of *M. grisea* in buffers of different pH on Cellophane after 24 h in the light

Buffered pH	3.0	4.0	5.0	6.0	7.0	8.0	Water (Control)
Germ tube length (μm)							
differentiated	38.5	59.5	73.9	90.0	69.8	16.2	81.5
	± 7.0	± 13.2	± 14.5	± 26.3	± 22.4	± 10.2	± 12.4
*undifferentiated	77.1	168.2	131.0	132.2	78.2	70.8	185.1
	± 20.2	± 30.0	± 23.8	± 29.6	± 7.1	± 12.7	± 43.9

*: Results represent 4 replicates from one experiment instead of the normal 9 replicates from 3 experiments

4.2.3 Appressorium formation

4.2.3.1 Light and substratum

To investigate the influence of contact with a surface and the influence of different substrata on appressorium formation, differentiation was quantified in hanging drops and on various substrata. The influence of light on appressorium formation in the different treatments was also evaluated.

Table 9 shows that on rice leaves 98% of germinated conidia differentiated appressoria in the light whilst fewer (92%) did so in the dark. On the artificial substrata, differentiation was ≥ 69% in the light and 20-30% lower in the dark. On each substratum, the percentage differentiation in the light was significantly greater than in the dark ($P < 0.01$). Comparisons of all the light-grown treatments, or all of the dark-grown treatments, showed that percentage differentiation on rice leaves was significantly higher ($P < 0.02$) than on any of the artificial substrata. The results were subjected to a two-way analysis of variance to detect significance of difference between the effects of the light/dark treatments and the type of substratum used. The analysis showed a significant influence ($P < 0.01$) of light and the substratum type, but no significant interaction between these factors, on the percentage of appressoria formed. In the hanging drops, it was notable that after 24 h none of the germ tubes differentiated appressoria unless they made contact with the glass surfaces from which the drops were suspended.

Table 9. Percentage differentiation of *M. grisea* appressoria on rice leaves, Cellophane, Teflon and glass in the light and in the dark after 24 h

	Rice Leaf	Cellophane	Teflon	Glass	Means
Light	98.0	79.9	91.2	69.0	84.5
Dark	91.5	54.5	68.1	39.0	63.3
Means	94.7	67.2	79.6	54.0	1% LSD 1.9

Four patterns of differentiation were representative of > 90% of all patterns exhibited by sporelings (Fig. 6, section 4.2.1.1). The relative proportion of sporelings within each of these four classes did not differ significantly ($P < 0.05$) on all substrata. Furthermore, the percentage of sporelings in the four differentiation patterns did not differ significantly ($P < 0.05$) if conidia were incubated in the light or in the dark on any of the surfaces investigated.

To investigate the effect of light on differentiation in further detail, appressorium formation on Cellophane was quantified after certain time intervals in the light and in the dark. Germ tube differentiation began 5 h post-inoculation in both the light and the dark (Fig. 11). However, the first morphological indicator of appressorium formation (hook formation; Bourett & Howard, 1990) was observed 1 h earlier in the light than in the dark (data not shown). Under both conditions, differentiation of appressoria ceased 14 h post-inoculation. The number of appressoria which differentiate per unit of time over the 6-12 h period was approximately 50% higher in the light than in the dark (Fig. 11).

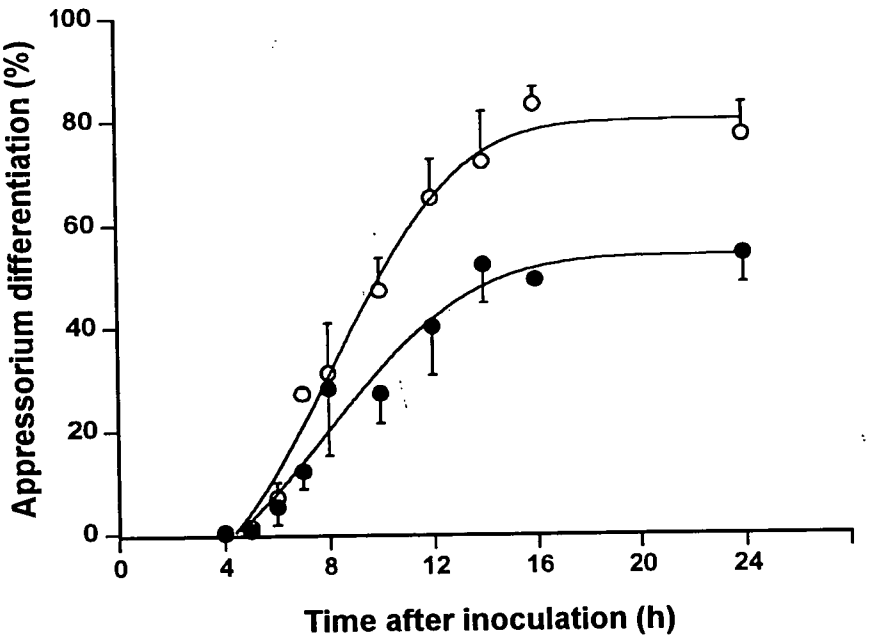

Fig. 11. Time course of differentiation of *M. grisea* appressoria on Cellophane in the light (○) and in the dark (●). Bars represent SEMs.

Although light *per se* enhanced the number of appressoria formed (Table 9), the photon flux density (15-110 μmol photons·m^{-2}·s^{-1}) did not seem to be important in this response (Table 10). Under all light intensities tested, the percentage of conidia which produced appressoria was > 20% higher than in the dark. This difference was highly significant for all treatments ($P < 0.01$) and no significant difference between light intensities was found.

Table 10. Influence of photon flux density on percentage differentiation of *M. grisea* appressoria after 24 h incubation on Cellophane

	Photon flux density (μmol photons·m^{-2}·s^{-1})					1% LSD
	110	60	30	15	0	
% Appressorium Differentiation	87.0	85.7	86.4	80.9	58.9	3.6

4.2.3.2 Nutrients

To investigate the influence of nutrients on the differentiation process, conidia were incubated in solutions of various sugars, ammonium nitrate and a complete nutrient medium (yeast extract plus casein hydrolysate plus sucrose) in the light or in the dark on Cellophane. In high concentrations of the complete medium, < 4% of germ tubes differentiated appressoria in the dark (Fig. 12). In the light > 43% of germ tubes differentiated under the same nutrient conditions. A 1:20 dilution of the nutrient solution increased the proportion of appressoria formed to > 17.0 in the dark and > 81.0 in the light.

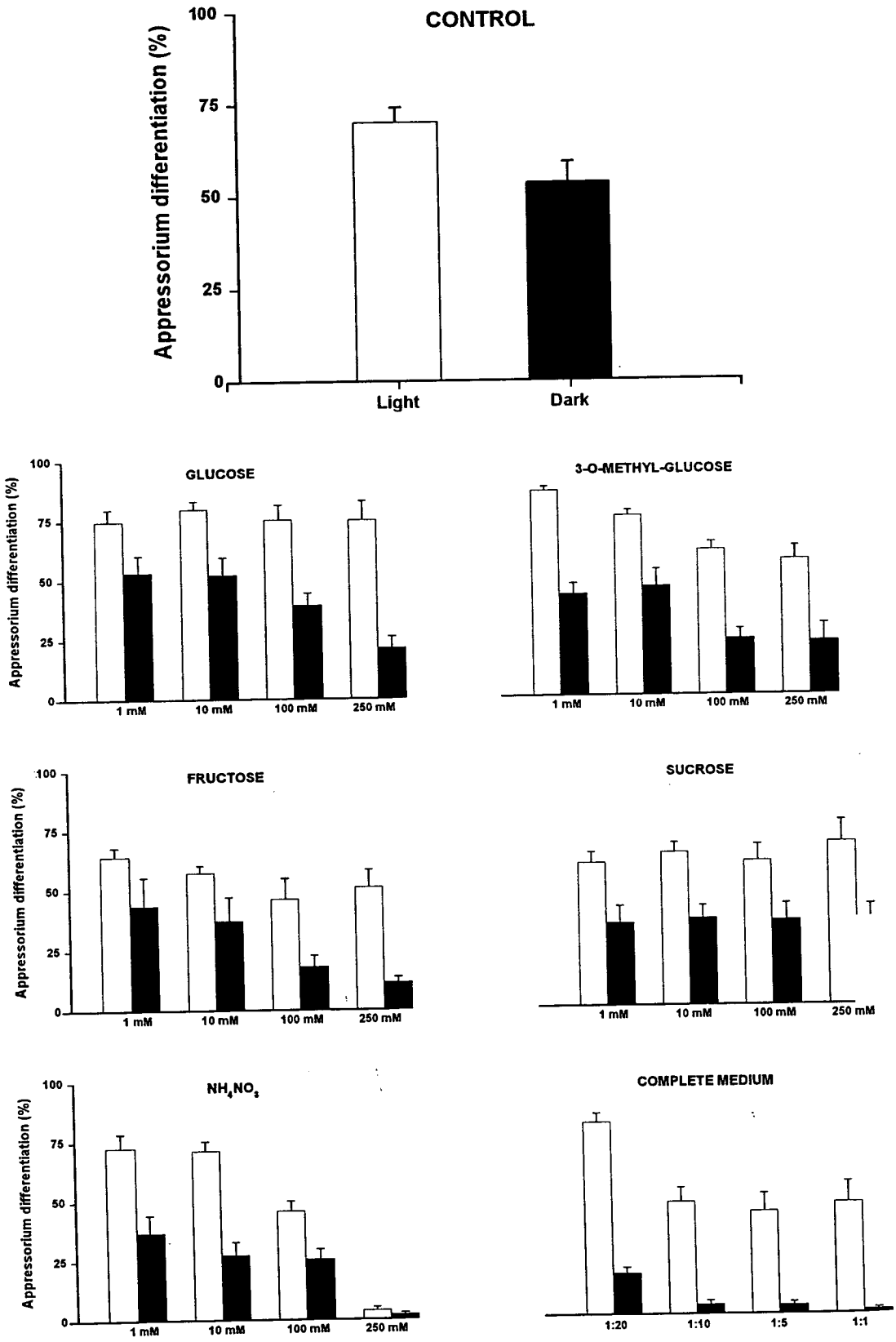

Fig. 12. Percentage differentiation of *M. grisea* appressoria in solutions of various nutrients on Cellophane in the light (□) and in the dark (■) after 24 h. Bars represent SEMs.

In high concentrations (100 mM and 250 mM) of the monosaccharides tested (glucose, 3-o-methyl-glucose and fructose) the percentage of germ tubes undergoing differentiation decreased. This effect was more notable in the dark than in the light. Sucrose had no effect on appressorium formation at all concentrations tested (1 mM - 250 mM).

Less than 4% of germ tubes formed appressoria in 250 mM ammonium nitrate in either the light or the dark. No other source of nitrogen was tested.

None of the nutrient treatments significantly increased the percentage of germ tubes differentiating appressoria.

4.2.3.3 pH

To assess the effect of pH on differentiation, conidia were incubated in buffers of different pH values. In buffered solution the average percentage of appressorium formation on Cellophane in the light was lower than in water over the pH range from 3 to 8 (Table 11). The highest number of appressoria were formed at pH 4.0, where > 42% of germ tubes differentiated.

Table 11. Percentage differentiation (± SEM) of *M. grisea* appressoria in buffer of different pH on Cellophane after 24 h in the light

Buffered pH	3.0	4.0	5.0	6.0	7.0	8.0	Water (Control)
% Appressorium formation	20.9 ± 9.1	42.6 ± 9.8	39.7 ± 12.9	32.1 ± 15.0	12.5 ± 2.7	3.0 ± 1.3	71.5 ± 6.9

4.2.3.4 Temperature

The influence of temperature on differentiation was characterised by incubating hydrated conidia at different temperatures in the light and in the dark on Cellophane. The percentage differentiation of appressoria in the light was significantly greater than in the dark over the 15-30°C temperature range ($P < 0.05$). Thus the promotive effect of light on appressorium differentiation was independent of temperature. At 30°C, far fewer appressoria were formed in both treatments (Fig. 13).

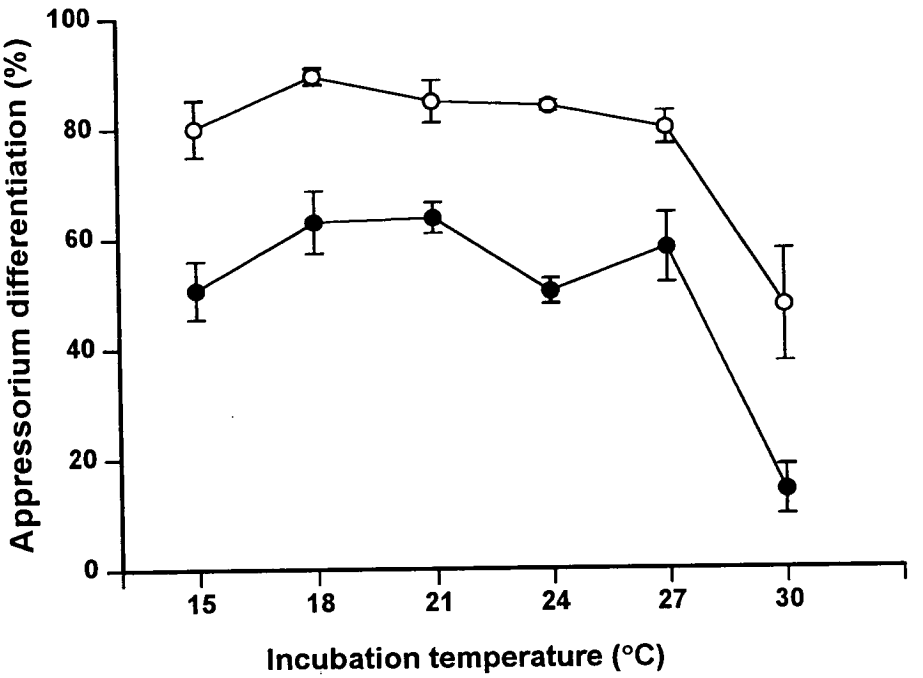

Fig. 13. Differentiation of *M. grisea* on Cellophane at different temperatures after 24 h in the light (O) and in the dark (●). Bars represent SEMs.

4.3 Discussion

The data presented here indicate that the pre-penetration phase of infection by *M. grisea* involves a programme of growth and differentiation triggered at spore germination and regulated by multiple signals from the host and surrounding environment.

4.3.1 Role of contact sensing

Surface contact was found to be essential for appressorium induction but not conidium germination. It is well established that contact of a germ tube with a solid surface is an essential prerequisite for appressorium formation in many plant pathogens (Emmett & Parbery, 1975; Hoch & Staples, 1991; Read *et al.*, 1992a). The present study does not support the conclusions of Lee & Dean (1993a) who reported for *M. grisea* that contact with a surface induces conidium germination whilst a high surface hydrophobicity, as found on a rice leaf, induces appressorium formation. These authors did show that appressoria differentiated readily on substrata with a high hydrophobicity (wax paper, polystyrene and polyester) but not on glass and agarose which were more hydrophilic. In contrast to these findings, Xiao *et al.* (1994a,b) reported that *M. grisea* forms appressoria readily on hydrophilic and hydrophobic surfaces and concluded that surface contact *per se* was triggering appressorium formation. Additionally, *M. grisea* has been shown to form appressoria on hydrophilic substrata such as Cellophane (Hashioka, 1972; Araki & Miyagi, 1977; Uchiyama *et al.*, 1979; Hirooka *et al.*, 1982; Bourett & Howard, 1990; Xiao *et al.*, 1994a) and glass (Uchiyama *et al.*, 1979; Yaegashi *et al.*, 1987; Uchiyama & Okuyama, 1990; Xiao *et al.*, 1994a), and the results presented here confirm this.

There is an interesting discrepancy in the literature regarding appressorium formation on glass. Although, as indicated, a number of works have shown that appressoria of *M. grisea* can develop on this substratum, other workers have reported that they do not (Hamer *et al.*, 1988, 1989; Howard *et al.*, 1991a; Lee & Dean, 1993). The reason for this inconsistency is not clear but may be attributable to differences in the type of glass used, strain variation or instability of certain genes involved in appressorium formation. In relation to the latter point, of possible significance is that *M. grisea* is highly mutable at

certain genetic loci (Valent & Chumley 1991). One such locus is *SMO* (*s*pore *mo*rphology) and Hamer *et al.* (1989) found that *Smo*$^-$ mutants, in contrast to the wild type from which they were isolated, formed significant numbers of appressoria on glass.

The ability of germ tubes to differentiate into appressoria may be related to how they adhere to their substratum - an important aspect of plant-pathogen interactions about which little is known (Nicholson & Epstein, 1991). Xiao *et al.* (1994b) found evidence that glycoproteins contained in an extracellular sheath around the germ tube are mediating contact sensing in *M. grisea.* It has been also suggested that a hydrophobin-like protein produced by the *MPG1* gene may be important for appressorial adhesion through hydrophobic interactions with the rice leaf (Talbot *et al.*, 1993). However, it seems unlikely that such a mechanism is involved in the adhesion of appressoria to Cellophane considering the latter's hydrophilic nature.

Evidence was found for germ tubes, but not conidia, exhibiting contact sensing. Firstly, a solid surface was required for germ tubes to differentiate. Secondly, a high substratum hydrophobicity (of Teflon or rice leaves) resulted in shorter differentiated germ tubes than on more hydrophilic substrata (glass and Cellophane). This may be a result of earlier differentiation, or alternatively slower growth, on the hydrophobic substrata. However, it should be noted that the conidia used in the present analysis lacked spore tip mucilage (Hamer *et al.*, 1988) and it is conceivable that this may play a role in conidial contact sensing. This aspect needs to be addressed in a future study.

4.3.2 Role of light

There is a dearth of knowledge on the significance of light in regulating the pre-penetration phase of plant pathogens (Emmett & Parbery, 1975). The data presented here show that on rice leaves and Cellophane the lengths of differentiated germ tubes were, on average, shorter in the light than in the dark. A possible explanation of this phenomenon is that light stimulates germ tubes to differentiate earlier after germination than in the dark, but this needs to be confirmed by further analysis. On all substrata, germinated conidia incubated in the light consistently produced more appressoria than those kept in the dark.

The mechanistic basis of how light is perceived by germ tubes is unknown. However, it was interesting to note that the lengths of differentiated germ tubes, but not the number of appressoria formed, were significantly influenced by the intensity of light. Thus the effect on the length of differentiated germ tubes was a graded response to the intensity of light whilst increased appressorium numbers were not. This distinction suggests that these two responses involve different signal transduction pathways.

Increasing light levels usually are associated with higher temperatures in those parts of the world where rice blast is endemic. The data here demonstrated that temperatures above 30°C reduced appressorium formation. Conidia of *M. grisea* are dispersed mainly at night (Ou, 1985). Since it takes several hours after spore deposition for appressoria to be initiated, this process will sometimes occur in early daylight as temperatures start to rise. The advanced formation of appressoria at this time before temperatures rise too high may be a distinct advantage for *M. grisea*, particularly since appressoria can endure more adverse conditions than germ tubes (Emmett & Parbery, 1975).

4.3.3 Role of nutrients

Starvation has been implicated as a signal influencing appressorium formation in *M. grisea* (Talbot *et al.*, 1993). The present study is the first time that the effects of nutrients on differentiation of germ tubes in *M. grisea* have been studied in detail. Glucose, but none of the other nutrients tested, was found to increase the number of longer differentiated germ tubes in the dark. This probably indicates that appressorium differentiation was delayed, suggesting that exhaustion of internal stores of glucose (e.g. from glycogen hydrolysis) might play a role in signalling appressorium formation. Interestingly, this effect was not observed in the light, indicating that light can override this effect. No specific effect of any other sugar on appressorium formation was found. The other notable finding was that incubation with a complete nutrient medium inhibited appressorium formation in the dark but not in the light. None of the treatments increased the numbers of appressoria formed. These results are substantially different from those obtained by Kaminskyj & Day (1984) who showed that simple sugars and complete media induced infection structure formation in

several rust species. However, their findings and the results presented here indicate that the germ tube is able to respond to external nutrients. Howard (1994) reported that in the presence of exogenous nutrients a single conidium will commonly give rise to many germ tubes from one conidial cell in *M. grisea*. This is a significant deviation from the germination pattern observed under conditions without nutrients. To respond to nutrients by increasing the number of germ tubes per conidium, and at the same time inhibiting differentiation, is a useful adaptation to environmental changes. The main reason for a hemibiotrophic fungus to penetrate into the host tissue from the nutrient-deprived leaf surface is to acquire nutrients from the host. If nutrients are present before penetration, no energy has to be wasted in breaching the host surface. Accordingly, a lack of nutrients (e.g. glucose) could be a signal for appressorium induction. In support of this is the finding that RNA transcripts of the *MPG1* gene, which is differentially expressed at a high level during appressorium formation, are also elevated in cultures starved of a carbon or nitrogen source (Talbot *et al.*, 1993). Furthermore, cAMP, which is elevated in response to starvation in some eukaryotes (e.g. in *Dictyostelium*, Gerisch, 1987), also seems to be involved in appressorium induction in *M. grisea* (Lee & Dean, 1993).

None of the single nutrients applied to germ tubes mimicked the dramatic inhibitory effects of the complete medium on appressorium formation in the dark. This suggests that either a combination of nutrients or an unidentified factor in the complete medium is responsible for this effect. Light served partially to overcome this inhibitory effect. This result indicates that light and certain nutrients, or other factors in the complete medium, interact through a common signalling pathway.

4.3.4 Role of external pH

Spore germination was found to be mainly unaffected by the external pH. The formation of appressoria was favoured at low pH values (pH 4.0-5.0). A preference to form appressoria in an acidic environment has also been reported for *Colletotrichum capsici* and *Uromyces appendiculatus* (Muruganandam *et al.*, 1991; Stumpf *et al.*, 1991). The interpretation of these results is difficult due to the possible effect of counter-ions used to adjust the buffer pH. Furthermore, the low number of appressoria formed in the present

study indicates that the buffer used had toxic effects. Therefore, the results presented here need to be compared with results from experiments using different buffers. Despite the apparent inhibitory effect of the buffer used, the ability of *M. grisea* to form appressoria over such a large pH range (pH 3.0-8.0) seems remarkable. How far the external pH actually affects intracellular pH is reported and discussed in the next chapter.

4.3.5 A 'conducive environment' is required for appressorium initiation

Signalling during the pre-penetration phase of infection by *M. grisea* inevitably involves an extremely complex network of interactions rather than independent, linear pathways of signalling events. Visualising appressorium initiation in *M. grisea* as being controlled by just one or even a few external factors is probably too simplistic. Instead, a network of external and internal signals may exert control, but each component of the network to varying extents (e.g. see: Kacser & Porteous 1987; Trewavas 1987). Appressorium initiation might be achieved in a variety of ways depending on the precise mixture and balance of signals and signal-transduction elements present. Emmett & Parbery (1975) concluded that few plant pathogens require specific external stimuli for appressorium induction but instead, need a *conducive environment* for the process to take place. The presented results suggest that what comprises a conducive environment may vary depending on the signalling capabilities of the germ tube and the environmental factors prevalent.

The germ tube seems to act as a specialised 'sense organ' which grows out from the conidium. So which environmental signals, influencing its differentiation into an appressorium, does it sense? The evidence presented here shows that surface contact, surface hydrophobicity, light, light intensity, nutrients, temperature and to a lesser extent pH are all important. However, other factors are also influential, including water and signals derived from the host. Free water is required for conidium germination and a high relative humidity is essential for infection (Ou, 1985). Host-derived signals must also be important because the results presented here show that consistently higher numbers of appressoria were formed on rice leaves than on any of the artificial substrata used in this study. Rice leaves consistently provided the most conducive environment for appressorium formation under the

different illumination conditions employed. Whether these host-derived signals are chemicals or physical attributes (e.g. microstructure) of the leaf surface, is not clear.

Of signals identified as playing a role in regulating the pre-penetration phase, we can distinguish between those that are essential and those which are not. The essential factors (e.g. surface contact and a high relative humidity) seemed to be passive in effect rather than providing active stimulation of appressorium formation. The passive role of surface contact is indicated by the observation that germ tubes did not differentiate immediately on making contact with a surface but grew to different lengths before forming appressoria. Other factors (e.g. light and the precise physical and chemical make-up of the contact surface) may not be indispensable but can play important roles as *modulatory signals* providing the conducive environment necessary for appressorium initiation. It is possible that all of these external signals act in concert to make the germ tube competent to respond to an, as yet unidentified, internal signal (see next section).

Although most fungal leaf pathogens, like *M. grisea*, do not seem to rely on specific external signals for appressorium formation (Emmett & Parbery, 1975), some clearly do so. In this respect, rusts deserve special mention. A number of rusts respond to well-defined topographical features as primary signals of appressorium induction (Allen *et al.*, 1991a; Hoch & Staples 1991; Read *et al.* 1992a). For example, > 90% of germ tubes of the bean rust (*U. appendiculatus*) grown on artificial substrata are optimally induced to differentiate appressoria over steps with a height of 0.5 μm (Hoch *et al.*, 1987; Allen *et al.*, 1991a). This topographical signal was closely correlated with the guard cell lip (or ledge) of the host plant *Phaseolus vulgaris* (Hoch *et al.*, 1987; Allen *et al.*, 1991b; Terhune *et al.*, 1991). Rusts have evolved this type of sensing process in order to locate precisely appressoria over stomata through which they penetrate. *M. grisea* and many other leaf pathogens, however, have no requirement for such a mechanism because they penetrate directly through the leaf cuticle and thus do not need to form appressoria at specific locations on the leaf surface. However, the direct penetrating *Colletotrichum spp.* which infect tomato, avocado and banana seem to rely on a specific external signal to synchronise appressorium formation with fruit ripening (Flaishman & Kolattukudy, 1994). Spores of these fungi remain dormant until the respective fruit ripens and releases ethylene, a plant hormone involved in fruit ripening. Ethylene then induces germination and appressorium formation. This signal

enables the fungus to invade the host during the most susceptible phase of fruit development.

4.3.6 Induction of conidium germination and appressorium differentiation

The work presented here shows that the pre-penetration phase of *M. grisea* involves a defined programme of cell lineage to which the fungus becomes committed at conidium germination. A similar conclusion was reached by Howard *et al.* (1991b) who described this succession of growth and developmental events as comprising together a *morphogenetic unit*. What triggers germination is not known precisely. However, since percentage germination was > 92% in the light and in the dark on all substrata and in liquid suspension, this indicates that water is probably important because it was a common, external factor in all these experiments. However, whether spore hydration provides a primary stimulus for germination, or whether water allows the release from spores of a germination self-inhibitor (Macko, 1981), remains to be determined.

As indicated earlier, no evidence was found for an external inductive signal for appressorium differentiation. This suggests that appressorium initiation is dependent on intracellular signalling. Since the whole of the pre-penetration phase can occur in water, devoid of external nutrients, starvation may provide this stimulus.

It is clear from the present study that the different artificial substrata did not completely mimic results obtained on the more conducive environment of rice leaves. This indicates a shortcoming of solely using *in vitro* systems to analyse experimentally the pre-infection phase in *M. grisea*, and probably other pathogens as well. It emphasises the need to perform experiments in parallel on the natural host substratum.

5. CYTOSOLIC pH OF GERM TUBES DURING GROWTH AND DIFFERENTIATION

5.1 INTRODUCTION

In this chapter, confocal ratio imaging has been used to analyse cytosolic pH (pH_c) in germ tubes of *M. grisea* during growth and appressorium formation *in vitro*. Additionally, the influence of external pH and nutrients on pH_c were assessed. Much of the work described involved a critical assessment of dual emission confocal ratio imaging of the pH-sensitive dye 5(6)-carboxyseminaphthorhodafluor-1 (SNARF-1) as a tool to study pH_c in living cells.

The role of ion gradients, especially H^+ gradients, in tip-growing cells is not well understood (see section 2.5.4). Proton gradients have been imaged in living cells and their presence correlated with tip growth but their relationship with cell polarity is still unclear (Turian *et al.*, 1985; Roncal *et al.*, 1993; Gibbon & Kropf, 1994). The present study is the first in which pH_c has been imaged in germ tubes of a fungal plant pathogen during the pre-penetration phase. This phase in the infection cycle of a plant pathogen involves repeated switches between polar and non-polar growth patterns (see section 2.2) and therefore offers an interesting system in which to study the relationship between pH_c and fungal morphogenesis.

Confocal ratio imaging was chosen as the best technique to obtain measurements of pH_c because of the high spatial and temporal resolution which can be achieved in living cells (see Chapter 2, Table 3). However, the ion imaging and quantitation using fluorescence dyes is fraught with potential problems including those arising from:

(a) dye cytotoxicity;
(b) autofluorescence, background fluorescence and stray light;
(c) dye photobleaching and irradiation damage;
(d) dye sequestration into organelles and leakage from cells;
(e) uneven dye distribution within the cells;
(f) optical and image processing artefacts; and
(g) calibration of the dye signal.

Fluorescent dyes have been used in numerous studies to quantify intracellular pH in yeast cells (e.g. Slavik, 1982; Slavik & Kotyk, 1984; Eraso *et al.*, 1987; Haworth *et al.*, 1991; Haworth & Fliegel, 1993) and filamentous fungi (Turian *et al.*, 1985; Davies *et al.*, 1990; Roncal *et al.*, 1993; Slayman *et al.*, 1994). However, in none of these studies were the necessary precautions taken, or the critical controls performed, to account for ***all*** the aforementioned problems. The present study has attempted to address the significance of all of these problems in the interpretation of pH_c measurements made in *M. grisea*.

5.2 RESULTS

5.2.1 Dye loading and imaging

The following requirements had to be fulfilled to allow satisfactory imaging of pH_c in ***living*** germ tubes:

(a) the method of dye-loading, concentration of dye and length of dye loading had to perturb as little as possible conidium germination, germ tube growth and appressorium formation;
(b) the dye had to be predominantly localised within the cytosol;
(c) the dye concentration had to be sufficient to provide a strong enough signal intensity for imaging and pH quantification;
(d) the dye introduced into the cytosol had to exhibit a significant shift in its emission spectrum; and
(e) the conditions used for imaging (e.g. laser intensity) had to have insignificant effects on germination, growth and development.

5.2.1.1. Dye loading

To load conidia and germ tubes with the pH-sensitive fluorescent dye SNARF-1, the cells were incubated in the non-fluorescent esterified form of the dye. In this state the dye molecule is non-polar and therefore able to permeate through the plasma membrane. Once in the cytosol, non-specific esterases remove the ester residues from the dye molecule. In this way, the dye molecule becomes pH-sensitive and fluorescent. Additionally, the dye molecule becomes charged, membrane impermeant and, in theory, it remains within the cytosol. In principle this loading method should be preferable to any other presently available method (e.g. microinjection, iontophoretic injection, electroporation) because it should cause less damage to the cell and because it is easy to perform.

Cytotoxicity. A common problem with the use of many fluorescent probes is their cytotoxicity. Cytotoxicity will depend on the concentration of the probe employed, the duration of its application and its interaction with cellular constituents. To investigate potential deleterious effects of SNARF-1, three different approaches were used:

(1) microscopic examination of loaded cells;
(2) quantification of germination and appressorium formation after dye loading;
(3) measurement of growth rates of loaded cells under imaging conditions.

Germ tubes loaded with 2-50 μM SNARF-1 did not reveal any signs of plasmolysis, increased vacuolation or abnormal swelling of the germ tubes, which were observed to be typical stress responses.

Loading 50 μM SNARF-1 (20 times the concentration used in subsequent experiments) for 15 min did not affect germination and appressorium formation significantly ($P < 0.01$) (Fig. 14). Longer loading times reduced the number of appressoria formed compared with numbers obtained from unloaded cells. However, in subsequent experiments loading times of < 10 min were used because they were found to be sufficient for pH_c imaging and quantification.

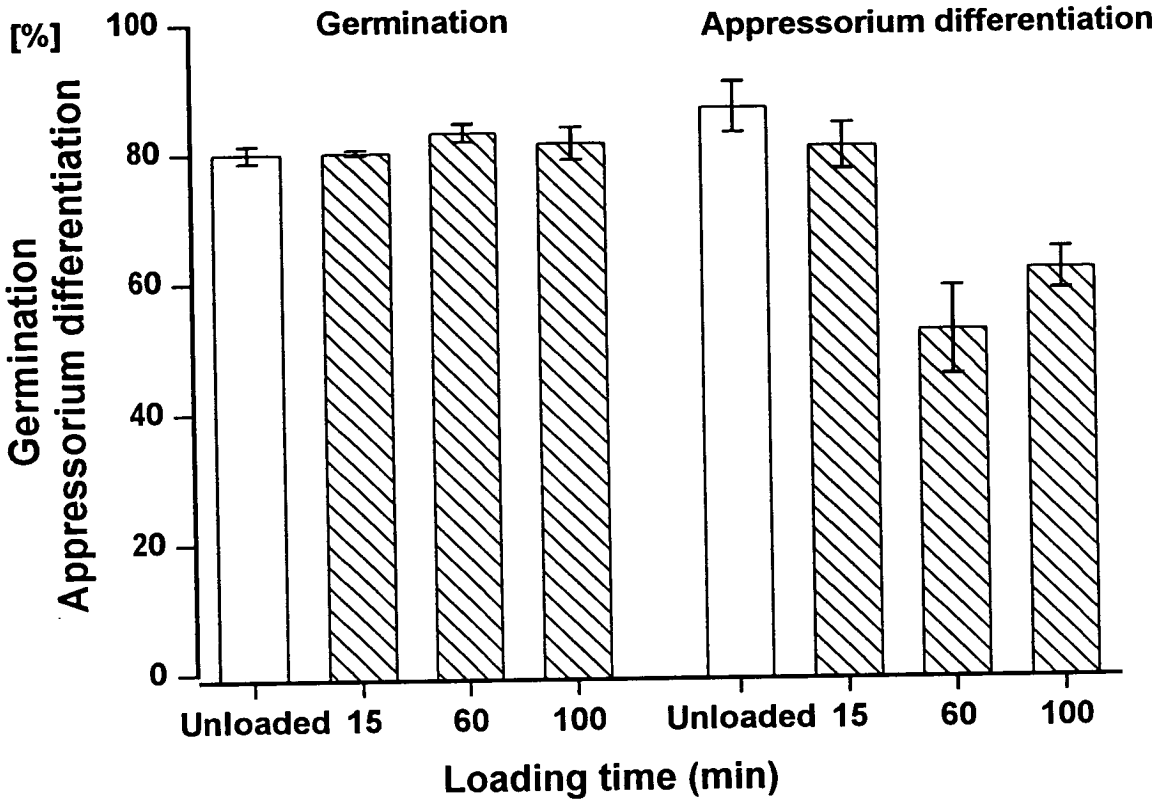

Fig. 14. Percentage germination and appressorium formation of *M. grisea* conidia loaded with 50 μM SNARF-1 for various periods of time. Data obtained after 24 h incubation on Cellophane. Bars represent SEMs.

When germlings were incubated in 2.5 μM SNARF-1 (the concentration used for all subsequent experiments) the growth rates of both loaded and unloaded germ tubes were found to be the same (0.37 $\mu m \cdot min^{-1}$, see section 5.2.1.2) and thus unaffected by introduction of the dye.

Dye sequestration and leakage. Some fluorescent dyes can be sequestered by cell organelles other than those of interest or, alternatively, can leak out of cells (Oparka & Read, 1994). In both cases the dye signal will become weaker, or even lost altogether, from the

cell compartment under study. Sequestration of the dye into the wrong compartment may also mask the dye fluorescence of interest. Recent work has highlighted the problems of dye sequestration and leakage in filamentous fungi (Read *et al.*, 1992b; Knight *et al.*, 1993; Slayman *et al.*, 1994). Esterified dyes, in particular, seem to be prone to sequestration since partial hydrolysis of the dye in the cytosol allows further passage of the dye into organelles (Slayman *et al.*, 1994). In yeast this seems to be less of a problem as it has been found that SNARF-1 is clearly excluded from the vacuole and has a long half-life (> 1.5 h) in the cytosol (Haworth *et al.*, 1991).

Careful microscopic examination of germinated conidia and germ tubes was performed to determine the extent of visible organelles such as vacuoles. Using differential interference contrast (DIC) light microscopy, no conspicuous organelles were observed in germ tubes. Germinated conidia, however, were significantly vacuolated in each of the three cells (Fig. 15).

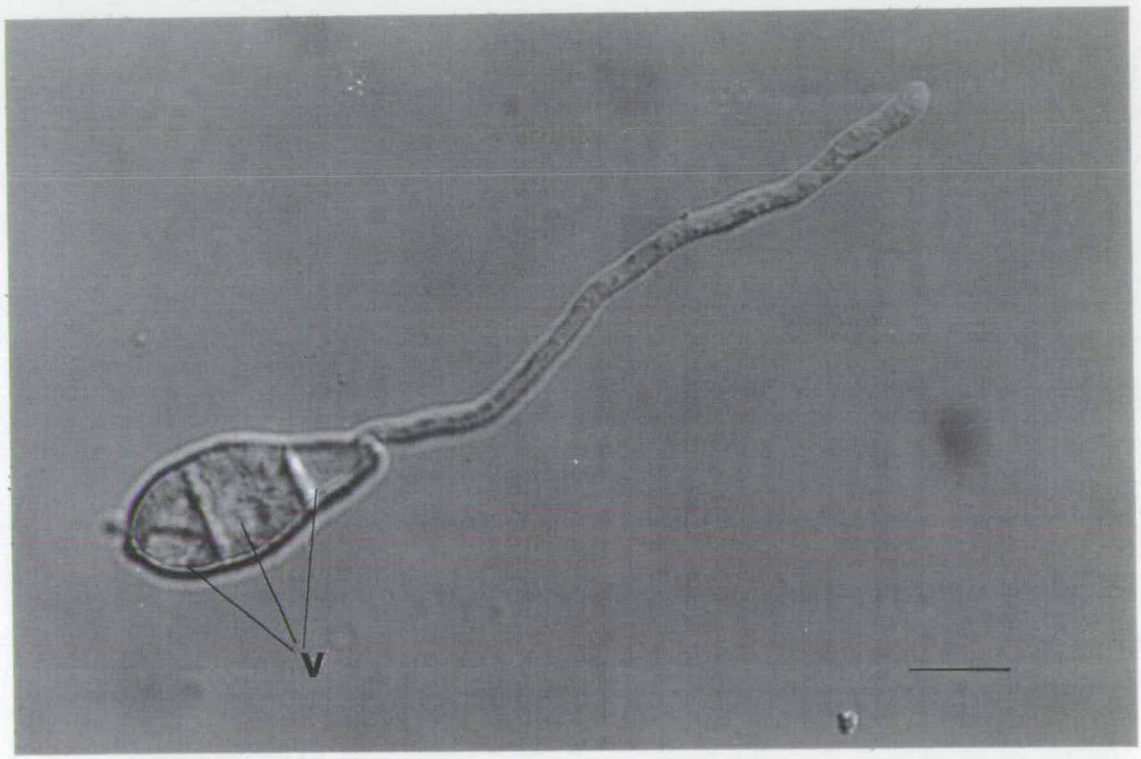

Fig. 15. Differential interference light micrograph of a conidium and germ tube of *M. grisea* 6 h after hydration. Note the large vacuoles (v) in each of the conidial cells. Bar represents 10 μm.

A more sensitive technique than DIC microscopy is to use the fluorescence dye carboxyfluorescein-diacetate to localise the vacuolar system in fungi (Rees *et al.*, 1994; Oparka & Read, 1994). Pronounced dye fluorescence, clearly indicative of a vacuolar system, was mainly localised 30 μm back from the germ tube tip although a low uniform background fluorescence was observed throughout the germ tube. Significant fluorescence was evident in the vacuoles of the germinated conidium (Fig. 16).

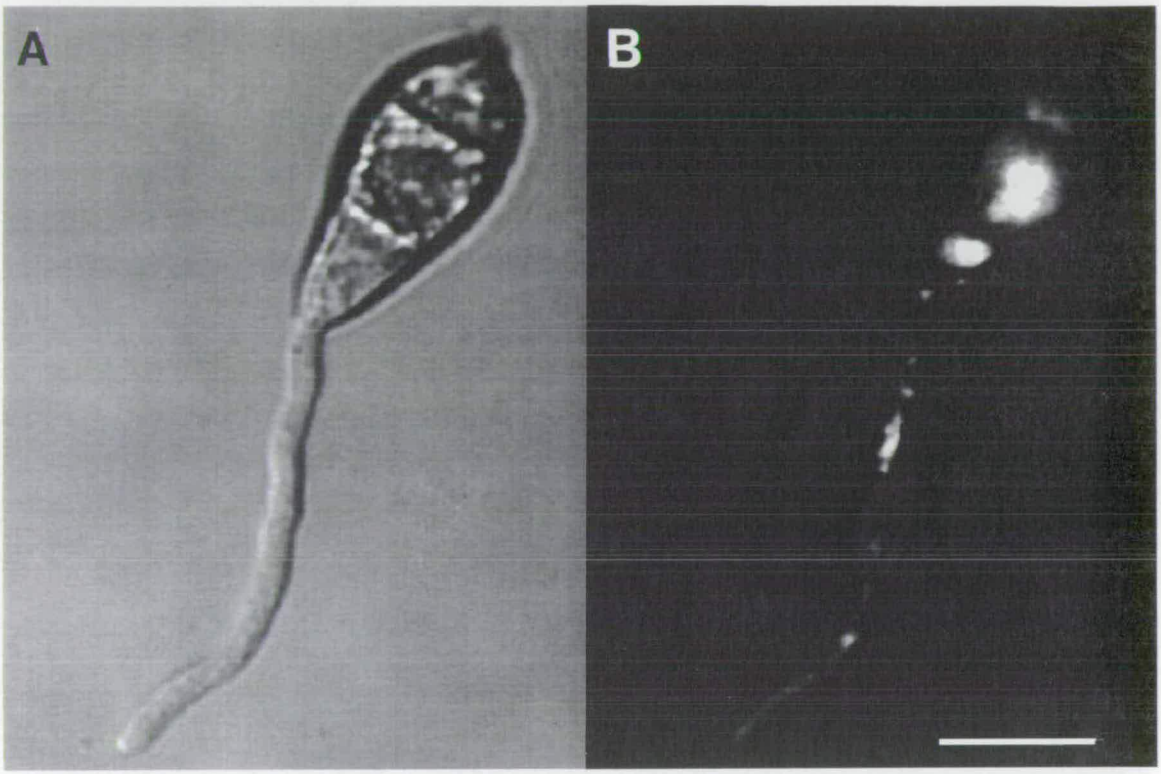

Fig. 16. Carboxyfluorescein-loaded conidium and germ tube of *M. grisea* 6 h after hydration. **A**. Brightfield laser scanned image. **B**. Simultaneously acquired confocal fluorescence image. Note that the 20-30 μm long apical region directly behind the germ tube tip is not intensely fluorescent indicating that it does not contain large vacuole compartments. Bar represents 10 μm.

Dye leakage from loaded germ tubes was not directly observed and any problem arising from dye sequestration or leakage was minimised by the immediate analysis of the cell under investigation within 15 min of the end of dye loading.

5.2.1.2 Imaging

Autofluorescence, background fluorescence, and stray light. A common problem in fluorescence microscopy is masking of the dye signal by autofluorescence, background fluorescence, or stray light. Autofluorescence may result from the biological specimen itself, or various other sources such as glass slides, coverslips or immersion oils (Oparka & Read, 1994). To determine whether these other sources of light would present problems, unloaded sporelings were examined at the wavelengths (580 nm and 640 nm) used to image SNARF-1 emission. With the parameters used for confocal ratio imaging (see Table 12, this section), no light other than from the dye was detected. This was partially due to the confocal imaging of optical sections which are free of out-of-focus light, much of which can be from autofluorescence, background fluorescence or stray light (Webb *et al.*, 1990; Sandison & Webb, 1994).

Dye photobleaching and irradiation damage. A further problem in fluorescence microscopy is the fading of fluorochromes during illumination. This photobleaching is mainly due to photochemical reactions induced by the excitation light (Oparka & Read, 1994). To account for this effect, all experiments were performed in a semi-dark laboratory environment. The excitation light was reduced to the minimum level, which still produced sufficient fluorescence intensity for ratio analysis (see below and Table 12, this section). The time the cell was exposed to the excitation light was significantly reduced by setting up imaging parameters to be used on a nearby cell and then switching to the cell to be analysed. Focusing on the cell under investigation was done with the shortest possible dwell time of the laser (0.25 sec/frame at 128 lines/frame). For ratio imaging of pH_c, each cell was scanned no more than twice.

Uneven dye distribution. Uneven dye distribution in the cell compartment under investigation produces a more intense fluorescence signal from areas containing high amounts of dye compared with areas which contain low amounts of dye. Uneven dye distribution can be the result of regional differentiation within the compartment examined or due to a variation in dye concentration within the cytoplasm. The use of a dual emission

ratio dye, such as SNARF-1, greatly reduced any problem arising from uneven dye distribution because the ratio values, which can be calibrated as ion concentrations, are independent of the amount of dye measured as long as the dye signal is sufficiently strong (see below). Additionally, the use of a confocal microscope allowed the investigation of optical sections free of out-of-focus information from the rest of the cell under examination. It has been found that in order to obtain accurate ratio values representing different pH values, the signal at each of the two emission wavelengths detected must have a minimum pixel intensity of 50 (R.M. Parton, in preparation). The calculation of ratio values when the signal intensity at each wavelength, or at one of the wavelengths, is < 50 produces inaccurate ratios. This latter effect caused regions of low emission intensity (e.g. at the edges of cells, Fig. 17) to appear to have a different pH from regions of higher signal intensity. This *edge effect* required balancing measures which increased the signal intensity (e.g. use of higher dye concentration, higher excitation intensity, longer excitation periods and signal acquisition from thicker optical sections) against the harmful effects of these different parameters on cell function. The edge-effect artefact was further reduced by subtraction of pixels with low signal intensity from images before calculating ratio values. However, the edge effect could not be completely eliminated. Measures to increase signal intensity also increased harmful side effects to the cell. A further problem was that by increasing the signal intensity in regions of low signal intensity, the signal strength in other parts of the cell sometimes became saturated (i.e. had a pixel intensity of 255). This also produced erroneous ratio values.

A.

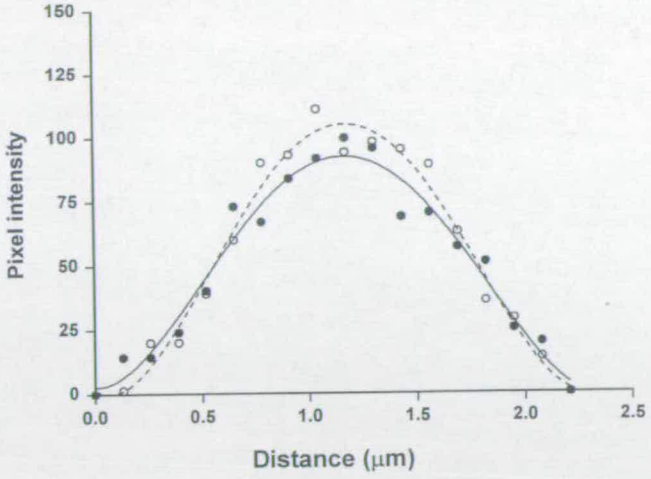

B.

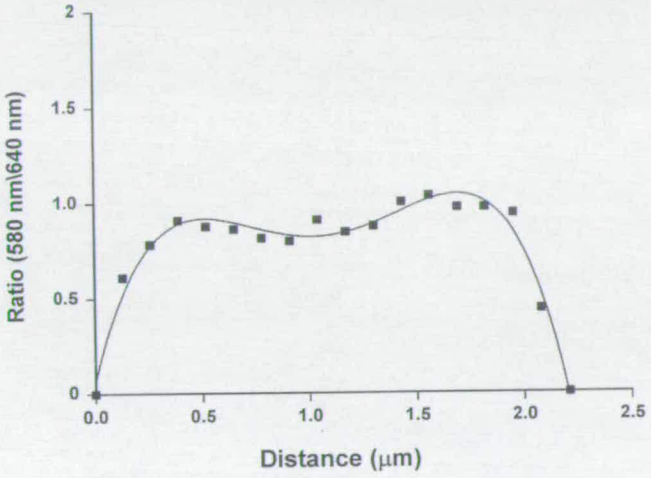

C.

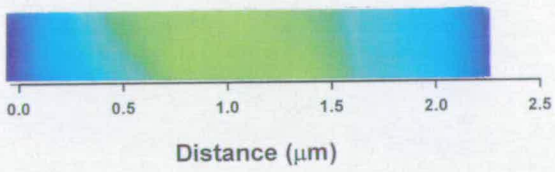

Fig. 17. Signal intensity across widths of SNARF-1 loaded germ tubes of *M. grisea* (n = 5). **A.** Intensity of dye fluorescence in both channels (○, channel 1, 640 nm; ●, channel 2, 580 nm). Pixel-by-pixel measurement. Results from individual germ tubes had to be modified to correct variations in germ tube width. **B.** Ratio values from processed image. **C.** Colour-coded ratio image of part of a SNARF-1 loaded germ tube of *M. grisea* showing the effects of low fluorescence on ratio values. The dark blue at the edges represents the lowest ratio values whilst green in the middle represents the highest ratio value.

Optimal imaging parameters. The conditions which were found to be optimal for ratio imaging of unperturbed, living cells of *M. grisea* are listed in Table 12.

Table 12. Conditions used for SNARF-1 ratio imaging of germ tubes of *M. grisea*

Dye concentration	2.5 μM
Loading time	10 min
Laser intensity	approximately 0.3 mW at 514 nm (neutral density filter 2)
Confocal aperture	33% opened (optical section ~ 2.5 μm)
Electronic signal amplification: Channel 1 (640 nm emission) Channel 2 (580 nm emission)	 low signal ON; gain 55% low signal ON; gain 64%
Scan speed	3 sec/image (512 lines)
Objective Electronic zoom Pixel size	x 40 plan apo, 0.95 numerical aperture x 4 116 x 116 nm
Image accumulation	2 times

The electronic amplification used to detect fluorescence was adjusted to give a similar intensity of the signal at the two wavelengths at around pH 7.0. This allowed for the highest sensitivity of the system in the pH_c range found under normal physiological conditions.

Germ tubes loaded with SNARF-1 and imaged, using the parameters given in Table 12, continued to grow and differentiate (Fig. 18). To evaluate the effect of these imaging conditions on the growth rates of germ tubes, loaded and imaged germ tubes were compared with unloaded germ tubes imaged with a laser intensity which was 3 times lower

(approximately 0.1 mW). The growth rate of unloaded and SNARF-1 loaded germ tubes in the first 6 h after hydration of the conidia was 0.37 μm $\cdot min^{-1}$ (SEM for unloaded cells: ± 0.11 μm $\cdot min^{-1}$; SEM for loaded cells 0.13 μm $\cdot min^{-1}$; n = 10). In addition, it was observed that cells which were brightly fluorescent tended to be more susceptible to growth inhibition after scanning with the laser beam than were less fluorescent cells. Therefore, dye concentration and laser intensity were chosen to give a sufficient fluorescence signal without deleterious effects on germ tube growth.

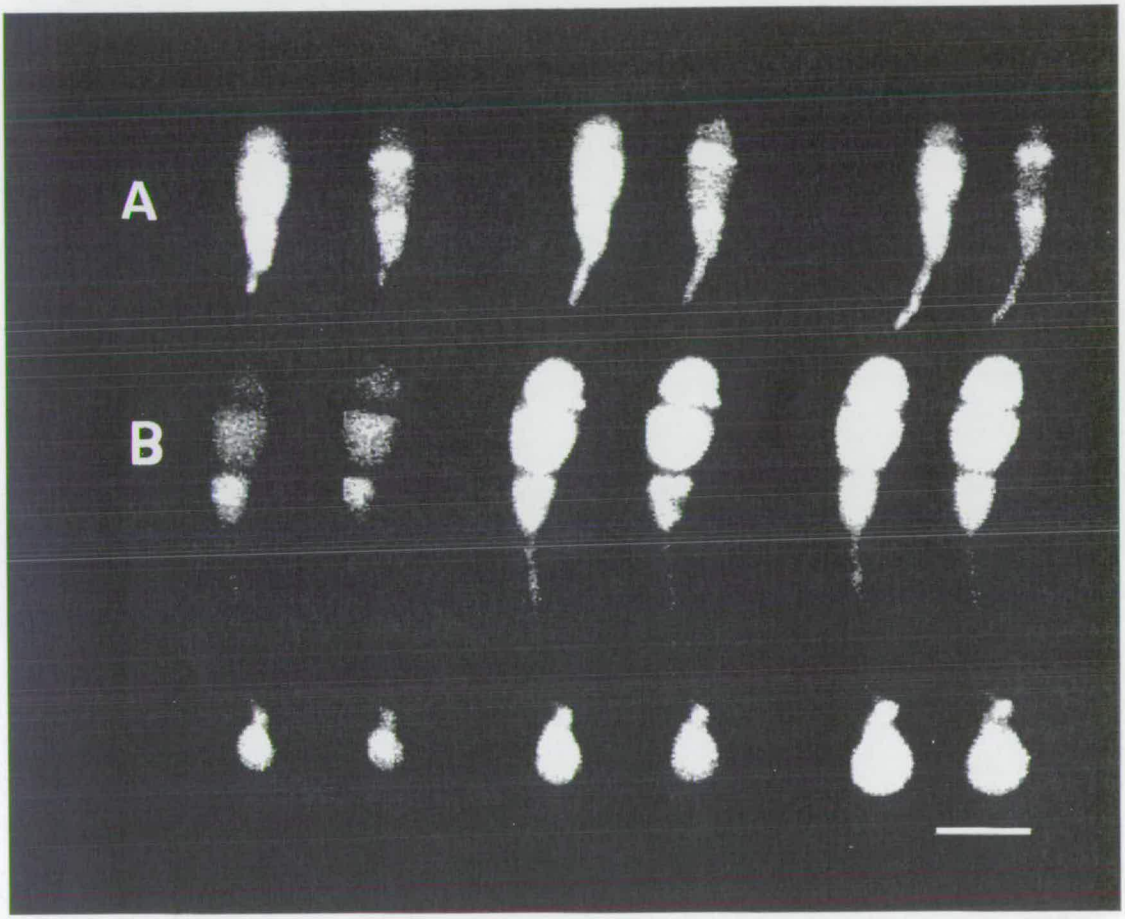

Fig. 18. Pairs of simultaneously acquired fluorescence images of two sporelings of *M. grisea* loaded with SNARF-1. Each pair of images represents fluorescence detected at 580 and 640 nm. **A**. Germinated conidium. **B**. Appressorium development. The pairs of images were taken in 15 min intervals 1 h (**A**) or 3.5 h (**B**) after conidium hydration. Bar represents 10 μm.

5.2.2 Imaging artefacts

Imaging artefacts can arise from the optical properties of the equipment and sample examined or from digital image processing. Three different imaging artefacts were identified as significant in the work described here.

Chromatic aberration. The differential refraction of light of different wavelengths (*chromatic aberration*) led to a misalignment of the two simultaneously acquired images at the two different emission wavelengths of SNARF-1 (580 nm and 640 nm). During the pixel-by-pixel calculation of the ratio values, the misalignment caused pixels from adjacent areas, rather than exactly the same area in the sample, to be ratioed. This artefact was particularly evident in regions close to the edges of cells and resulted in apparently lower ratio values because in one channel a pixel from outside the cell area was used in the calculation. Furthermore, misalignment of the signals from the two emission wavelengths was affected by adjustment of mirrors in the light path of the confocal microscope and this had to be regularly corrected. When misalignment occurred it was corrected before the calculation of the ratio values. The correction was made by moving of one of the two simultaneously acquired images by one pixel using the CoMOS *move* command until the two images were in perfect register (Fig. 19).

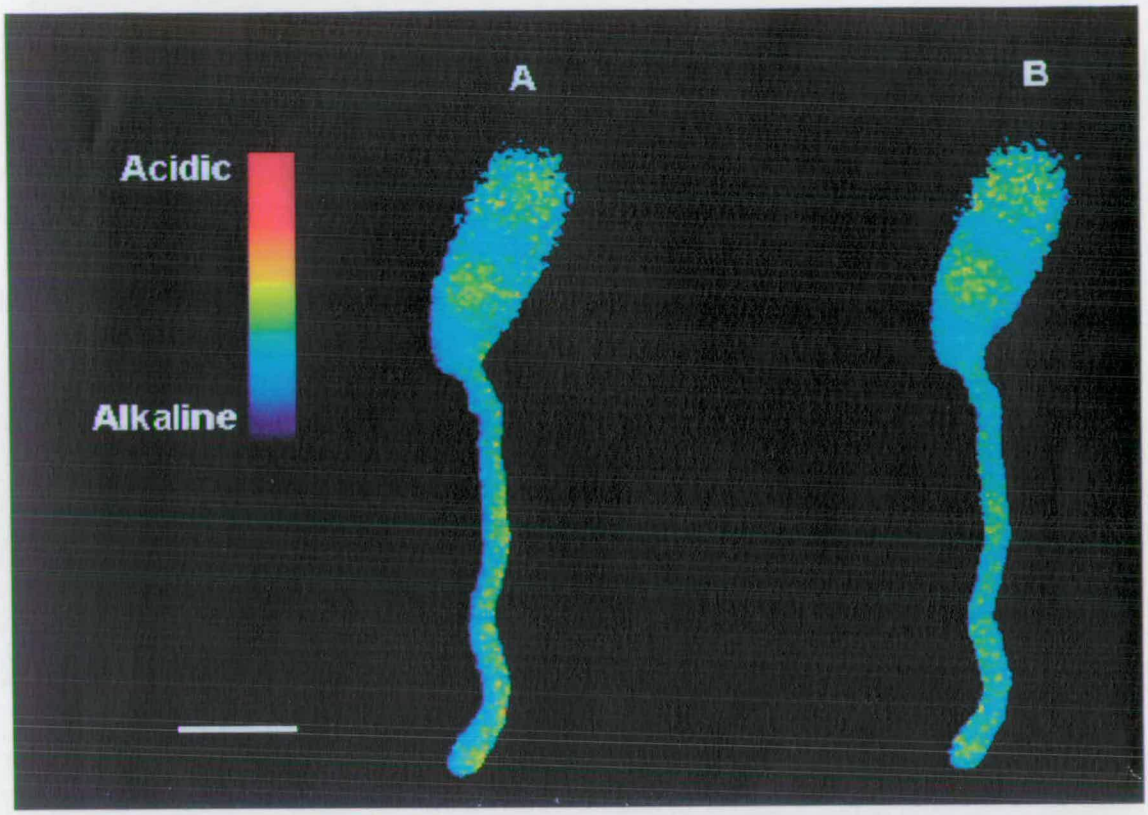

Fig. 19. Pseudocoloured ratio image of a germinated conidium of *M. grisea* loaded with SNARF-1. **A**. Ratio image obtained from misaligned fluorescence images. **B**. Ratio image obtained after correction of the misalignment of the fluorescence images. Bar represents 10 μm.

Signal attenuation. The optical properties of the germ tube caused differential signal attenuation at each wavelength which resulted in a change in ratio values as one focused through the z-axis of a cell. Light detected from optical sections close to the objective gave lower ratio values than light from sections further away. To test that this did not really represented a pH-gradient in the z-plane of a germ tube, the same germ tube was imaged right-side up and upside down. In either case the apparent gradient indicated a lower pH value for the plane closest to the objective (Fig. 20).

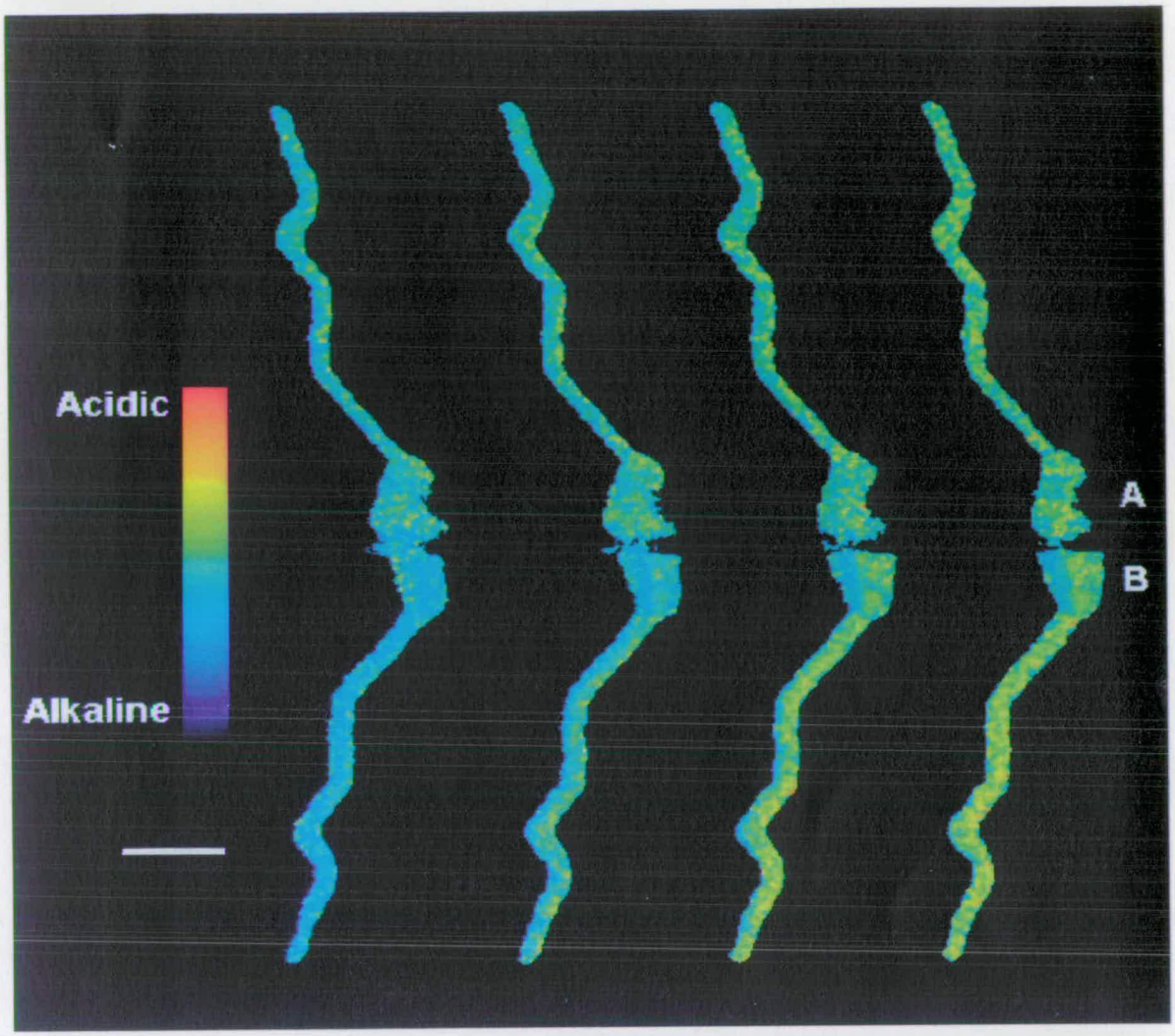

Fig. 20. Pseudocoloured ratio images indicating apparent pH_c of successive z-planes of a germinated conidium of *M. grisea* loaded with SNARF-1. Images showing, from left to right, subsequent overlapping focal planes in 0.3 μm intervals starting within the plane closest to the substratum. **A**. Specimen right-side up. **B**. Specimen upside down. Note in either case the apparent more alkaline pH_c in the optical sections closer to the substratum. Bar represents 10 μm.

To minimise the influence of signal attenuation in different images, all images were acquired from median focal planes of the germ tubes. Signal attenuation was therefore similar in all images and thus ratio values could be directly compared in different germ tubes.

Processing artefacts. Digital image enhancement caused an edge effect different from that previously mentioned (see section 5.2.1.2). This edge effect gave lower ratio values for pixels bordering the edge of the cell. A commonly used method for improving the appearance of images is to adjust pixel intensity in pixel arrays of variable size depending on the overall intensity of all pixels in the array. This process, called *median filtering* or *ranking*, transforms the individual intensities of pixels in a square of, for example, 3 x 3 pixels into the median value of all pixel intensities in this square. In cases where some of the pixels in this square are part of a region outside a cell, which can have a pixel intensity of zero, or close to zero, the median of the 3 x 3 pixels square can be considerably below the value calculated if none of those pixels outside the cell were included in the calculation (Fig. 21).

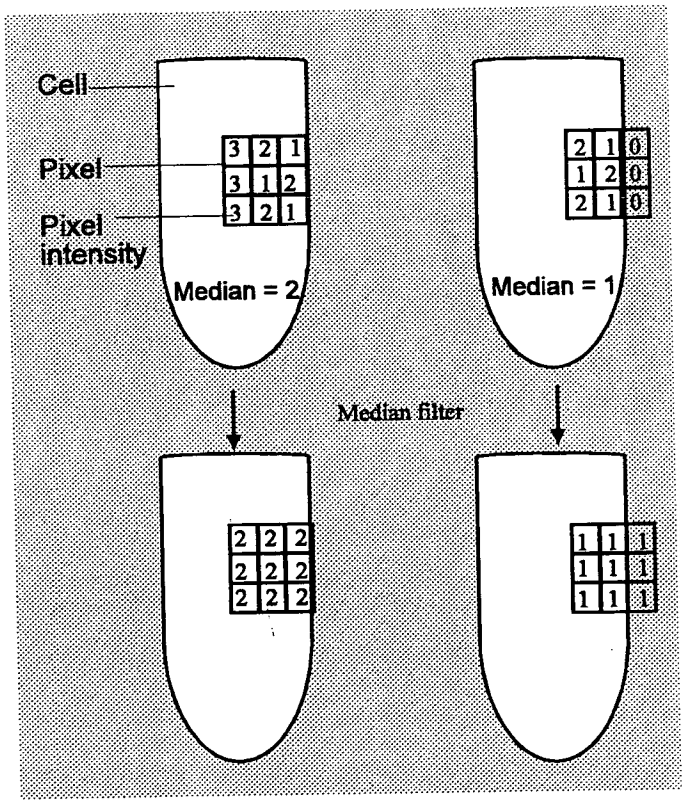

Fig. 21. Schematic representation of the effect of *median filtering* on the pixels close to the edge of a germ tube. Note that the pixel size, relative to the size of the germ tube, is significantly larger than normal.

Because of this effect, image enhancement by median filtering was kept to an absolute minimum and image areas affected by this edge effect were excluded from numerical quantifications. The significance of this imaging artefact was found to be much less than that caused by low signal intensities at the edge of cells.

5.2.3 Calibration of SNARF-1

A critical step in the use of SNARF-1 to precisely quantify pH_c is the calibration of the fluorescence signal in relation to different pH values. Four different calibration methods were used:

(1) *In vitro* (in buffer): the signal of the SNARF-1, either as its free acid or as a 70 kDa dextran conjugate, was measured in buffers with different pH values. Dextran-dye conjugates are commonly used to avoid dye sequestration within organelles (Gibbon & Kropf, 1994).

(2) *In vitro* (in pseudocytoplasmic buffer): the signal of the SNARF-1 free acid was measured in buffers with different pH values which mimicked the cytoplasm in their composition and viscosity.

(3) *In situ* (within dead cells): the fluorescence signal from cells loaded with the fluorescent dye was measured and the pH_c equilibrated with the pH of the external medium by using an ionophore (e.g. amphotericin). Treatment with ionophores usually causes cell death.

(4) *In vivo* (within living cells): the fluorescence signal from cells loaded with SNARF-1 was measured over a range of pH values, and the pH_c equilibrated with the external pH using a weak organic acid (e.g. propionic acid) and a weak base (e.g. ammonium hydroxide).

The pH range was between pH 6.0 and 8.0 for the comparison of the calibration methods and was well within the dynamic range of SNARF-1 (Haugland, 1992).

In vitro calibrations. For all methods used, the pH-dependent change in the fluorescence ratio of SNARF-1 was nearly linear between pH 6.5 and pH 7.5 (Fig. 22). The *in vitro* calibration curves for the SNARF-1 free acid in the pseudocytoplasmic buffer and in a simple MES-HEPES buffer, were very similar. The *in vitro* calibration of the 70 kDa SNARF-1 dextran conjugate showed that this dye exhibited a significantly smaller dynamic range of the ratio values, in response to changes in pH, than did the SNARF-1 free acid. Furthermore, the signal intensity of the SNARF-1 dextran was found to be 5 times lower than the intensity of the SNARF-1 free acid at equivalent dye concentrations (data not shown).

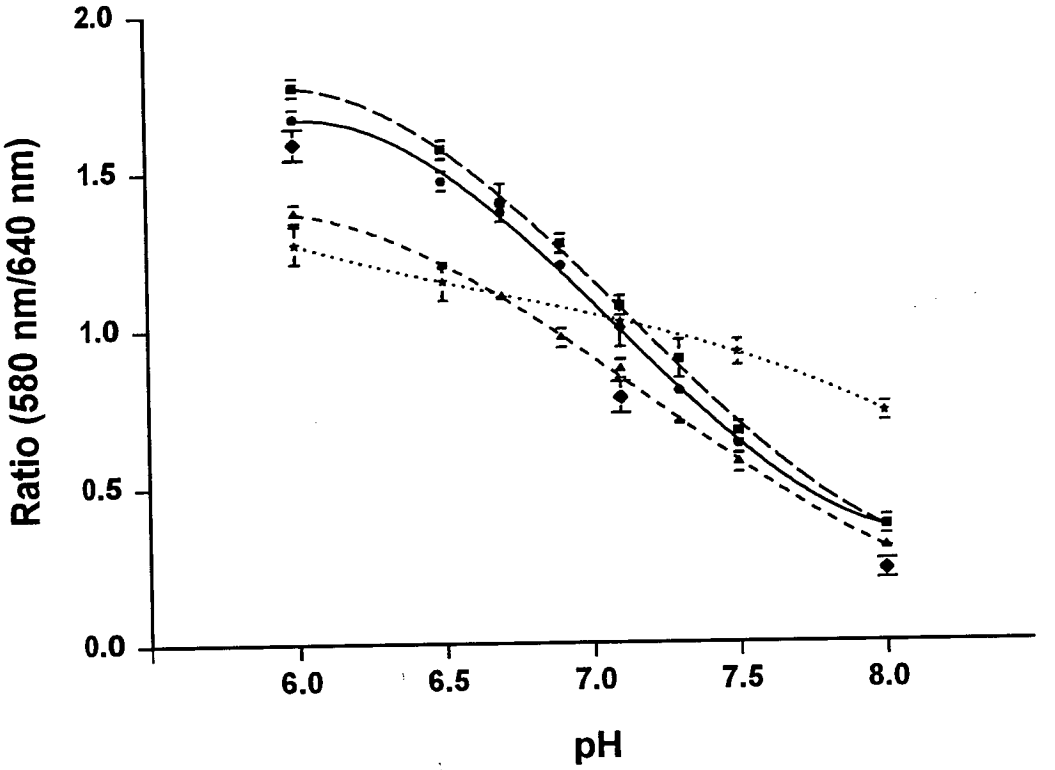

Fig. 22. Comparison of different calibration curves obtained from SNARF-1 and SNARF-1 dextran. ■ —— : *In vitro*, SNARF-1 free acid in pseudocytoplasmic buffer. ● ——: *In vitro*, SNARF-1 free acid, in simple buffer. ▲---- : *In vitro*, SNARF-1 dextran in simple buffer. ★..... : *In situ*, SNARF-1 AM in dead cells. ◆ : *In vivo*, SNARF-1 AM in live cells. Bars represent SEMs. (The measurements made to obtain the *in vitro* curves were done in collaboration with R.M. Parton.)

The calculation of the regression for the linear part of the calibration curve obtained with SNARF-1 free acid in simple buffer gave a slope of this part of the curve of -1.15 and an intersect with the x-axis at 8.24. Ratio values were therefore converted to pH values by using following equation:

$$pH = ratio \cdot (-1.15) + 8.24$$

The limits of precision for pH measurements under ideal conditions (as used to obtain the *in vitro* calibrations) were determined by electronic noise generated by the hardware used. The standard errors of measurements of the pixel intensity in individual ratio images, used to calculate the *in vitro* calibration curves, were well below 0.1 (number of pixels: 98304, measured in a 2530 μm^2 square sized area). The conversion of pixel intensities into ratio values (pixel intensities 1-255 converted into ratio values 1-4) gave a standard error of a ratio value for each ratio image of $<< 0.01$. The 99.9% confidence limits of the ratio value were $<< 0.03$. After conversion of the ratio value into pH values using the equation given above, this indicated a precision of $<< \pm 0.03$ pH units of the mean value for each ratio image obtained with the standard settings given in Table 12.

Table 13 shows a representative set of results from an *in vitro* calibration. Additional to the software-generated ratio values (produced from pixel-by-pixel division), ratio values based on division of the **average** intensities of the two simultaneously acquired fluorescence images, have also been added. This was done as an internal control to assess the effects (if any) of misalignment and image processing (see previous section).

Table 13. Representative results from one *in vitro* calibration experiment of SNARF-1 free acid. Ratio values were obtained in two different ways. For the results shown in column B the mean fluorescent intensities of the simultaneously acquired fluorescent images from column A were divided. For the results in column C the pixel intensities in the simultaneously acquired fluorescent images were divided on a pixel-by-pixel basis by the TCSM software and the mean ratios of the resulting images determined.

	A	B	C
pH	Mean intensity of fluorescence image (after background subtraction) Channel 1 / Channel 2 (SEM << 0.1)	Ratio calculated Channel 2 / Channel 1	Mean ratio from pixel-by-pixel calculated ratio image (SEM << 0.01)
6.0	22.0 / 48.6*	2.20	1.68
6.0	66.1 / 110.4	1.67	1.66
6.5	71.2 / 103.3	1.45	1.49
6.5	65.3 / 96.8	1.48	1.52
6.7	66.3 / 91.1	1.37	1.40
6.7	71.0 / 98.6	1.39	1.40
6.9	74.4 / 90.8	1.22	1.24
6.9	81.3 / 96.9	1.19	1.21
7.1	79.5 / 82.5	1.04	1.05
7.1	85.8 / 86.7	1.01	1.02
7.3	112.1 / 92.8	0.83	0.83
7.3	115.8 / 95.3	0.82	0.83
7.5	101.8 / 69.2	0.68	0.69
7.5	93.2 / 64.2	0.69	0.69
8.0	132.0 / 53.1	0.40	0.39
8.0	134.1 / 55.0	0.41	0.41

*: Data discarded since pixel intensity was below 50

In situ calibration. The antibiotic amphotericin was used to modify the pH_c. Amphotericin, a polyene type antibiotic, binds to sterol-type membrane components which are particularly prominent in fungal cells. It specifically promotes permeability of the plasma membrane for H^+ and K^+ ions (Bolard, 1986). When used at a concentration of 50 μM, germ tube growth was completely inhibited and did not recover after washing out the antibiotic (data not shown). The dynamic range of the pH dependent response of SNARF-1 between pH 6.0 and 8.0 was much smaller under these conditions than that obtained with any of the other calibration methods (see Fig. 22). Attempts were also made to equilibrate the intracellular and extracellular pH with the ionophores nigericin and valinomycin. Neither ionophore caused a measurable effect on pH_c in germ tubes at concentrations up to 50 μM for 60 min incubation periods, even when the two ionophores were combined.

In vivo calibration. Changing pH_c with either a weak acid (propionic acid) or a weak base (ammonium hydroxide) did not inhibited germ tube growth (data not shown) and thus this method can be regarded as a true *in vivo* calibration. The fluorescence ratios obtained with this approach gave a good agreement over the pH 6.0-8.0 range with the results obtained *in vitro* with SNARF-1 free acid (Fig. 22). In Fig. 23 pseudocoloured ratio images are shown, indicating pH_c of growing germ tubes of *M. grisea* loaded with SNARF-1 and incubated in either weak organic acids or bases at pH 6.0, 7.0 or 8.0.

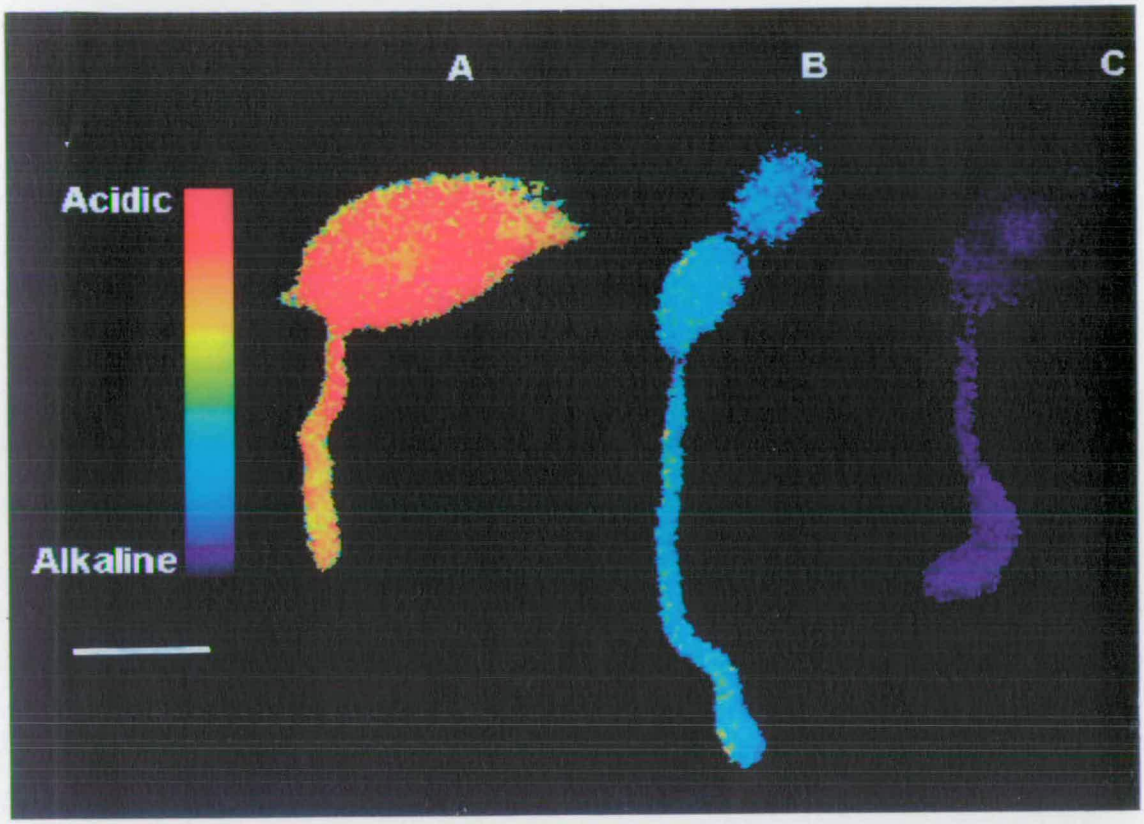

Fig. 23. Pseudocoloured ratio image indicating pH_c of growing germ tubes of *M. grisea* loaded with SNARF-1 incubated in either weak organic acids or bases at different pH values. **A.** Propionic acid, pH 6.0. **B.** Ammonium hydroxide, pH 7.0. **C.** Ammonium hydroxide, pH 8.0. Bar represents 10 μm.

For the interpretation of all subsequent experiments *in vitro* calibrations of the free acid in buffer were used in combination with *in vivo* calibrations to determine pH_c values because the two calibrations showed close agreement with each other (see Fig. 22). It should be noted, however, that the precision of pH_c measurements obtained *in vivo* was lower than the precision achieved for *in vitro* measurements. This lower precision for *in vivo* measurements was due to the smaller size of the measurable area within germ tubes; this gave a smaller number of pixels averaged for the mean ratio value of an individual image. However, the 99.9% confidence limit for *in vivo* measurements was in all cases $< \pm 0.06$ pH units.

5.2.4 Cytosolic pH in germ tubes during the pre-penetration phase

Cytosolic pH was initially investigated and quantified in 1.5-4 h old growing germ tubes with a maximal length of approximately 80 µm. The measurements were performed on the first apical 20-30 µm of the growing germ tube. Measurements in more distal regions were more difficult due to bends in the germ tubes and to the presence of the vacuolar system (Fig. 16).

When germ tubes were grown on glass in double-distilled water, the average ratio value of the SNARF-1 fluorescence in growing germ tubes was found to be 0.89 ± 0.01 (SEM) (n = 13). On the basis of the *in vitro* calibration (see previous section), this ratio value indicated a mean cytosolic pH value of 7.22 (Fig. 24). The lowest mean cytosolic pH measured for an individual growing germ tube was pH 7.09; the most alkaline mean pH_c for a growing germ tube was pH 7.28.

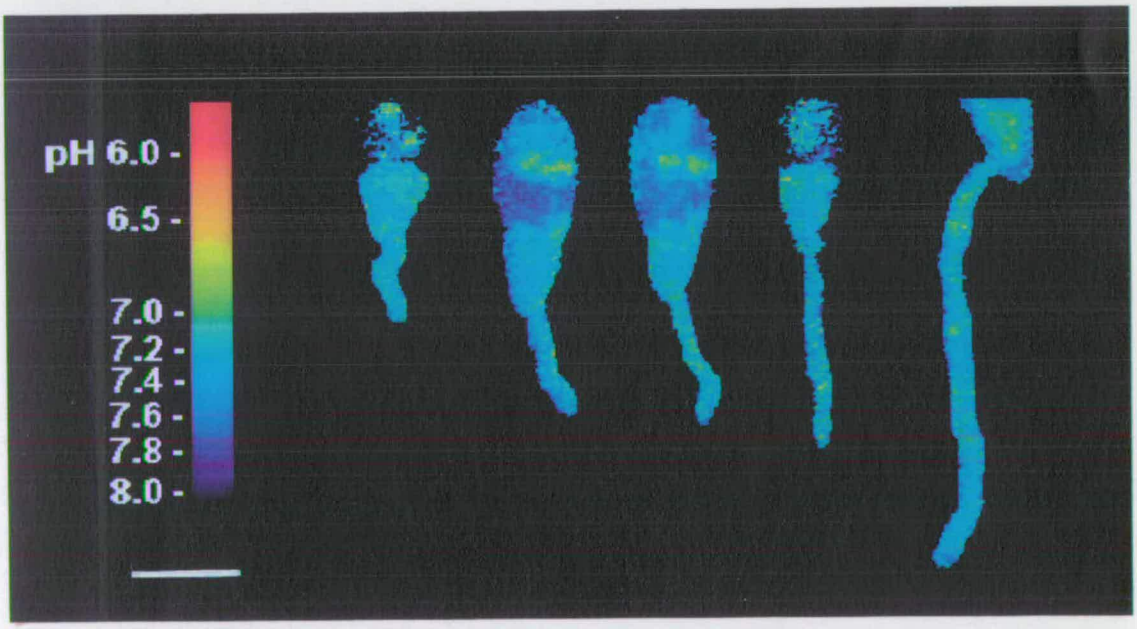

Fig. 24. Pseudocoloured ratio image indicating pH_c of growing germ tubes of *M. grisea* loaded with SNARF-1. Bar represents 10 µm.

When germ tubes were grown on glass and incubated in a complete nutrient medium, the mean ratio value of the SNARF-1 fluorescence in growing germ tubes was found to be 0.84 ± 0.01 (SEM) (n = 10). This indicated a mean pH_c value of 7.27. The lowest mean pH_c found in any one of those germ tubes was 7.21; the highest mean pH_c of an individual germ tube was pH 7.34.

To analyse localised variation in pH_c within growing germ tubes, ratio values were measured at defined intervals along a one-pixel-wide mid-line through the first apical 30 µm of ratio images of these cells. The measurements of individual pixels along this mid-line gave ratio values between 1.08 and 0.56. This corresponded to pH_c values between 7.0 and 7.6 (Fig. 25A). However, much of this variation represented noise generated during the detection of low fluorescence from the germ tubes. By averaging pixel intensities in 2 x 2 µm squares along the lengths of these germ tubes, much of the noise was averaged out and ratio values were found to be between 0.78 ± 0.02 (SEM) and 0.87 ± 0.02 (SEM). This indicated pH_c values between pH 7.35 and pH 7.24 (Fig. 25B).

The influence of nutrient supply on localised differences in pH_c was tested by incubating germinating conidia in a complete nutrient source. The complete medium used had marked effects on germ tube growth and differentiation (see sections 4.2.2.2 and 4.2.3.2). Averaging pixel intensities in 2 x 2 µm squares along the lengths of growing germ tubes indicated mean ratio values varying between 0.77 ± 0.03 (SEM) and 0.85 ± 0.02 (SEM). This represented pH_c values between pH 7.35 and pH 7.26 (Fig. 25C).

These results strongly suggested that pronounced pH_c gradients were not present in germ tubes grown in either distilled water or nutrient medium.

A.

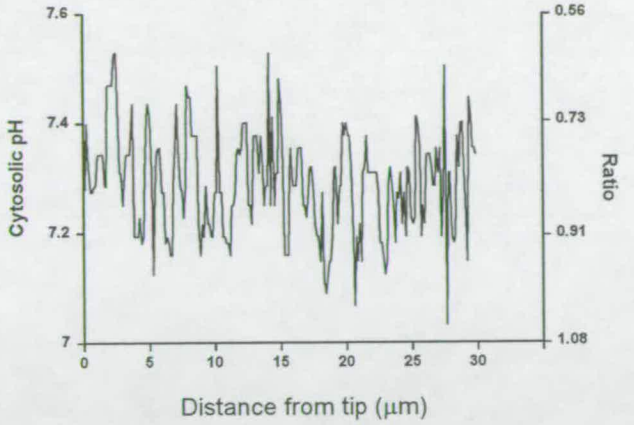

B.

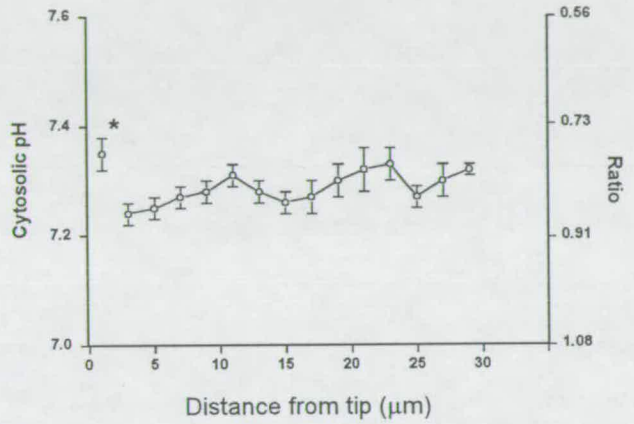

C.

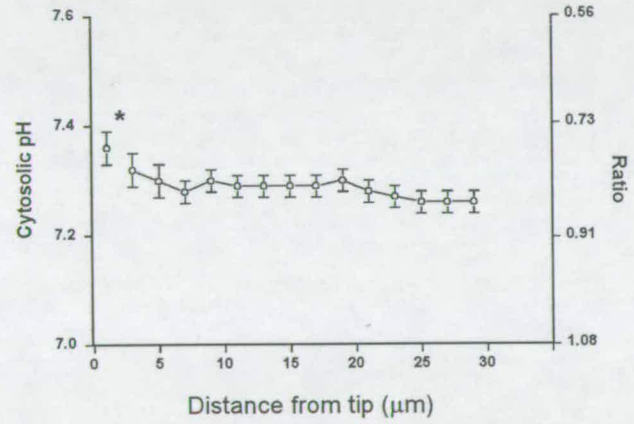

Fig. 25. Ratio values and corresponding pH_c values of growing germ tubes of *M. grisea* in successive regions behind the germ tube tip. **A.** Pixel-by-pixel measurements along a one-pixel-wide mid-line of an individual germ tube growing on glass in distilled water (pixel size 113 x 113 nm). **B.** Values of ratios and pH averaged over 2 x 2 μm squares along the lengths of germ tubes growing on glass in distilled water (n = 10) **C.** Values of ratios and pH averaged over 2 x 2 μm squares along the lengths of germ tubes growing on glass in complete nutrient medium (n = 10). The data set marked by * is based on weak fluorescence and thus erroneous but has been added for completeness (see following section). Bars represent SEMs.

In the first 2 µm of the germ tube apex the fluorescence signal detected at each emission wavelength was usually below the intensity of 50 which was found necessary for reliable ratiometric measurements (see section 5.2.1.2). The primary reason for this problem was the shape of the germ tube tip which caused less volume of cytosol to contribute to the voxel (3-dimensional pixel) in this region (Fig. 26).

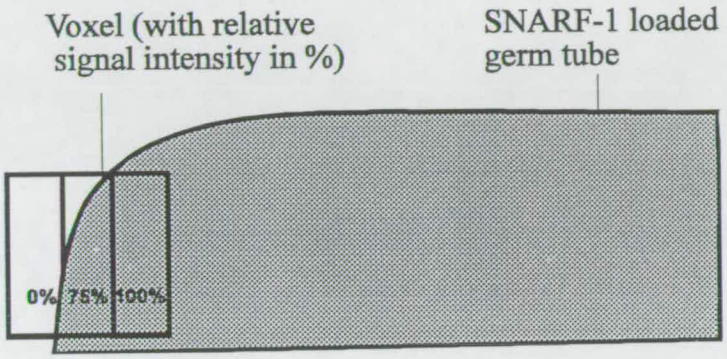

Fig. 26. Schematic representation of the influence of the germ tube shape on the signal intensity of dye detected from within the germ tube. A voxel represents the smallest 3-dimensional unit the hardware can resolve. Digitisation of the signal converts the information received from voxels into 2-dimensional pixels in the image.

Older germ tubes, which could be > 100 µm long, were imaged at lower magnification (using a x 20 objective instead of a x 40 objective) in order to visualise the entire length of a germ tube in one field of view. As before, this study was performed on germ tubes grown on glass for 24 h in either double-distilled water or in a complete nutrient medium. No pronounced gradients in pH_c along the full lengths of these germ tubes were observed (data not shown).

To investigate possible temporal changes in pH_c of living germ tubes following germination and up to and including the early stages of appressorium formation, SNARF-1 fluorescence ratio values were measured at specific developmental stages. Four distinct stages were chosen for closer investigation (Fig. 27). These were:

(A) germ tubes shortly after germination (3-5 μm in length; germ tubes shorter than this gave unreliable ratio values; see Figs. 25 and 26);

(B) germ tubes 6-80 μm in length;

(C) germ tubes which have swollen (early stage of appressorium formation before the septum is formed); and

(D) differentiated germ tubes (stage of appressorium formation after septum has formed).

Areas of the germ tubes in which the pH_c was investigated are indicated in Fig. 27.

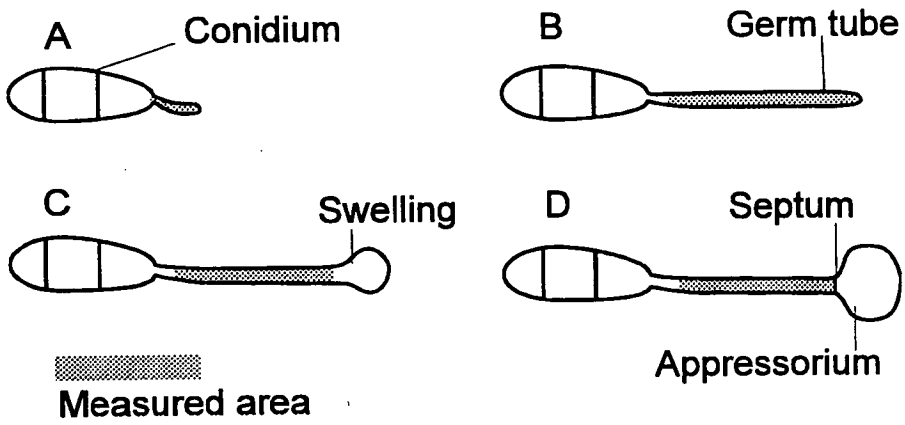

Fig. 27. Developmental stages of *M. grisea* during which pH_c in germ tubes was investigated. Shaded regions indicate areas on which the measurements were performed. **A.** Germ tubes shortly after germination. **B.** Germ tubes 6-80 μm in length. **C.** Germ tubes which have swollen (no septum has been formed). **D.** Differentiated germ tubes (after septum has formed).

The ratio values obtained for germ tubes at these developmental stages are summarised in Table 14. The ratio values ranged between 0.80 ± 0.01 (SEM) and 0.88 ± 0.02 (SEM) with no significant differences between the results. This equates to pH_c values between 7.32 and 7.23 (Fig. 28).

Table 14. Ratio values and corresponding pH values obtained from SNARF-1 loaded cytosol of *M. grisea* germ tubes at different developmental stages. Swollen and differentiated parts of the germ tubes were not included in the investigated area.

Developmental phase	Time after hydration (h)	Ratio values (± SEM)	Mean cytosolic pH	Number of measured individuals
Germ tubes 3-5 µm in length	0.5 - 1.5	0.80 ± 0.01	7.32	15
Germ tubes 6-80 µm in length	1.5 - 4.0	0.89 ± 0.01	7.22	12
Germ tubes swollen	4.0 - 6.0	0.84 ± 0.03	7.27	15
Differentiated germ tubes	6.0 - 9.0	0.85 ± 0.02	7.27	20

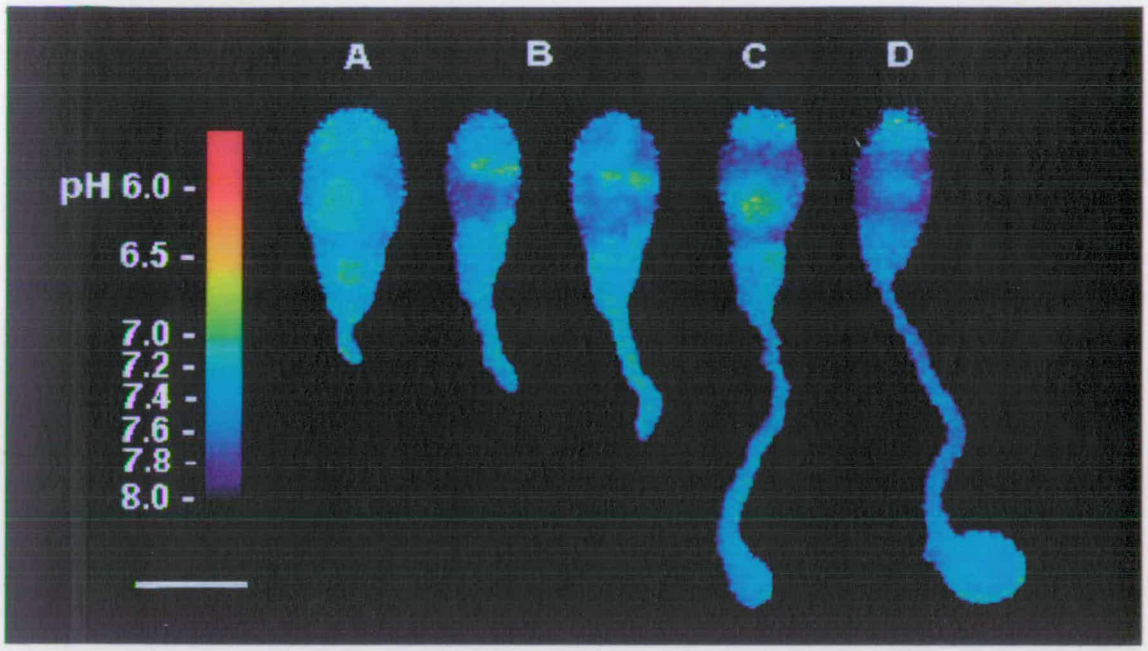

Fig. 28. Pseudocoloured ratio image indicating pH_c in sporelings of *M. grisea* at different developmental stages following loading with SNARF-1. **A**. Germinated conidium 1 h after hydration. **B**. Same growing germ tube at 3 h and 3.25 h after hydration. **C**. Swelling germ tube 5 h after hydration before a septum has formed between germ tube and appressorium. **D**. Differentiated germ tube 7 h after hydration after a septum has formed between germ tube and appressorium. Bar represents 10 μm.

Analysis of the swollen region of the germ tube before septum formation gave a mean ratio value of the SNARF-1 fluorescence of 0.85 ± 0.02 (SEM) indicating a mean pH_c value of 7.26 (n = 15). The lowest mean pH_c found in one of these swellings was 7.10, whilst the highest mean pH_c of an individual swelling was pH 7.43.

In the present study, the imaging parameters and calibrations had been carefully optimised for accurate ratio measurements of SNARF-1 fluorescence in growing germ tubes. Different parameters will have to be used to obtain similar measurements in appressoria and conidia because differences in their cell structure and the biochemical and biophysical properties of their cytosol will have a significant influence on the outcome (see sections 5.2.1-5.2.3). For this reason, a detailed and rigorous analysis of pH_c within these cells was not attempted.

5.2.5 Response of pH_c to external pH

To investigate the effects of changes in extracellular pH on the pH_c of germ tubes and thus internal pH homeostasis, 4-6 h old germlings were grown in 25 mM MES-HEPES buffer of different pH values.

To check for the viability of the germ tubes grown under the imaging conditions (Table 12), SNARF-1 loaded germ tubes were assessed for growth. Fig. 29 shows that germlings continued growth after double-distilled water was replaced with buffers of pH 6.0, 7.0 or pH 8.0.

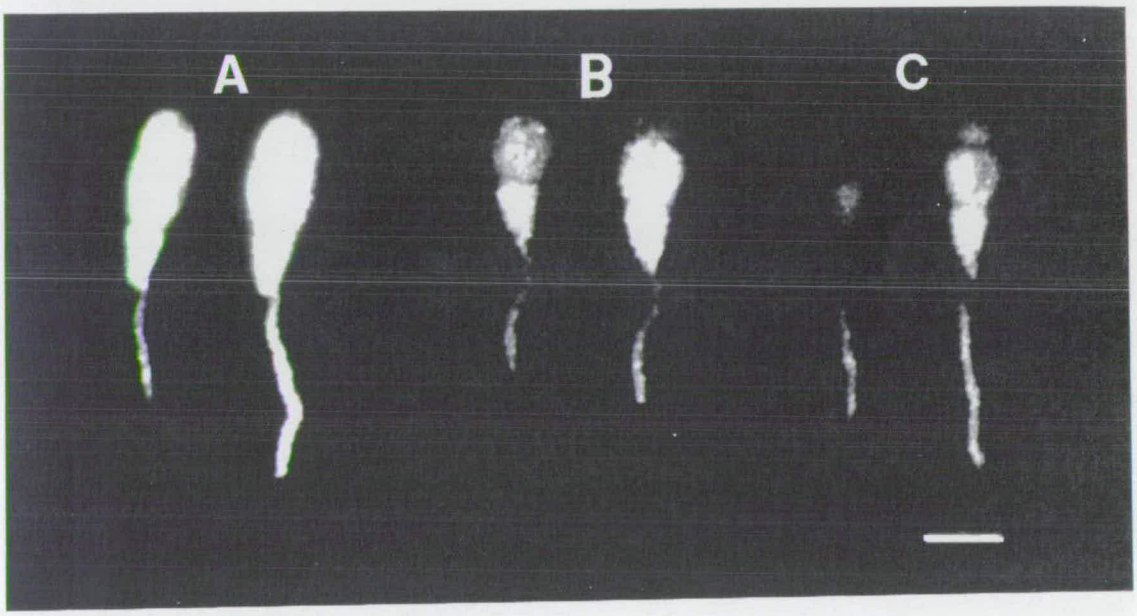

Fig. 29. Fluorescence images of growing germ tubes of *M. grisea* loaded with SNARF-1 and incubated in buffer of pH 6.0 (**A**), pH 7.0 (**B**) and pH 8.0 (**C**). Emission wavelength 640 nm. Time interval between two images of each germ tube was 15 min. Bar represents 10 μm.

When germ tubes were grown in buffer of slightly acidic (pH 6.0) or neutral pH (pH 7.0) the ratio of the fluorescence emission of SNARF-1 was 0.88 ± 0.02 (SEM) and 0.86 ± 0.01 (SEM), (n = 12). This represented a mean pH_c of pH 7.23 and 7.25, respectively. In slightly alkaline buffer (pH 8.0), the ratio of the emission signal was 0.80 ± 0.02 (SEM) indicating a mean cytosolic pH in growing germ tubes of 7.31 (n = 12) (Fig. 30). The results were subjected to an analysis of variance to detect significance of differences between the effects of the buffer treatments. The analysis showed a significant difference ($P < 0.01$) between the ratios obtained from germ tubes grown in acidic and neutral buffer when compared with the ratio values obtained from germ tubes grown in alkaline buffer.

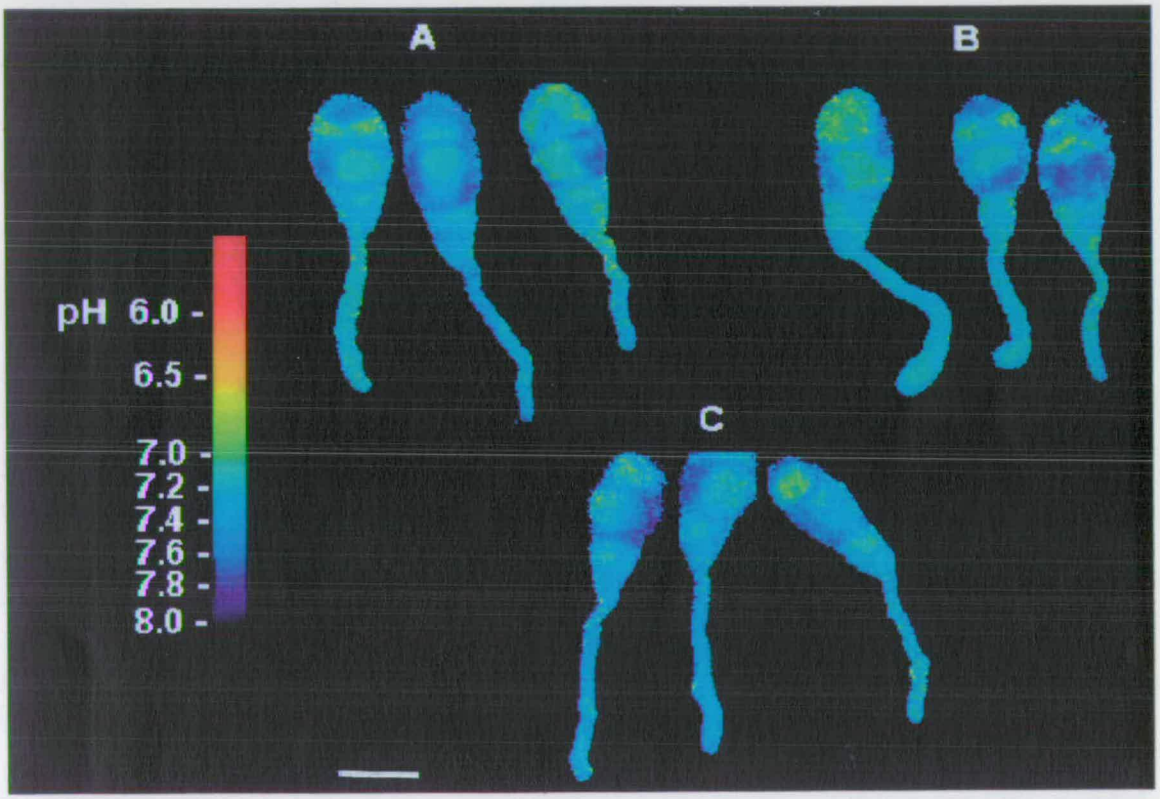

Fig. 30. Pseudocoloured ratio images indicating pH_c in growing germ tubes of *M. grisea* loaded with SNARF-1 and incubated in buffers of pH 6.0 (**A**), pH 7.0 (**B**), and pH 8.0 (**C**). Bar represents 10 μm.

To check whether a slow equilibration between external pH and pH_c occurred, some germlings were grown for > 1 h in the appropriate buffer. No change of the measured ratio values of the SNARF-1 emission was observed over this period (data not shown).

5.3 DISCUSSION

The results presented here have critically assessed and improved confocal ratio imaging of SNARF-1 as a high precision method for the spatial analysis and quantification of pH_c in living fungal cells. Employing this technology, the pH_c in germ tubes of *M. grisea* was found to be tightly regulated between pH 7.2 and pH 7.3 during germ tube growth and the induction of appressoria. Furthermore, the pH_c within germ tubes was largely independent of the presence of external nutrients or changes in extracellular pH. No pronounced pH gradients were observed in growing germ tubes.

5.3.1 Assessment of method of pH measurement

Dual emission confocal ratio imaging of the H^+-sensitive dye SNARF-1 can give high precision quantification, with a high spatial and temporal resolution, of the pH_c in living germ tubes. Under ideal conditions, as achieved with *in vitro* calibrations, this method could achieve a precision of ± 0.03 pH units. This is similar to the degree of precision obtained with methods involving weak acids and bases and pH-sensitive microelectrodes which have previously been used to measure pH_c in fungal cells (Table 3, section 2.5.3; Sanders & Slayman, 1982; Kaur & Mishra, 1994). All of these methods provide more precise measurements of pH_c than has been achieved with NMR of fungal cells (Stewart *et al.*, 1988). The measurement precision, however, was lower for *in vivo* measurements due to the fact that information from smaller areas was averaged and therefore random noise from the hardware had a proportionately greater influence on the measurements obtained. The measurement precision that can be achieved therefore depends on the size of the measured area, which in turn is dependent on the type of specimen analysed and the magnification used. The temporal resolution of simultaneous dual emission ratio imaging is only limited by the hardware used (laser scan speed and data saving time). For pH_c measurements, only microelectrodes can achieve a similar or greater temporal resolution. The spatial resolution of fluorescence imaging is far superior to any of the other methods employed for pH_c measurements and this is limited only by the optical properties of the microscope used and sample imaged.

Imaging artefacts were found to influence extensively the results if the necessary precautions were not taken. Imaging artefacts have been identified as a significant cause in the misinterpretation of results from ratiometric measurements (Silver *et al.*, 1992). However, in most studies involving ratio analysis of pH-sensitive fluorescence dyes (Roncal *et al.*, 1993; Gibbon & Kropf, 1994 and references given in Table 15) imaging artefacts have not been addressed in a satisfactory way. Recently Slayman *et al.* (1994) emphasised the problem of sequestration of esterified pH-indicator dyes, including SNARF-1, within organelles of *Neurospora* hyphae. They concluded that the interference between the fluorescence of organelle-sequestered dye with that of cytosolic-located dye can be greatly reduced by using confocal microscopy. Confocal microscopy, as has been used in the present study, allows the exclusion of out-of-focus signals from organelles above and below the optical section under investigation (Webb *et al.*, 1990; Sandison & Webb, 1994). Furthermore, Slayman *et al.* (1994) stressed the importance of correlative structural analysis of the cell under investigation to interpret the location of intracellular fluorescence from pH-sensitive dyes.

In the present study, the first 30 μm of the germ tube apex was found to be free of large organelles, notably parts of the vacuolar network, which might significantly influence the measurements of pH_c.

It was found essential to reduce image processing to a minimum because this could cause imaging artefacts. The use of a median filter on adjacent pixels led both to a loss of spatial resolution and to an edge effect where pixels from around a cell contributed to the pixel value attributed to areas inside the cell. The interpretation of ratio values obtained close to the edges of cells is additionally complicated by the weak fluorescence signal obtained from this region. The weak signal received from the cell periphery is usually due to the smaller volume of cytosol in this part of the cell and thus the smaller amount of dye available for measurements. The low signal and the effects of image processing make interpretation of the results obtained close to the cell periphery difficult. Roos (1992) reported an acidic layer of peripheral cytoplasm in protoplasts of *Gossypium hirsutum* and *Penicillium cyclopium.* No details of the image processing employed in Roos's study were given, so interpretation of the data is difficult, if not impossible. Roncal *et al.* (1993), using

fluorescence ratio imaging of fluorescein, observed a similar layer of apparently more acidic cytoplasm in hyphae of *P. cyclopium* but were aware of the problem of the low signal intensity, and thus inaccuracy of pH_c measurements, in this region of the cell.

The present study provides the first detailed comparison of different calibration methods for SNARF-1: *in vitro* (in buffer); *in vitro* (in pseudocytoplasmic buffer); *in situ* (in dead cells); and *in vivo* (in live cells). In Table 15 significant studies employing SNARF-1 for intracellular pH measurements are listed. In none of these studies has all four calibration methods been compared.

In the present study, marked differences were found between some of the calibration methods. Whereas the *in vivo* calibration was in good agreement with the *in vitro* calibrations using SNARF-1 free acid, results obtained *in situ*, and from SNARF-1 dextran *in vitro*, differed significantly from the other calibration methods. The reasons why results obtained *in vivo* by using weak acids/bases and *in situ* by using an antibiotic were different are not immediately clear. Discrepancies between results from *in vitro* calibrations of SNARF-1 and calibrations obtained intracellularly using ionophores have been reported before (Seksek *et al.*, 1991; Owen, 1992; Owen *et al.*, 1992; Opitz *et al.*, 1994). The observed shift in the pK_a of the fluorescent dye inside cells, compared with *in vitro*, was attributed to the binding of the probe to cellular proteins. The results presented here do not support those findings reporting discrepancies between *in vitro* and *in vivo* calibrations of SNARF-1. However, good agreement between *in vitro* and *in vivo* calibrations of SNARF-1 have been reported in studies on *Saccharomyces cerevisiae* (Haworth *et al.*, 1991; Haworth & Fliegel, 1993). In these analyses saponine, a glycoside, was used to equilibrate extracellular pH and pH_c. It may well be that the ionophores (some of which are proteins themselves) used in those studies reporting discrepancies between *in vitro* and *in vivo* calibrations of SNARF-1 (Seksek *et al.*, 1991; Owen, 1992; Owen *et al.*, 1992; Opitz *et al.*, 1994), interfered with the dye molecules rather than the cellular proteins, as suggested in these works. This potential problem of interactions between dye molecules and ionophores was avoided in the present study by the use of weak acids/bases to equilibrate the extracellular pH with the pH_c of living cells.

Table 15. Calibration methods used for SNARF-1 ratio imaging

Calibration method	Buffer or Ionophore	Cell type	Reference
in vitro (in buffer)	HEPES	N.A.	Opitz *et al.*, 1994
	MES + HEPES		Martinez-Zaguilan *et al.*, 1991
			Roos, 1992
	MES + HEPES + Bicine		Owen *et al.*, 1992
	Mops		Haworth *et al.*, 1991
	Phosphate buffered saline		Owen, 1992
	Ethanol/water		Owen *et al.*, 1992
in vitro (in pseudo-cytoplasmic buffer)	Sonicated cells	Hamster spleen	Owen, 1992
		Hamster ovary	Owen *et al.*, 1992
	Not specified	*Pelvetia* rhizoid	Gibbon & Kropf, 1994
in situ (in dead cells)	Nigericin	Human glioma	Opitz *et al.*, 1994
		Rat carotid body	Buckler & Vaughan-Jones, 1990
		Rabbit proximal tube	Dubbin *et al.*, 1993
		Rat muscle and glioma	Cody *et al.*, 1993
		Mouse fibroblasts	Martinez-Zaguilan *et al.*, 1991
in vivo (in live cells)	Nigericin/	Rat carotid body	Seksek *et al.*, 1991
	Valinomycin	Murine lymphocyte	Owen, 1992*
		Hamster spleen Hamster ovary	Owen *et al.*, 1992*
	Saponine	*S. cerevisiae*	Haworth *et al.*, 1991*

*: Cell viability not tested

5.3.2 Measurements of cytosolic pH in germ tubes

Cytosolic pH in germ tubes of *M. grisea* was shown to be tightly regulated between 7.2 and 7.3. This is in good agreement with measurements of pH_c in hyphae of other filamentous fungi (Sanders & Slayman, 1982; Davies *et al.* 1990; Roncal *et al.*, 1993; S. Fischer, personal communication). In the present study the pH_c of germ tubes was not found to be markedly influenced by variations in external pH between pH 6.0 and pH 8.0. This result, and the fact that conidium germination and germ tube growth were little affected by external pH in the range between pH 3.0 and pH 8.0 (see section 4), suggests that pH_c in conidia and germ tubes is well maintained. Sanders & Slayman (1982) reported similar results for *N. crassa* hyphae from measurements using pH-sensitive microelectrodes, and these have been confirmed recently by confocal ratio imaging of SNARF-1 in the same species (S. Fischer, personal communication). The data from Sanders & Slayman (1982), which included results obtained after inhibiting the plasma membrane H^+-ATPase, led them to discuss the possibility that the plasma membrane of *N. crassa* was less permeable for H^+ than previously thought. This would imply that no regulation of pH_c in response to changes in extracellular pH would be required. The present study does not provide any insight regarding the mechanisms involved in maintaining pH_c in *M. grisea*. This will require further experimentation, including perturbation of the plasma membrane H^+-ATPase and other proteins involved in fungal pH_c homeostasis (see section 2.5.2). Nevertheless, the ability to grow unaffected by external pH has adaptive value for any immotile organism which might need to survive and grow in a microenvironment markedly different in pH. However, deleterious effects of extreme external pH values on appressorium formation (see section 4.2.3.3) suggest that this differentiation process is more sensitive to changes in external pH than are conidium germination or germ tube growth.

Measurements of pH_c along the length of growing germ tubes did not reveal any marked gradients in pH. Pronounced pH_c gradients have also not been observed in vegetative hyphae of *N. crassa* ratio imaged in the same way as in the present study (S. Fischer, personal communication). These data suggest that prominent pH_c gradients are not important for tip growth in filamentous fungi as has been suggested for the polarised growth of *Pelvetia* rhizoids (Gibbon & Kropf, 1994).

No pronounced differences in pH_c during germ tube growth or early stages of appressorium differentiation were observed. In other filamentous fungi, a change in pH_c during distinct developmental phases has been reported. Turian (1983) showed a polarised acidification at germ tube outgrowth from spores of *Morchella* and conidia of *Neurospora* although in this study is was not clear that the cells were unperturbed by the loaded dye. Roncal *et al.* (1993) presented results indicating a role for changes in pH_c during conidiation of *Penicillium cyclopium*. In *Candida albicans*, a yeast which can switch from yeast-like to hyphal-like growth, pH_c changes have been clearly correlated with the outgrowth of germ tubes from yeast-like cells (Kaur *et al.*, 1988; Stewart *et al.*, 1988; Kaur & Mishra, 1994). Based on these results Gadd (1995) discusses the role of intracellular pH as a *second messenger* in the dimorphic regulation of this fungus. To establish the idea that protons act as intracellular signals in this process would, however, need more experimental support. One type of experiment which might contribute further evidence to support the signalling role of protons in the dimorphic switch could involve the use of photoactivated *caged* probes such as Diazo-3 (a form of caged protons). Diazo-3 can be introduced into a cell in various ways and protons can be released in response to illumination with UV-light. The initiation of a specific process due to the intracellular elevation in the concentration of a putative signal molecule provides good evidence for it having a role in signalling that process (Read *et al.*, 1993).

Most of the studies on the importance of protons in filamentous fungi have been on indirect measurements of external currents using the *vibrating probe* (Gow, 1989, 1995b). In recent years more evidence has accumulated which suggests that the inwardly directed H^+ currents reveal sites where H^+-driven nutrient transport is localised. This indicates that the measured H^+ current is mainly concerned with local nutrient uptake rather than having a primary function in tip growth (reviewed by Gow, 1995b). Considering that the germ tube and conidium of *M. grisea* are self-contained systems in which nutrients are probably in many cases exclusively supplied from stores within the conidium, the need for nutrient uptake by symport with protons may not arise and thus extracellular or intracellular H^+-gradients might not be generated. Results presented in sections 4.2.2.2 and 4.2.3.2, however, indicated that the supply of a rich external nutrient medium can influence the morphogenesis of the germ tube. The observed effects suggest that the germ tube is

competent to take up nutrients such as glucose. The measurements of pH_c in germ tubes incubated in complete medium did not reveal any gradient in the pH. Whether this finding indicates that nutrients are taken up in all parts of the germ tube rather than just in the tip region, or whether any gradients in pH_c, if they exist, are too small to be resolved by confocal ratio imaging, is not clear. Also, little is known about the buffering capacity of the cytosol in *M. grisea* germ tubes, which, if large enough, could prevent any build up of a pronounced pH_c gradient.

Most of the electrical currents associated with tip growth extend over more than 200 μm behind the hyphal tips of fungi (Gow, 1984; Kropf *et al.*, 1984; McGillviray & Gow, 1987; Takeuchi *et al.*, 1988). A pH_c gradient linked to this current might then be extended to stretch over a similar distance. Gow *et al.* (1984) reported a pH gradient in the external medium corresponding to the electrical current surrounding the hyphae of *Achlya bisexualis*. This external pH gradient was assumed to be generated by the spatially separated apical uptake and sub-apical release of protons over the apical 200 μm, or so, of the hypha. Germ tubes of *M. grisea* were shown to be usually between 1 and 100 μm long (see section 4.2.2.1). Gradients of pH_c, of the type which might possibly exist in *A. bisexualis*, may not be evident in the short germ tubes of *M. grisea*. However, recent studies have reported that pH_c gradients occur over the first 30 μm behind the tips of *Penicillium* hyphae (Roncal *et al.*, 1993) and *Pelvetia* rhizoids (Gibbon & Kropf, 1994).

In summary, the work in this chapter has shown that:

(a) no changes in $pH_c > 0.1$ pH unit are involved during germ tube growth and induction of appressoria in *M. grisea*;

(b) the pH_c is little affected by external factors such as pH or nutrients; and

(c) pronounced gradients in pH_c associated with tip growth and/or nutrient uptake are not evident.

6. SUMMARY

The objectives of the first part of this study were to investigate the influence of external factors on the pre-penetration phase of infection of *M. grisea*. Surface contact was found to be essential for appressorium induction but not conidium germination. Other factors such as light, surface properties, temperature and pH had modulatory influences on the pre-penetration events of infection. However, a high concentration of a complete nutrient source prevented differentiation in the dark but not in the light. Higher numbers of appressoria differentiated on rice leaves than on artificial substrata suggesting that the host provides additional factors, and thus a more conducive environment, for promoting appressorium formation. Overall, the results indicated that the pre-penetration phase of rice blast infection involves a programme of growth and differentiation triggered at conidium germination and regulated by multiple signals from the host and environment.

In the second part of this work confocal ratio imaging of the pH-sensitive dye 5(6)-carboxyseminaphthorhodafluor-1 (SNARF-1) has been shown to be a highly precise method for the analysis of cytosolic pH (pH_c) in growing germ tubes. However, it was found that considerable precautions have to be taken to avoid the numerous artefacts which can arise during dye loading, imaging, image processing and image analysis to obtain accurate imaging and quantitation of pH_c. Measurements of pH_c in growing germ tubes of *M. grisea* during germ tube growth and early differentiation showed it to be remarkably stable between pH 7.2 and pH 7.3 and no changes in $pH_c > 0.1$ pH unit during these processes were observed. Furthermore, the pH_c was little affected by external factors such as pH or nutrients, and pronounced gradients in pH_c associated with tip growth and/or nutrient uptake were not evident.

7. FUTURE WORK

7.1 THE ROLE OF EXTERNAL SIGNALS IN REGULATING THE PRE-PENETRATION PHASE OF INFECTION

(a) Conidium germination appears to initiate a programme of growth and differentiation which leads to the formation of infection structures (see section 4.3). The events involved in the induction of germination thus seem to be critical for this process to occur. Studies using inhibitors of intracellular signalling pathways (see section 2.4) could be useful to further understand the signalling processes involved.

(b) The importance of contact with a surface for appressorium formation (see section 4.2.3.1) suggests the involvement of mechanosensitive ion channels and/or transmembrane signalling by integrins (or integrin-like proteins) in the plasma membrane of the germ tube. Possible roles of these plasma membrane components could be initially investigated using suitable inhibitors (e.g. Gd^{3+} for stretch-activated channels and RGD peptides for integrins).

(c) The application of single, or combinations of, nutrients could reveal which component(s) of the complete nutrient medium, used in this study, fully inhibited appressorium formation in the dark (see section 4.2.3.2). This analysis might indicate which signalling processes are involved in preventing differentiation.

(d) The promotion of appressorium formation by light could be further investigated by producing an action spectrum of wavelengths which are effective in this process. This should give an indication of what type of photoreceptor mediates this response (e.g. blue light or red light receptor).

7.2 Role of cytosolic pH during the pre-penetration phase of infection

(a) Because of the novelty of dual emission ratio imaging of SNARF-1 to investigate pH_c in living cells, the results obtained here would benefit from being compared with results obtained using an independent method of pH_c measurement. However, the small size of *Magnaporthe* germ tubes does not allow the use of pH-sensitive microelectrodes for analysing pH_c in these cells, and other methods do not provide the necessary spatial resolution (see section 2.5.3). Therefore, larger hyphae of another fungus (e.g. *Neurospora crassa*) should be used to obtain these correlative measurements with pH-sensitive microelectrodes.

(b) Although the pH_c in germ tubes does not seem to change markedly during growth and appressorium induction, there may be important changes in pH_c during the complex differentiation events which follow (see Table 1, section 2.2) Therefore, confocal ratio imaging of SNARF-1 could be used to analyse pH_c during the formation of appressoria, infection pegs and infection hyphae which can all be studied *in vitro*.

(c) The role of the plasma membrane H^+-ATPase in the regulation of pH_c in *M. grisea* could be investigated by application of specific inhibitors of this enzyme (e.g. vanadate).

(d) Precise manipulation of pH_c by applying weak organic acids or bases or by the intracellular photorelease of caged protons (e.g. Diazo-3), could be used to investigate further the importance of the pH_c during the pre-penetration phase of *M. grisea*.

8. REFERENCES

ABE, T. (1931) On the effect of sunlight on the infection of the rice plant by *Piricularia oryzae*. *Forschungen aus dem Gebiet der Pflanzenkrankheiten*, **1**: 46-53. [In Japanese].

ALBERTS, B., BRAY, D., LEWIS, J., RAFF, M., ROBERTS, K. & WATSON, J.D. (1994) *The Molecular Biology of the Cell*, Garland Publishing, Inc., New York.

ALLEN, P.J. & DUNKEL, L.D. (1970) Natural activators and inhibitors of spore germination. In: *Morphological and Biochemical Events in Plant-Parasite Interactions* (ed. Akai, S. & Ouchi, S.), pp. 23-58. Phytopathological Society of Japan, Tokyo.

ALLEN, E.A., HAZEN, B.E., HOCH, H.C., KWON, Y., LEINHOS, G.M.E., STAPLES, R.C., STUMPF, M.A. & TERHUNE, B.T. (1991a) Appressorium formation in response to topographical signals by 27 rusts. *Phytopathology*, **81**: 323-331.

ALLEN, E.A., HOCH, H.C., STAVELY, J.R. & STEADMAN, J.R. (1991b) Uniformity among races of *Uromyces appendiculatus* in response to topographic signaling for appressorium formation. *Phytopathology*, **81**: 883-887.

ARAKI, F. & MIYAGI, Y. (1977) Effects of fungicides on penetration by *Pyricularia oryzae* as evaluated by an improved cellophane method. *Journal of Pesticide Science*, **2**: 457-461.

BAILEY, J.A., O'CONNELL, R.J., PRING, R.J. & NASH, C. (1992) Infection strategies of *Colletotrichum* species. In *Colletotrichum. Biology, Pathology and Control.* (ed Bailey, J.A. & Jeger, M.J.), pp. 88-120, CAB International, Wallingford.

BERTL, A. & SLAYMAN, C.L. (1992) Complex modulation of cation channels in the tonoplast and plasma membrane of *Saccharomyces cerevisiae*: single channel studies. *Journal of Experimental Biology*, **172**: 271-287.

BOLARD, J. (1986) How do the polyene macrolide antibiotics affect the cellular membrane properties? *Biochimica et Biophysica Acta*, **864**: 257-304.

BOURETT, T.M. & HOWARD, R.J. (1990) *In vitro* development of penetration structures in the rice blast fungus *Magnaporthe grisea*. *Canadian Journal of Botany*, **68**: 329-342.

BOURETT, T.M. & HOWARD, R.J. (1992) Actin in penetration pegs of the fungal rice blast pathogen, *Magnaporthe grisea*. *Protoplasma*, **168**: 20-26.

BOURETT, T.M., PICOLLELLI, M.A. & HOWARD, R.J. (1993) Postembedment labeling of intracellular concanavalin A-binding sites in freeze-substituted fungal cells. *Experimental Mycology*, **17**: 223-235.

BOWMAN, B.J. & BOWMAN, E.J. (1986) H^+-ATPases from mitochondria, plasma membranes and vacuoles of fungal cells. *Journal of Membrane Biology*, **94**: 83-97.

BOWMAN, B.J., DSCHIDA, W.J. & BOWMAN, E.J. (1992) Vacuolar ATPase of *Neurospora crassa*: electron microscopy, gene characterisation and gene inactivation/mutation. *Journal of Experimental Biology*, **172**: 57-66.

BRUNTON, A.H. & GADD, G.M. (1989) The effect of exogenously supplied nucleosides and nucleotides and the involvement of adenosine 3′-5′-cyclic monophosphate (cyclic-AMP) in the yeast-mycelium transition of *Ceratocystis* (= *Ophiostoma*) *ulmi*. *FEMS Microbiology Letters*, **60**: 49-53.

BRUNTON, A.H. & GADD, G.M. (1991) Evidence for an inositol lipid signal pathway in the yeast-mycelium transition of *Ophiostoma* (*Ceratocystis*) *ulmi*, the Dutch elm disease fungus. *Mycological Research*, **95**: 484-491.

BUCKLER, K.J. & VAUGHAN-JONES, R.D. (1990) Application of a new pH-sensitive fluoroprobe (carboxy-SNARF-1) for intracellular pH measurement in small, isolated cells. *Pfluegers Archives*, **417**: 234-239.

BUSH, D.R. (1993) Proton-coupled sugar and amino acid transporters in plants. *Annual Review of Plant Physiology*, **44**: 513-542.

CAMERON, J.N. & CARLILE, M.J. (1980) Negative chemotaxis of zoospores of the fungus *Phytophthora palmivora*. *Journal of General Microbiology*, **120**: 347-353.

CASSONE, A., CARPINELLI, G., ANGIOLLELA, L., MADDALUNO, G. & PODO, F. (1983) ^{31}P Nuclear magnetic resonance study of growth and dimorphic transition in *Candida albicans*. *Journal of General Microbiology*, **129**: 1569-1575.

CHANG, H.-S. & CALPOUZOS, L. (1973) Phototropism of the uredospore germ tubes of *Puccinia graminis tritici*. *Botanical Bulletin of the Academia Sinicia*, **14**: 35-40.

CODY, S.H., DUBBIN, P.N., BEISCHER, A.D., DUNCAN, N.D., HILL, J.S., KAYE, A.H. & WILLIAMS, D.A. (1993) Intracellular pH mapping with SNARF-1 and confocal microscopy. I: A quantitative technique for living tissues and isolated cells. *Micron*, **24**: 573-580.

CRAWFORD, M.S., CHUMLEY, F.G., WEAVER, C.G. & VALENT, B. (1986) Characterization of the heterokaryotic and vegetative diploid phases of *Magnaporthe grisea*. *Genetics*, **114**: 1111-1129.

DAVIES, D.D. (1986) The fine control of cytosolic pH. *Physiologia Plantarum*, **67**: 702-706.

DAVIES, J.M., BROWNLEE, C. & JENNINGS, D.H. (1990) Measurement of intracellular pH in fungal hyphae using BCECF and digital imaging microscopy. *Journal of Cell Science*, **96**: 731-736.

DE SILVA, L.R., YOUATT, J., GOODAY, G.W. & GOW, N.A.R. (1992). Inwardly directed ionic currents of *Allomyces macrogynus* and other water moulds indicate sites of proton-driven nutrient transport but are incidental to tip growth. *Mycological Research*, **96**: 925-931.

DILLON-WESTON, W.A.R. (1931) Effect of light on the urediniospores of black stem rust of wheat, *Puccinia graminis tritici. Nature*, **128**: 67-68.

DOBLINGER, R. & TROMBALLA, H.W. (1982) The effect of glucose on chloride uptake by *Chlorella*. 2. Effect of intracellular acidification on chloride uptake. *Planta*, **156**: 16-20.

DONALDSON, S.P. & DEACON, J.W. (1992) Role of calcium in adhesion and germination of zoospore cysts of *Pythium*: a model to explain infection of host plants. *Journal of General Microbiology*, **138**: 2051-2059.

DUBBIN, P.N., CODY, S.H. & WILLIAMS, D.A. (1993) Intracellular pH mapping with SNARF-1 and confocal microscopy. II: pH gradients within single cultured cells. *Micron*, **24**: 581-586.

DUBOIS, E. & GRENSON, M. (1979) Methylamine/ammonia uptake systems in *Saccharomyces cerevisiae*: multiplicity and regulation. *Molecular and General Genetics*, **175**: 67-76.

DUFOUR, J.P., GOFFEAU, A. & TSONG, T.Y. (1982) Active proton uptake in lipid vesicles reconstituted with the purified yeast plasma membrane ATPase - fluorescence quenching of 9-amino-6-chloro-2-methoxyacridine. *Journal of Biological Chemistry*, **257**: 9365-9371.

EDDY, A.A. & HOPKINS, P.G. (1985) The putative electrogenic nitrate-proton symport of the yeast *Candida utilis*. Comparison with the systems absorbing glucose or lactate. *Biochemical Journal*, **231**: 291-297.

EDWARDS, M.C. & BOWLING, D.J.F. (1986) The growth of rust germ tubes towards stomata in relation to pH gradients. *Physiological and Molecular Plant Pathology*, **29**: 185-196.

EMGE, R.G. (1958) The influence of light and temperature on the formation of infection-type structures of *Puccinia graminis* var. *tritici* on artificial substrates. *Phytopathology*, **48**: 649-652.

EMMETT, R.W. & PARBERY, D.G. (1975) Appressoria. *Annual Review of Phytopathology*, **13**: 147-167.

EPSTEIN, L., STAPLES, R.C. & HOCH, H.C. (1989) Cyclic AMP, cyclic GMP, and bean rust uredospore germlings. *Experimental Mycology*, **13**: 100-104.

ERASO, P., MAZON, M.J. & GANCEDO, J.M. (1987) Internal acidification and cAMP increase are not correlated in *Saccharomyces cerevisiae*. *European Journal of Biochemistry*, **165**: 671-674.

FELLE, H. (1989) K^+/H^+-antiport in *Riccia fluitans* - an alternative to the plasma membrane H^+-pump for short term pH-regulation. *Plant Science*, **61**: 9-15.

FELLE, H. & JOHANNES, E. (1990) The regulation of proton amino-acid symport in *Riccia fluitans* L. by cytosolic pH and proton pump activity. *Journal of Experimental Botany*, **41**: 587-592.

FLAISHMAN, M.A. & KOLATTUKUDY, P.E. (1994) Timing of fungal invasion using host's ripening hormone as a signal. *Proceedings of the National Academy of Sciences, USA*, **91**: 6579-6583.

FRACHISSE, J.M., JOHANNES, E. & FELLE, H. (1988) The use of weak acids as physiological tools - a study of the effects of fatty-acids on intracellular pH and electrical plasmalemma properties of *Riccia fluitans* rhizoid cells. *Biochimica et Biophysica Acta*, **938**: 199-210.

FRENCH, R.C. & WEINTRAUB, R.L. (1957) Pelargonaldehyde as an endogenous germination stimulator of wheat rust spores. *Archives of Biochemistry and Biophysics*, **72**: 235-237.

FREYTAG, S., BRUSCAGLIONI, L., GOLD, R.E. & MENDGEN, K. (1988) Basidiospores of rust fungi (*Uromyces* species) differentiate infection structures *in vitro*. *Experimental Mycology*, **12**: 275-283.

GADD, G.M. (1993) Interactions of fungi with toxic metals. *New Phytologist*, **124**: 25-60.

GADD, G.M. (1995) Signal transduction in fungi. In: *The Growing Fungus* (ed. Gow, N.A.R. & Gadd, G.M.) pp. 183-210, Chapman & Hall, London.

GARRILL, A. (1995) Transport. In: *The Growing Fungus* (ed. Gow, N.A.R. & Gadd, G.M.), pp. 163-181, Chapman & Hall, London.

GARRILL, A., LEW, R.R. & HEATH, I.B. (1992) Stretch-activated Ca^{2+} and Ca^{2+}-activated K^+-channels in the hyphal tip plasma membrane of the oomycete *Saprolegnia ferax*. *Journal of Cell Science*, **101**: 721-730.

GARRILL, A., JACKSON, S.L., LEW, R.R. & HEATH, I.B. (1993) Ion channel activity and tip growth: tip localised stretch-activated channels generate an essential Ca^{2+}-gradient in the oomycete *Saprolegnia ferax*. *European Journal of Cell Biology*, **60**: 358-365.

GERISCH, G. (1987) Cyclic AMP and other signals controlling cell development and differentiation in *Dictyostelium*. *Annual Review of Biochemistry*, **56**: 853-879.

GHISLAIN, M., SCHLESSER, A. & GOFFEAU, A. (1987) Mutation of a conserved glycine residue modifies the vanadate sensitivity of the plasma membrane H^+-ATPase from *Schizosaccharomyces pombe*. *Journal of Biological Chemistry*, **262**: 17549-17555.

GIBBON, B.C. & KROPF, D.L. (1994) Cytosolic pH gradients associated with tip growth. *Science*, **263**: 1419-1421.

GILLIES, R.J., UGURBIL, K., DEN HOLLANDER, J.A. & SHULMAN, R.G. (1981) ^{31}P NMR studies of intracellular pH and phosphate metabolism during cell division cycle of *Saccharomyces cerevisiae*. *Proceedings of the National Academy of Sciences, USA*, **78**: 2125-2129.

GOW, N.A.R. (1984) Transhyphal electrical currents in fungi. *Journal of General Microbiology*, **130**: 3313-3318.

GOW, N.A.R. (1989) Circulating ionic currents in micro-organisms. *Advances in Microbial Physiology*, **30**: 89-123.

GOW, N.A.R. (1995a) Yeast-hyphal dimorphism. In: *The Growing Fungus* (ed. Gow, N.A.R. & Gadd, G.M.), pp. 403-422, Chapman & Hall, London.

GOW, N.A.R. (1995b) Tip growth and polarity. In: *The Growing Fungus* (ed. Gow, N.A.R. & Gadd, G.M.), pp. 277-299, Chapman & Hall, London.

GOW, N.A.R., KROPF, D.L. & HAROLD, F.M. (1984) Growing hyphae of *Achlya bisexualis* generate a longitudinal pH gradient in the surrounding medium. *Journal of General Microbiology*, **130**: 2967-2974.

GRAMBOW, H.J. (1977) The influence of volatile leaf constituents on the *in vitro* differentiation and growth of *Puccinia graminis* f. sp. *tritici*. *Zeitschrift für Pflanzenphysiology*, **85**: 361-372.

GRESIK, M., NADEZDA, K. & FARKAS, V. (1991) Hyperpolarization and intracellular acidification in *Trichoderma viride* as a response to illumination. *Journal of General Microbiology*, **137**: 2605-2609.

GUERN, J., FELLE, H., MATHIEU, Y. & KURKDJIAN, A. (1991) Regulation of intracellular pH in plant cells. *International Review of Cytology*, **127**: 111-173.

GUSTIN, M.C., MARTINAC, B., SAIMI, Y., GULBERTSON, M.R & KUNG, C. (1986) Ion channels in yeast. *Science*, **233**: 1195-1197.

GUSTIN, M.C., ZHOU, X.-L., MARTINAC, B. & KUNG, C. (1988) A mechanosensitive ion channel in the yeast plasma membrane. *Science*, **242**: 762-765.

HAMER, J.E., HOWARD, R.J., CHUMLEY, F.G. & VALENT, B. (1988) A mechanism for surface attachment in spores of a plant pathogenic fungus. *Science*, **239**: 288-290.

HAMER, J.E., VALENT, B. & CHUMLEY, F.G. (1989) Mutations at the SMO genetic locus affect the shape of diverse cell types in the rice blast fungus. *Genetics*, **122**: 351-361.

HANSEN, U.-P. & SLAYMAN, C.L. (1978) Current-voltage relationships for a clearly electrogenic cotransport system. In *Coupled Transport Phenomena in Cells and Tissue* (ed. Hoffmann, J.F.), pp. 141-154, Raven Press, New York.

HAROLD, F.M. & CALDWELL, J.H. (1990) Tips and currents: electrobiology of apical growth. In: *Tip Growth in Plant and Fungal Cells* (ed. Heath, I.B), pp. 59-90, Academic Press, London.

HASHIOKA, Y. (1972) Fine structure of the rice blast. IX. Scanning electronmicroscopical observations on appressoria of the rice blast fungus and other species of *Pyricularia*. *Research Bulletin of the Faculty of Agriculture, Gifu University*, **33**: 65-73.

HAUGLAND, R.P. (1992) *Handbook of Fluorescent Probes and Research Chemicals*, 5th Edition, p. 129. Molecular Probes Inc., Eugene, Oregon.

HAWORTH, R.S. & FLIEGEL, L. (1993) Intracellular pH in *Schizosaccharomyces pombe* - comparison with *Saccharomyces cerevisiae*. *Molecular and Cellular Biochemistry*, **124**: 131-140.

HAWORTH, R.S., LEMIRE, B.D., CRANDALL, D., CRAGOE, E.J. Jr. & FLIEGEL, L. (1991) Characterisation of proton fluxes across the cytoplasmic membrane of the yeast *Saccharomyces cerevisiae*. *Biochimica et Biophysica Acta*, **1098**: 79-89.

HEATH, I.B. (1990) *Tip Growth in Plant and Fungal Cells.* Academic Press, London.

HEDRICH, R. & SCHROEDER, J.I. (1989) The physiology of ion channels and electrogenic pumps in higher plants. *Annual Review of Plant Physiology and Plant Molecular Biology*, **40**: 539-569.

HIROOKA, T., MIYAGI, Y., ARAKI, F., KUNOH, H. & ISHIZAKI, H. (1982) The effect of isoprothiolane on the emergence of infection pegs from appressoria of *Pyricularia oryzae*. *Pesticide Science*, **13**: 379-386.

HOAGLAND, D.R. & ARNON, H. (1950) The water culture method for growing plants without soil. *University of California Agricultural Experimental Station Circular*, **347.**

HOCH, H.C. & STAPLES, R.C. (1984) Evidence that cAMP initiates nuclear division and infection structure formation in the bean rust fungus, *Uromyces phaseoli*. *Experimental Mycology*, **8**: 37-46.

HOCH, H.C. & STAPLES, R.C. (1991) Signaling for infection structure formation in fungi. In: *The Fungal Spore and Disease Initiation in Plants and Animals* (ed. Cole, G.T. & Hoch, H.C.), pp. 25-46, Plenum Press, New York.

HOCH, H.C., STAPLES, R.C., WHITEHEAD, B., COMEAU, J. & WOLF, E.D. (1987) Signaling for growth orientation and cell differentiation by surface topography in *Uromyces*. *Science*, **235**: 1659-1662.

HORAK, J. (1986) Amino acid transport in eukaryotic microorganisms. *Biochimica et Biophysica Acta*, **864**: 223-256.

HOWARD, R.J. (1994) Cell biology of pathogenesis. In: *Rice Blast Disease* (ed. Zeigler, R.S, Leong, S.A. & Teng, P.S.), pp. 3-22, CAB International, Wallingford.

HOWARD, R.J. & FERRARI, M.A. (1989) Role of melanin in appressorium function. *Experimental Mycology*, **13**: 403-418.

HOWARD, R.J., BOURETT, T.M. & FERRARI, M.A. (1991a) Infection by *Magnaporthe*: an *in vitro* analysis. In: *Electron Microscopy of Plant Pathogens* (ed. Mendgen, K. & Lesemann, D.-E.), pp. 251-264, Springer Verlag, Berlin.

HOWARD, R.J., FERRARI, M.A., ROACH, D.H. & MONEY, N.P. (1991b) Penetration of hard substrates by a fungus employing enormous turgor pressures. *Proceedings of the National Academy of Sciences, USA*, **88**: 11281-11284.

KACSER, H. & PORTEOUS, J.W. (1987) Control of metabolism: what do we have to measure? *Trends in Biochemical Sciences*, **12**: 5-12.

KAMINSKYJ, S.G.W. & DAY, A.W. (1984) Chemical induction of infection structures in rust fungi. *Experimental Mycology*, **8**: 63-72.

KAUR, S. & MISHRA, P. (1994) Differential increase in cytoplasmic pH at bud and germ tube formation in *Candida albicans*: studies of a nongerminative variant. *Canadian Journal of Microbiology*, **40**: 720-723.

KAUR, S., MISHRA, P. & PRASAD, R. (1988) Dimorphism-associated changes in intracellular pH of *Candida albicans*. *Biochimica et Biophysica Acta*, **972**: 277-282.

KNIGHT, H., TREWAVAS, A.J. & READ, N.D. (1993) Confocal microscopy of living fungal hyphae microinjected with Ca^{2+}-sensitive fluorescent dyes. *Mycological Research*, **97**: 1505-1515.

KNIGHTS, I.K. & LUCAS, J.A. (1980) Photosensitivity of *Puccinia graminis* f. sp. *tritici* urediniospores *in vitro* and on the leaf surface. *Transactions of the British Mycological Society*, **74**: 543-549.

KROPF, D.L., LUPA, M.D.A., CALDWELL, J.H. & HAROLD, F.M. (1983) Cell polarity: endogenous ion currents precede and predict branching in the water mould *Achlya*. *Science*, **220**: 1385-1387.

KROPF, D.L., CALDWELL, J.H., GOW, N.A.R. & HAROLD, F.M. (1984) Transcellular ion currents in the water mold *Achlya*. Amino acid proton symport as a mechanism of current entry. *The Journal of Cell Biology*, **99**: 486-496.

KURKDJIAN, A. & GUERN, J. (1989) Intracellular pH: measurement and importance in cell activity. *Annual Review of Plant Physiology and Plant Molecular Biology*, **40**: 271-303.

KWON, Y.H., HOCH, H.C. & STAPLES, R.C. (1991) Cytoskeletal organisation in *Uromyces* urediospores germling apices during appressorium formation. *Protoplasma*, **165**: 37-50.

LACCETTI, L., STAPLES, R.C. & HOCH, H.C. (1987) Purification of calmodulin from bean rust urediospores. *Experimental Mycology*, **11**: 231-235.

LEE, Y.-H. & DEAN, R.A. (1993) cAMP regulates infection structure formation in the plant pathogenic fungus *Magnaporthe grisea*. *The Plant Cell*, **5**: 693-700.

LEUNG, H. & TAGA, M. (1988) *Magnaporthe grisea* (*Pyricularia* species), the blast fungus. *Advances in Plant Pathology*, **6**: 175-188.

LOWENDORF, H.S., BAZINET, G.F. Jr. & SLAYMAN, C.W. (1975) Phosphate transport in *Neurospora crassa*: derepression of a high affinity transport system during phosphate starvation. *Biochimica et Biophysica Acta*, **389**: 541-549.

LUCAS, J.A. & KNIGHTS, I.K. (1987) Spores on leaves: endogenous and exogenous control of development. In: *Fungal Infection of Plants* (ed. Pegg, G.F. & Ayres, P.G.) pp. 45-59, Cambridge University Press, Cambridge.

LUTTRELL, P.(1974). Parasitism of fungi on vascular plants. *Mycologia*, **66**: 1-15.

MACKO, V. (1981) Inhibitors and stimulants of spore germination and infection structure formation. In: *The Fungal Spore: Morphogenetic Controls* (ed. Turian, G. & Hohl, H.R.) pp. 565-584, Academic Press, New York.

MACKO, V., RENWICK, J.A.A. & RISSLER, J.F. (1978) Acrolein induces differentiation of infection structures in the wheat stem rust fungus. *Science*, **199**: 442-443.

MADSHUS, I.H. (1988) Regulation of intracellular pH in eukaryotic cells. *Biochemical Journal*, **250**: 1-8.

MARRE, E. (1979) Fusicoccin: a tool in plant physiology. *Annual Review of Plant Physiology*, **30**: 273-288.

MARTINEZ-ZAGUILAN, R., MARTINEZ, G.M., LATTANZIO, F. & GILLIES, R.J. (1991) Simultaneous measurement of intracellular pH and Ca^{2+} using the fluorescence of SNARF-1 and fura-2. *American Journal of Physiology*, **260**: C297-C307.

MARZLUF, G.A. (1970) Genetic and metabolic controls for sulfate metabolism in *Neurospora crassa*: isolation and study of chromate-resistant and sulfate transport-negative mutants. *Journal of Bacteriology*, **102**: 716-721.

MATHIEU, Y., GUERN, J., PEAN, M., PASQUIER, C., BELOEIL, J.-C. & LALLEMAND, J.Y. (1986) Cytoplasmic pH regulation in *Acer pseudoplatanus* cells. II. Possible mechanisms involved in pH regulation during acid-load. *Plant Physiology*, **82**: 846-852.

McGILLVIRAY, A.M. & GOW, N.A.R. (1987) The transhyphal electrical current of *Neurospora crassa* is carried principally by protons. *Journal of General Microbiology*, **133**: 2875-2881.

MELLMAN, I., FUCHS, R. & HELENIUS, A. (1986) Acidification of the endocytic and exocytic pathways. *Annual Review of Biochemistry*, **55**: 663-700.

MERCER, P.C., WOOD, R.K.S. & GREENWOOD, A.D. (1971) Initial infection of *Phaseolus vulgaris* by *Colletotrichum lindemuthianum*. In *Ecology of Leaf Surface Micro-organisms* (ed. Preece, T.F. & Dickinson, C.H.), pp. 381-389, Academic Press, London.

MONK, B.C., KURTZ, M.B., MARRINAN, J.A. & PERLIN, D.S. (1991) Cloning and characterisation of the plasma membrane H^+-ATPase from *Candida albicans*. *Journal of Bacteriology*, **173**: 6826-6836.

MONK, B.C., NIIMI, M. & SHEPHERD, M.G. (1993) The *Candida albicans* plasma membrane and H^+-ATPase during yeast growth and germ tube formation. *Journal of Bacteriology*, **175**: 5566-5574.

MOSS, M.A. & TREVATHAN, L.E. (1987) Environmental conditions conducive to infection of ryegrass by *Pyricularia oryzae*. *Phytopathology*, **77**: 863-866.

MOUNT, M.S. & SLESINSKI, R.S.(1971) Characterization of primary development of powdery mildew. In: *Ecology of Leaf Surface Micro-organisms*. (ed. Preece, T.F. & Dickinson, C.H.), pp. 301-322, Academic Press, London.

MURPHY, T.M., MATSON, G.B. & MORRISON, S.L. (1983) Ultraviolet-stimulated $KHCO_3$ efflux from rose cells - regulation of cytoplasmic pH. *Plant Physiology*, **73**: 20-24.

MURUGANANDAM, V., VENKATACHALAM, S. & SURYANARAYANAN, R.S. (1991) Potassium enhances thigmotropically stimulated appressorium formation in *Colletotrichum capsici*. *Cryptogamie Mycologie*, **12**: 155-159.

MUTHUKUMAR, G., & NICKERSON, K.W. (1984) Ca(II)-Calmodulin regulation of fungal dimorphism in *Ceratocystis ulmi*. *Journal of Bacteriology*, **159**: 390-392.

MUTHUKUMAR, G., KULKARNI, R.K. & NICKERSON, K.W. (1985) Calmodulin levels in the yeast and mycelial phases of *Ceratocystis ulmi*. *Journal of Bacteriology*, **162**: 47-49.

NICHOLSON, R.L. & EPSTEIN, L. (1991) Adhesion of fungi to the plant surface: prerequisite for pathogenesis. In: *The Fungal Spore and Disease Initiation in Plants and Animals* (ed. Cole, G.T. & Hoch, H.C.), pp. 3-23, Plenum Press, New York.

NUTMAN, F.J. & ROBERTS, F.M. (1963) Studies on the biology of *Hemileia vestatrix*, Berk & Br. *Transactions of the British Mycological Society*, **46**: 27-48.

OPARKA, K.J. & READ, N.D. (1994) The use of fluorescent probes for studies of living plant cells. In: *Plant Cell Biology. A Practical Approach.* (ed. Harris, S. & Oparka, K.J.), pp. 27-50, IRL Press, Oxford.

OPITZ, N., MERTEN, E. & ACKER, H. (1994) Evidence for redistribution-associated intracellular p*K* shifts of the pH-sensitive fluoroprobe carboxy-SNARF-1. *Pfluegers Archives*, **427**: 332-342.

OU, S.H. (1980) A look at worldwide rice blast disease control. *Plant Disease*, **64**: 439-445.

OU, S.H. (1985) *Rice Diseases*.2nd ed. Commonwealth Mycological Institute, Kew.

OWEN, C.S. (1992) Comparison of spectrum-shifting intracellular pH probes 5′(and 6′)-carboxy-10-dimethylamino-3-hydroxyspiro[7H-benzo[c]xanthene-7,1′(3′H)-isobenzofuran]-3′-one and 2′,7′-biscarboxyethyl-5(and6)-carboxyfluorescein. *Analytical Biochemistry*, **204**: 65-71.

OWEN, C.S., CARANGO, P., GRAMMER, S., BOBYOCK, S. & LEEPER, D.B. (1992) pH-dependent intracellular quenching of the indicator carboxy-SNARF-1. *Journal of Fluorescence*, **2**: 75-80.

PARTON, R.M. (1995) Imaging of intracellular pH and calcium in cells of *Dryopteris affinis*. *PhD Thesis*, University of Edinburgh, (in preparation).

PENG, Y.-L. & SHISHIYAMA, J. (1988) Temporal sequence of cytological events in rice leaves infected with *Pyricularia oryzae*. *Canadian Journal of Botany*, **66**: 730-735.

PERRIN, D.D. & DEMPSEY, B. (1974) *Buffers for pH and Metal Ion Control.* Chapman and Hall, London.

PETERSON, G.W. & WALLA, J.A. (1978) Development of *Dothistroma pini* upon and within needles of Austrian and ponderosa pines in eastern Nebraska.. *Phytopathology*, **68**: 1422-1430.

PODILA, G.K., ROGERS, L.M. & KOLATTUKUDY, P.E. (1993) Chemical signals from avocado surface wax trigger germination and appressorium formation in *Colletotrichum gloeosporioides*. *Plant Physiology*, **103**: 267-272.

PORTILLO, F. & SERRANO, R. (1989) Growth control strength and active site of yeast plasma membrane ATPase studied by site-directed mutagenesis. *European Journal of Biochemistry*, **186**: 501-507.

PRIOR, S.L., CUNNLIFFE, B.W., ROBSON, G.D. & TRINCI, A.P.J. (1993) Multiple isomers of phosphatidyl inositol monophosphate and inositol bisphosphates and trisphosphates from filamentous fungi. *FEMS Microbiology Letters*, **110**: 147-152.

PURKAYASTHA, R.P. & GUPTA, M.S. (1973) Studies on conidial germination and appressoria formation in *Colletotrichum gloeosporioides* Penz. causing anthracnose of jute (*Corchorus olitorius* L.) *Zeitschrift für Planzenkrankheiten und Pflanzenschutz*, **73**: 718-724.

QUAGLIARIELLO, E. & PALMIERI, F. (1992) *Molecular Mechanisms of Transport*. Elsevier, Amsterdam.

RATHAIAH, Y. (1977) Stomatal tropism of *Cercospora beticola* in sugarbeet. *Phytopathology*, **67**: 358-362.

READ, N.D., KELLOCK, L.J., KNIGHT, H. & TREWAVAS, A.J. (1992a) Contact sensing during infection by fungal pathogens. In *Perspectives in Plant Cell Recognition* (ed. Callow, J.A., & Green, J.R.), pp. 137-172, Cambridge University Press, Cambridge.

READ, N.D., ALLAN, W.T.G., KNIGHT, H., KNIGHT, M.R., MALHO, R., RUSSELL, A., SHACKLOCK, P.S. & TREWAVAS, A.J. (1992b) Imaging and measurement of cytosolic free calcium in plant and fungal cells. *Journal of Microscopy*, **66**: 57-86.

READ, N.D., SHACKLOCK, P.S., KNIGHT, M.R. & TREWAVAS, A.J. (1993) Imaging calcium dynamics in living plant cells and tissues. *Cell Biology International*, **17**: 111-125.

REES, B., SHEPHERD, V.A. & ASHFORD, A.E. (1994) Presence of a motile tubular vacuole system in different phyla of fungi. *Mycological Research*, **98**: 985-992.

REID, R.J. & WALKER, N.A. (1984) Control of Cl-influx in *Chara* by internal pH. *Journal of Membrane Biology*, **78**: 157-162.

REUSS, L., RUSSELL, J.M., Jr. & JENNINGS M.L. (1993) *Molecular Biology and Function of Carrier Proteins.* 46th Symposium, Society of General Physiologists. Rockefeller University Press, New York.

RODRIGUEZ-NAVARRO, A., BLATT, M.R. & SLAYMAN, C.L. (1986) A potassium-proton symport in *Neurospora crassa. Journal of General Physiology*, **87**: 649-674.

RONCAL, T., UGALDE, U.O. & IRASTORZA, A. (1993) Calcium-induced conidiation in *Penicillium cyclopium:* calcium triggers cytosolic alkalinization at the hyphal tip. *Journal of Bacteriology*, **175**: 879-886.

ROOS, W. (1992) Confocal pH topography in plant cells - acidic layers in the peripheral cytoplasm and the apoplast. *Botanica Acta*, **105**: 253-259.

ROSSMAN, A.Y., HOWARD, R.J. & VALENT, B. (1990) *Pyricularia grisea*, the correct name for the rice blast disease fungus. *Mycologia*, **82**: 509-512.

SANDERS, D. & SLAYMAN, C.L. (1982) Control of intracellular pH. Predominant role of oxidative metabolism, not proton transport, in the eukaryotic microorganism. *Journal of General Physiology*, **80**: 377-402.

SANDERS, D., SLAYMAN, C.L. & PALL, M.L. (1983) Stoichiometry of H^+/amino acid cotransport in *Neurospora crassa* revealed by current-voltage analysis. *Biochimica et Biophysica Acta*, **735**: 67-76.

SANDERS, D., SMITH, F.A. & WALKER, N.A. (1985) Proton chloride cotransport in *Chara* - mechanism of enhanced influx after rapid external acidification. *Planta*, **163**: 411-418.

SANDISON, D.R. & WEBB, W.W. (1994) Background rejection and signal-to-noise optimization in the confocal and alternative fluorescence microscopes. *Applied Optics*, **33**: 605-615.

SATO, T., OHSUMI, Y. & ANRAKU, Y. (1984) Substrate specificities of active transport systems for amino acids in vacuolar-membrane vesicles of *Saccharomyces cerevisiae* - evidence of 7 independent proton amino acid antiport systems. *Journal of Biological Chemistry*, **259**: 1505-1508.

SCARBOROUGH, G.A. (1980) Proton translocation catalyzed by the electrogenic ATPase in the plasma membrane of *Neurospora. Biochemistry*, **19**: 2925-2931.

SEKSEK, O., HENRY-TOULME, N., SUREAU, F. & BOLARD, J. (1991) SNARF-1 as an intracellular pH indicator in laser microspectrofluorometry: a critical assessment. *Analytical Biochemistry*, **193**: 49-54.

SERRANO, R., KIELLAND-BRANDT, M.C. & FINK, G.R. (1986) Yeast plasma-membrane ATPase is essential for growth and has a homology with ($Na^+ + K^+$), K^+- and Ca^{2+}-ATPases. *Nature*, **319**: 689-693.

SHARP, E.L., SCHMITT, C.G., STALEY, J.M. & KINGSOLVER, C.H. (1958) Some critical factors involved in establishment of *Puccinia graminis* var. *tritici*. *Phytopathology*, **48**: 469-474.

SILVER, A.R., WHITAKER, M. & BOLSOVER, S.R. (1992) Intracellular ion imaging using fluorescent dyes: artefacts and limits to resolution. *Pfluegers Archives*, **420**: 595-602.

SINGH, P. (1973) Effect of light, temperature and substrate during spore formation on the germinability of conidia of *Colletotrichum falcatum*. *Physiologia Plantarum*, **29**: 194-197.

SLAVIK, J. (1982) Intracellular pH of yeast cells measured with fluorescent probes. *FEBS Letters*, **140**: 22-26.

SLAVIK, J. & KOTYK, A. (1984) Intracellular pH distribution and transmembrane pH profile of yeast cells. *Biochimica et Biophysica Acta*, **766**: 679-684.

SLAYMAN, C.L (1965a) Electrical properties of *Neurospora crassa*. Effects of external cations on the intracellular potential. *Journal of General Physiology*, **49**: 69-92.

SLAYMAN, C.L. (1965b) Electrical properties of *Neurospora crassa*. Respiration and the intracellular potential. *Journal of General Physiology*, **49**: 93-116.

SLAYMAN, C.L. (1987) The plasma membrane ATPase of *Neurospora:* a proton-pumping electroenzyme. *Journal of Bioenergetics and Biomembranes*, **19**: 1-20.

SLAYMAN, C.L. & SLAYMAN, C.W. (1974) Depolarisation of the plasma membrane of *Neurospora* during active transport of glucose: evidence for a proton-dependent cotransport system. *Proceedings of the National Academy of Sciences, USA*, **71**: 1935-1939.

SLAYMAN, C.W. & SLAYMAN, C.L. (1975) Energy coupling in the plasma membrane of *Neurospora:* ATP-dependent proton-transport and proton-dependent sugar transport. In: *Molecular Aspects of Membrane Phenomena* (ed. Kaback, H.R., Neurath, H., Radda, G.K., Schwyzer, R. & Wiley, W.R.), pp. 233-248. Springer-Verlag, Berlin.

SLAYMAN, C.L., MOUSSATOS, V.V. & WEBB, W.W. (1994) Endosomal accumulation of pH indicator dyes delivered as acetoxymethyl esters. *Journal of Experimental Biology*, **196**: 419-438.

STAPLES, R.C. & HOCH, H.C. (1988) Preinfection changes in germlings of a rust fungus induced by host contact. In *Biotechnology for Crop Protection* (ed. Hedin, P.A., Menn, J.J. & Hollingworth, R.M.), pp. 82-93. American Chemical Society, Washington DC.

STAPLES, R.C., GRAMBOW, H.J. & HOCH, H.C. (1983) Potassium ion induces rust fungi to develop infection structures. *Experimental Mycology*, **7**: 40-46.

STEVENS, T.H. (1992) The structure and function of the fungal V-ATPase. *Journal of Experimental Biology*, **172**: 47-55.

STEWART, E., GOW, N.A.R. & BOWEN, D.V. (1988) Cytoplasmic alkalinization during germ tube formation in *Candida albicans*. *Journal of General Microbiology*, **134**: 1079-1087.

STEWART, E., HAWSER, S. & GOW, N.A.R. (1989) Changes in internal and external pH accompanying growth of *Candida albicans*: studies of non-dimorphic variants. *Archives of Microbiology*, **151**: 149-153.

STUMPF, M.A., LEINHOS, G.M.E., STAPLES, R.C. & HOCH, H.C. (1991) The effect of pH and K^+ on appressorium formation by *Uromyces appendiculatus* urediospore germlings. *Experimental Mycology*, **15**: 356-360.

SWINBURNE, T.R. (1986) Stimulation of disease development by siderophores and inhibition by chelated iron. In: *Iron, Siderophores and Plant Disease* (ed. Swinburne, T.R.), pp. 217-226. Plenum Press, New York.

SZE, H. (1984) H^+-translocating ATPases of the plasma-membrane and tonoplast of plant cells. *Physiologia Plantarum*, **61**: 683-691.

TAKEUCHI, Y., SCHMID, J., CALDWELL, J.H. & HAROLD, F.M. (1988) Transcellular ion currents and extension of *Neurospora crassa* hyphae. *Journal of Membrane Biology*, **101**: 33-41.

TALBOT, N.J. (1995) Having a blast: exploring the pathogenicity of *Magnaporthe grisea*. *Trends in Microbiology*, **3**: 9-16.

TALBOT, N.J., EBBOLE, D.J. & HAMER, J.E. (1993) Identification and characterization of *MPG1*, a gene involved in pathogenicity from the rice blast fungus *Magnaporthe grisea*. *The Plant Cell*, **5**: 1575-1590.

TERHUNE, B.T., ALLEN, E.A., HOCH, H.C., WERGIN, W.P. & ERBE, E.F. (1991) Stomatal ontogeny and morphology in *Phaseolus vulgaris* in relation to infection structure initiation by *Uromyces appendiculatus*. *Canadian Journal of Botany*, **69**: 477-484.

TREWAVAS, A.J. (1987) Many a mickle makes a muckle; network maxims may mitigate controversy. *BioEssays*, **7**: 84-86.

TREWAVAS, A. & GILROY, S. (1991) Signal transduction in plant cells. *Trends in Genetics*, **7**: 1-5.

TRIVEDI, B. & DANFORTH, W.H. (1966) Effect of pH on the kinetics of frog muscle phosphofructokinase. *The Journal of Biological Chemistry*, **241**: 4110-4114.

TURIAN, G. (1983) Polarized acidification at germ tube outgrowth from fungal spores (*Morchella* ascospores, *Neurospora* conidia). *Botanica Helvetica*, **93**: 27-32.

TURIAN, G., TON-THAT, T.C. & ORTEGA-PEREZ, R. (1985) Acid-tip linear growth in fungi: requirements for H^+/Ca^{2+} inverse gradients and cytoskeleton integrity. *Botanica Helvetica*, **95**: 311-322.

UCHIYAMA, T. & OKUYAMA, K. (1990) Participation of *Oryza sativa* leaf wax in appressorium formation by *Pyricularia oryzae*. *Phytochemistry*, **29**: 91-92.

UCHIYAMA, T.N., OGASAWARA, Y., NANBA, Y. & ITO, H. (1979) Conidial germination and appressorial formation of the plant pathogenic fungi on the cover glass or cellophane coated with various lipid components of plant leaf waxes. *Agricultural and Biological Chemistry*, **43**: 383-384.

VALENT, B. (1990) Rice blast as a model system for plant pathology. *Phytopathology*, **80**: 33-36.

VALENT, B. & CHUMLEY, F.G. (1991) Molecular genetic analysis of the rice blast fungus, *Magnaporthe grisea*. *Annual Review of Phytopathology*, **29**: 443-467.

VALENT, B., FARRALL, L. & CHUMLEY, F.G. (1991) *Magnaporthe grisea* genes for pathogenicity and virulence identified through a series of backcrosses. *Genetics*, **127**: 87-101.

WEBB, W.W., WELLS, K.S., SANDISON, D.R. & STRICKLER, J. (1990) Criteria for quantitative dynamical confocal fluorescence imaging. In: *Optical Microscopy for Biology* (ed. Herman, B. & Jacobson, K.), pp. 73-108, Wiley-Liss Inc., New York.

WEINTRAUB, R.L., MILLER, W.E. & SCHANTZ, E.J. (1958) Chemical stimulation of germination of spores of *Pyricularia oryzae*. *Phytopathology*, **48**: 7-10.

XIAO, J.-Z., WATANABE, T., KAMAKURA, T., OSHIMA, A. & YAMAGUCHI, I. (1994a) Studies on cellular differentiation of *Magnaporthe grisea*. Physicochemical aspects of substratum surfaces in relation to appressorium formation. *Physiological and Molecular Plant Pathology*, **44**: 227-236.

XIAO, J.-Z., OSHIMA, A., KAMAKURA, T., ISHIYAMA, T. & YAMAGUCHI, I. (1994b) Extracellular glycoprotein(s) associated with cellular differentiation in *Magnaporthe grisea*. *Molecular Plant-Microbe Interactions*, **7**: 639-644.

YAEGASHI, H., MATSUDA, I. & SATO, Z. (1987) Production of appressoria at the tips of hyphae of *Pyricularia oryzae*. *Annals of the Phytopathological Society of Japan*, **53**: 203-209.

YARWOOD, C.E. (1932) Reversible phototropism of the germ tubes of clover powdery mildew. *Phytopathology*, **22**: 31.

YOUATT, J., GOW, N.A.R. & GOODAY, G.W. (1988) Bioelectric and biosynthetic aspects of cell polarity in *Allomyces macrogynus*. *Protoplasma*, **146**: 118-126.

ZHOU, X.-L. & KUNG, C. (1992) A mechanosensitive ion channel in *Schizosaccharomyces pombe*. *EMBO Journal*, **11**: 2869-2875.

ZHOU, X.-L., STUMPF, M.A., HOCH, H.C. & KUNG, C. (1991) A mechanosensitive channel in whole cells and in membrane patches of the fungus *Uromyces*. *Science*, **253**: 1415-1417.

9. PUBLICATION

anta (1994) 194:471–477

Planta

Role of external signals in regulating the pre-penetration phase of infection by the rice blast fungus, *Magnaporthe grisea*

ill C. Jelitto, Helen A. Page, Nick D. Read

olecular Signalling Group, Institute of Cell and Molecular Biology, University of Edinburgh, Rutherford Building, dinburgh EH9 3JH, UK

eceived: 11 February 1994 / Accepted: 23 March 1994

bstract. The role of external signals (particularly the ıbstratum surface and light) in regulating the pre-pene-ation phase of *Magnaporthe grisea* (Herbert) Barr namorph, *Pyricularia grisea* Sacc.] were analysed on ce (*Oryza sativa* L.) leaves, artificial substrata and in quid suspension. Surface contact was found to be essen-al for appressorium induction but not conidium germi-ation. Both a high surface hydrophobicity and light fa-oured the formation of short differentiated germ tubes nd large numbers of appressoria, but neither factor was ssential for their induction. Light intensity had a graded ffect on the lengths of differentiated germ tubes but not n the number of appressoria formed. Higher numbers of ppressoria differentiated on rice leaves than on artificial ıbstrata suggesting that the host provides additional ctors, and thus a more conducive environment, for pro-ioting appressorium formation. Our study indicates that ne pre-penetration phase of rice blast infection involves programme of growth and differentiation triggered at onidium germination and regulated by multiple signals om the host and environment. No evidence was found or a single, external signal which initiates appressorium rmation. Starvation is suggested as providing the nec-ssary intracellular signal.

ey words: Appressorium – Contact sensing – Infection tructure – *Magnaporthe* – *Oryza* – Rice blast

ntroduction

Rice blast is considered the most important disease of ice in the world (Ou 1980, 1985). The causative agent, *Magnaporthe grisea* (Herbert) Barr [anamorph, *Pyricu-aria grisea* Sacc.], offers an excellent experimental system n which to address many of the most significant ques-ions in plant pathology. In recent years, studies of the cell biology and molecular genetics of this fungus have permitted a number of critical elements of host-pathogen interactions to be analysed (Valent 1990; Valent and Chumley 1991; Dobinson and Hamer 1992). One important aspect of study has been the pre-penetration phase of infection.

The initial stages of infection by *M. grisea* usually require the deposition and attachment of three-celled conidia to aerial parts of the rice plant. Attachment typically involves the immediate and persistent adhesion of a conidium to the rice leaf by means of a glue (the *spore tip mucilage*) released from the spore apex. The spore tip mucilage will also stick strongly to various artificial surfaces, including 'non-stick' Teflon (Hamer et al. 1988). Germination of the conidium can occur from any of its three cells and results in one or more germ tubes which, after a period of growth, can differentiate terminal, pigmented appressoria (Peng and Shishiyama 1988; Bourett and Howard 1990; Howard et al. 1991b). The appressorium is even more tenaciously adherent to the host surface than are conidia, and generates a hydrostatic pressure (> 80 bar) of unprecedented magnitude in living eukaryotic cells. This pressure provides a mechanical force which seems to be the primary mechanism by which an emergent penetration peg pushes through the rice leaf cuticle (Howard and Ferrari 1989; Howard et al. 1991a).

The pre-penetration phase of infection by *M. grisea* involves differential gene expression. Three genes, differentially expressed during appressorium formation, have been cloned (Lee and Dean 1993b; Talbot et al. 1993) and one encodes a hydrophobin-like protein (Talbot et al. 1993). Other genes involved in appressorium morphogenesis and pigmentation have also been identified by mutant analysis (Woloshuk et al. 1983; Hamer et al. 1989; Howard and Ferrari 1989; Chumley and Valent 1990). However, little is known about how these different genes are regulated by signals from the host, environment or from within the fungus itself. Nevertheless, recent evidence suggests that cAMP, but not Ca^{2+}, plays an important role as an intracellular signal in mediating appressorium formation (Lee and Dean 1993a).

Correspondence to: N.D. Read; FAX: 44 (31) 650 5392; e-mail: read@srv0.bio.ed.ac.uk

A useful approach to the experimental analysis of signals which influence the initial stages of infection is to study the process in vitro. In *M. grisea*, the pre-penetration phase readily occurs on artificial substrata in drops of water (e.g. see Bourett and Howard 1990). In this way, one can avoid the complex influences of the host which, itself, may also be affected by the same environmental factors that directly affect the fungus.

Two important factors which can influence pathogenesis are light and the physical nature of the host surface (Emmett and Parbery 1975; Hoch and Staples 1991; Read et al. 1992). However, the role of neither of these factors has been the subject of rigorous analysis during the pre-penetration phase of *M. grisea*. Nevertheless, it is well established that successful infection of rice plants can take place in either the light or dark (Ou 1985). Furthermore, appressoria have been shown to differentiate on a wide range of artificial substrata with marked differences in their hydrophobicity, hardness and other surface properties (Araki and Miyagi 1977; Uchiyama et al. 1979; Yaegashi et al. 1987; Bourett and Howard 1990; Uchiyama and Okuyama 1990; Howard et al. 1991a; Lee and Dean 1993a,b).

The aim of the present study was to determine the roles of external signals (particularly the substratum surface and light) in regulating the pre-penetration phase of infection by *M. grisea*. For this purpose, we have quantified conidium germination, germination patterns, germ-tube lengths, and appressorium formation in the fungus under light and dark conditions on rice leaves, cellophane, Teflon and glass, and in liquid suspension. Our study indicates that appressorium induction occurs within a conducive environment providing multiple regulatory signals rather than being exclusively stimulated by a single external signal.

Materials and methods

Organism and growth conditions. *Magnaporthe grisea*, strain 0-42 (kindly supplied by Dr. Barbara Valent, DuPont Co., Wilmington, Del., USA) was bulked up and stored as described by Valent et al. (1991). For experimentation, oatmeal-agar plates (1.5% agar containing 50 g per litre of Scottish porridge oat flakes) were inoculated with small pieces of filter paper bearing the fungus (Valent et al. 1991) and incubated at 25° C for 18–24 d under continuous light from fluorescent lamps at 45 μmol photons $\cdot m^{-2} \cdot s^{-1}$ in a cooled incubator. Conidia were isolated as described by Bourett and Howard (1990). The concentration of conidia in suspension was adjusted to $1 \cdot 10^4$–$2 \cdot 10^4 \cdot ml^{-1}$ in sterile, double-distilled water. At conidial concentrations higher than this, it was not possible to determine accurately the percentage conidium germination and appressorium formation. Illumination was minimised during conidial isolation by wrapping the centrifuge tubes containing conidia in aluminium foil. All conidia produced by this isolation procedure lacked spore tip mucilage.

In-vitro system on solid substrata. For all in vitro experiments, unused glass slides (Blue Star; Chance Propper, Warley, UK) were washed in Fairy Liquid detergent (Procter and Gamble, Newcastle upon Tyne, UK) and rinsed thoroughly with double-distilled water. Three silicon gaskets (Swinnex-13; Millipore, Bedford, Mass., USA), covered in melted dental wax (Anutex; Associated Dental Products, Swindon, UK), were applied to the slides to which they adhered once the wax cooled. The gasket rings prevented run-off of the inoculum drop during subsequent manipulations. To minimise microbial contamination during experimentation, the slides with gaskets were treated with UV-A irradiation for at least 4 h prior to inoculation. For experiments on cellophane (gauge 525, uncoated 'rayophane' from A.A. Packaging, Walmer Bridge, Lancs., UK) or Teflon (polytetrafluoroethylene from DuPont Co., Wilmington, Del., USA), 10-mm-diameter circles of the substrata were cut using a cork borer. After autoclaving, the circles were placed within the silicon gaskets. Experiments on glass were performed directly on the slides. A 20-μl conidium suspension was applied to the substratum and the slides placed in sterile, 12 cm · 12 cm square Petri dishes. To maintain high humidity, sterile tissue paper, saturated with sterile water, was placed in each dish which was then sealed with Parafilm. Except where stated, the fungal samples were grown for 24 h and incubated at 25° C under continuous light from fluorescent tubes at 45 μmol photons $\cdot m^{-2} \cdot s^{-1}$ in a cooled incubator. Dark-grown samples were covered in light-tight bags normally used to store photographic paper. To determine the effects of different light intensities, Petri dishes were wrapped in polyester neutral density filters (Lee Lighting, Glasgow, UK) of different grades (50%, 25% and 15% transmission). Temperature measurements with a digital thermometer showed that the temperatures within sealed Petri dishes grown in the light and dark, and within the incubator, were the same (± 0.5° C).

In-vitro system in liquid suspension. In order to analyse spore germination in liquid suspension, hanging-drop cultures were prepared. This involved adding 20-μl drops of spore suspension to glass slides, immediately inverting the slides, and then incubating them on a support over damp tissue paper in Petri dishes (as described in the previous section). Spore germination and appressorium formation in the hanging drops were assessed after 24 h using an Nikon Diaphot (Tokyo, Japan) inverted microscope.

Fixation and quantitative analysis. After 24 h (48 h for the temperature experiments), the silicon gaskets were removed and each sample immobilised and fixed by applying a molten drop of 20 μl 2% agarose (Type VIII; Sigma, Dorset, UK) containing 5% glutaraldehyde (Sigma) at 50° C. For the time-course experiments, samples were immobilised and fixed at the times indicated. Percentage conidium germination, germination patterns and appressorium formation were assessed using a Reichert-Jung Polyvar Photomicroscope with a × 10 plan apo objective and a total magnification of × 125. Germ-tube lengths were measured using a Bio-Rad (Watford, Herts., UK) MRC-600 laser scanning confocal system mounted on an Nikon Diaphot inverted microscope, and the images analysed with CoMOS (Bio-Rad) software. Unless stated otherwise, six replicates were performed for each experiment which was done at least twice. All conidia (100–300) were counted in each replicate. Percentage appressorium differentiation was taken as the percentage of germinated conidia (sporelings) that were differentiated. An appressorium was regarded as a rounded, pigmented, terminal swelling of a germ tube (Fig. 1). Statistical analyses were performed using either Fig P for Windows v. 1.0 (Biosoft, Cambridge, UK) or Microsoft Excel v. 4.0. Statistical tests (*t*-test and analysis of variance) were done after arcsine transformation.

Plant growth conditions and infection. Rice (*Oryza sativa* L.) plants (M-201; California Cooperative Rice Research Foundation Inc.) were grown in standard soil (Fisons, Type M3) and watered with Hoagland's nutrient solution (Hoagland and Arnon 1950). Plants were grown under a 14-h photoperiod at 27° C in the light (300 μmol photons $\cdot m^{-2} \cdot s^{-1}$) and 21° C in the dark. Plants were transferred to a cooled incubator 14–18 days after seed germination. The third or fourth leaf of each plant was placed in a Petri dish (50 mm diameter) by guiding it through small openings cut in the dishes. Care was taken not to damage the leaf or touch the leaf surface to be studied. Damp filter paper was placed in the base of the Petri dish to maintain a high humidity. Prior to inoculation, the leaves were left for at least 8 h in open Petri dishes, after which 8-μl drops of conidial suspension were pipetted onto the upper surfaces of

ves. The Petri dish lids were then replaced. For dark samples, the tri dishes were wrapped in black photographic bags in such a way at they were light-tight. Incubation conditions were as described the in-vitro system.

aining of infected leaves. Leaves were removed and sprayed with 05% Calcofluor M2R (Sigma, Poole, Dorset, UK) 24 h after inoc-ation. Quantitation of germination patterns and appressorium rmation was performed immediately afterwards by fluorescence croscopy, using the U1 filter block (containing a 330- to 380-nm citation filter, 420-nm dichroic mirror, and 418-nm-long path rrier filter) of the Reichert-Jung (Slough, UK) Polyvar micro-ope. Germ-tube lengths were measured using CoMOS image alysis software.

esults

onidium germination. The mean percentage of conidium rmination, on the different substrata and in hanging ops, ranged from 92.8 ± 3.5 (SE) to 98.3 ± 1.3 (SE) in e light and dark. In the hanging drops, it was notable at after 24 h none of the germ tubes differentiated ap-essoria unless they made contact with the glass surfaces om which the drops were suspended.

ermination and differentiation patterns. With the excep-on of the lengths of germ tubes (see below), the general ppearance of germinated conidia bearing appressoria as very similar on rice leaves and artificial substrata. Iature appressoria were pigmented and typically circu-r in profile (Figs. 1, 2). Sometimes, however, the appres-oria on rice leaves were irregular in outline (not shown) ecause they tend to mould themselves around papillae n the leaf surface (see Hirooka et al. 1982).

Four patterns of germination and differentiation were presentative of > 90% of all patterns exhibited by porelings (Fig. 3). The relative proportion of sporelings ithin each of these four classes was broadly the same on l substrata. Conidia germinated from one or more of eir three cells although < 2% germinated from their iddle cells. Greater than 70% of sporelings possessed

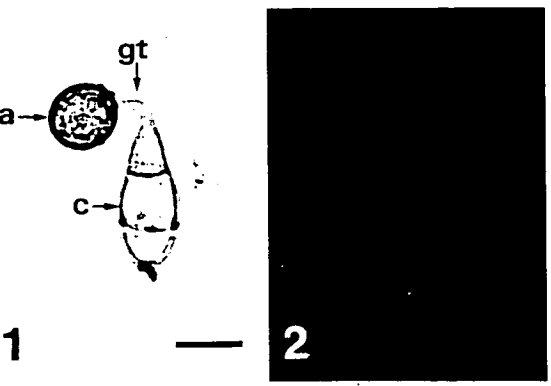

ig. 1. Brightfield light micrograph of a germinated conidium of *lagnaporthe grisea* (*c*) from which a germ tube (*gt*) has differentiat-d an appressorium (*a*) on Teflon. Bar = 10 μm

ig. 2. Fluorescence light micrograph of a germinated conidium om which a germ tube has differentiated an appressorium on a rice af. Magnification same as Fig. 1

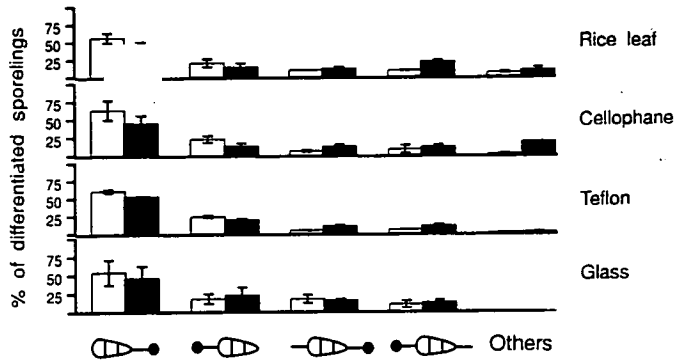

Fig. 3. Differentiation patterns of germinated *M. grisea* conidia on rice leaves, cellophane, Teflon and glass in the light (□) and dark (■) after 24 h. Bars represent SEs

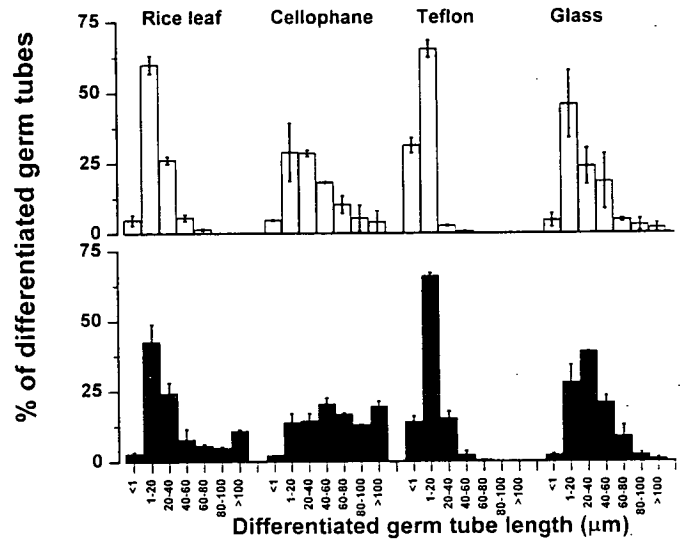

Fig. 4. Percentage of differentiated *M. grisea* germ tubes in defined length classes, on rice leaves, cellophane, Teflon and glass in the light (□) and dark (■) after 24 h. Bars represent SEs

one germ tube only; the most common type had one differentiated germ tube which had emerged from the apical cell of the conidium. The differentiation patterns did not differ significantly ($P < 0.05$) if conidia were incubated in the light or dark.

Lengths of differentiated germ tubes. On the rice leaf, germ tubes with appressoria showed a marked tendency to be shorter in the light than the dark: 97% and 77% of the germ tubes were < 60 μm long in the light and dark, respectively (Fig. 4). Of the artificial substrata, only differentiated germ tubes on cellophane were significantly shorter in the light (80% < 60 μm long) than the dark (51% < 60 μm long). On Teflon, 100% and 97% of germ tubes were < 60 μm in the light and dark, respectively; on glass, 93% and 90% were < 60 μm in the light and dark, respectively.

Appressorium differentiation. Table 1 shows that on rice leaves 98% of germinated conidia differentiated appressoria in the light whilst fewer (92%) did in the dark. On

Table 1. Percentage differentiation of *M. grisea* appressoria on rice leaves, cellophane, Teflon and glass in the light and dark after 24 h

	Rice Leaf	Cellophane	Teflon	Glass	Means
Light	98.0	79.9	91.2	69.0	84.5
Dark	91.5	54.5	68.1	39.0	63.3
Means	94.7	67.2	79.6	54.0	1% LSD 1.9

Table 2. Influence of photon flux density on percentage differentiation of *M. grisea* appressoria after 24 h incubation on cellophan

	Photon flux density ($\mu mol \cdot m^{-2} \cdot s^{-1}$)					1% LS
	110	60	30	15	0	
% Appressorium Differentiation	87.0	85.7	86.4	80.9	58.9	3.6

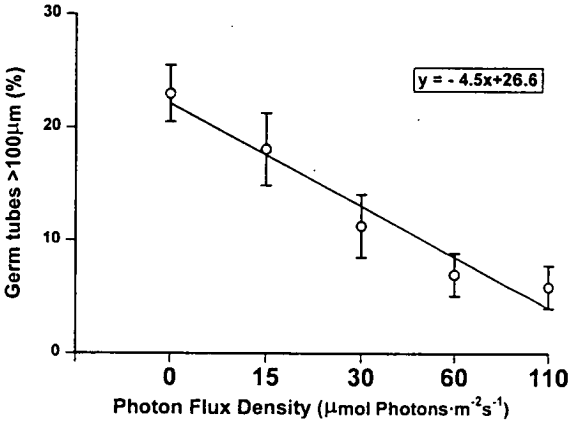

Fig. 5. Influence of photon flux density on the percentage differentiated of *M. grisea* germ tubes > 100 µm long after 24 h incubation on cellophane. Bars represent SEs of nine replicates per treatment. The line was fitted by regression analysis

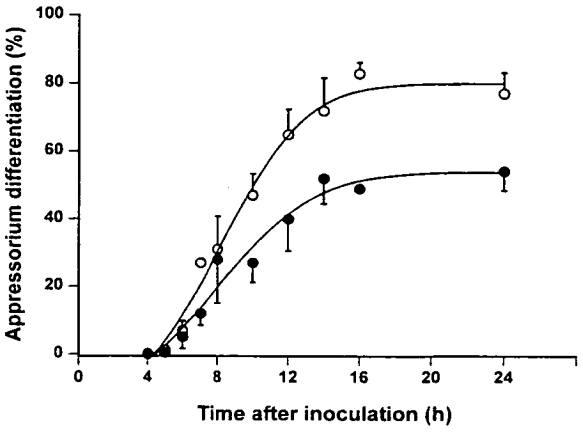

Fig. 6. Time course of differentiation of *M. grisea* appressoria in t light (○) and dark (●). Bars represent SEs

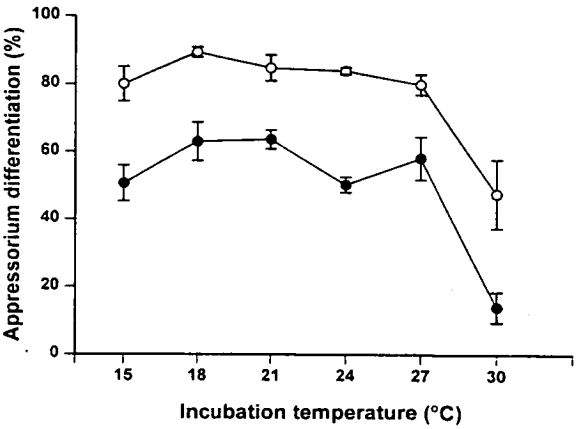

Fig. 7. Differentiation of *M. grisea* appressoria on cellophane different temperatures after 24 h in the light (○) or dark (●). Ba represent SEs

the artificial substrata, differentiation was ⩾ 69% in the light and 20–30% lower in the dark. On each substratum, the percentage differentiation in the light was significantly greater than in the dark ($P < 0.01$). Comparisons of all the light-grown treatments, or all of the dark-grown treatments, showed that percentage differentiation on rice leaves was significantly higher ($P < 0.02$) than on any of the artificial substrata. The results were subjected to a two-way analysis of variance to detect significance of difference between the effects of the light/dark treatments and the type of substratum used. The analysis showed a significant influence ($P < 0.01$) of light and the substratum type, but no significant interaction between these factors, on the percentage of appressoria formed.

Influence of irradiance. Of the three artificial substrata tested, only cellophane resembled rice leaves by inducing the fungus to produce shorter differentiated germ tubes in the light than the dark (Fig. 4). It was, therefore, chosen as a substratum to investigate the effects of irradiance on germ tube lengths and appressorium formation.

Irradiance had a marked effect on the lengths of differentiated germ tubes and this was a graded response: the higher the photon flux density, the lower the number of long (> 100 µm) differentiated germ tubes (Fig. 5).

Although light per se, enhanced the number of appressoria formed (Table 1), the photon flux density (15–110 µmol photons $\cdot m^{-2} \cdot s^{-1}$) did not seem to be important in this response (Table 2). Under all irradiances used, the percentage of conidia which produced appressoria was > 20% higher than in the dark. This difference was highly significant for all treatments ($P < 0.01$) and no significant difference between irradiances was found.

Time course of appressorium differentiation. On cellophane, conidium germination in the light and dark was completed within 8 h (data not shown). On the same substratum, germ-tube differentiation began 5 h post inoculation in both the light and dark (Fig. 6). However the first morphological indicator of appressorium formation (hook formation, Bourett and Howard 1990) was observed 1 h earlier in the light than the dark (data not shown). Under both conditions, differentiation of appressoria ceased 14 h post-inoculation. The number of a

essoria which differentiate per unit of time over the 6-12-h period was approximately 50% higher in the light an in the dark (Fig. 6).

fluence of temperature on appressorium differentiation. n cellophane, the percentage differentiation of appres-ria in the light was significantly greater than in the ark over the temperature range 15–30° C ($P < 0.05$). hus the promotive effect of light on appressorium differ-tiation was independent of temperature. At 30° C, far wer appressoria were formed in both treatments ig. 7).

iscussion

ur data indicate that the pre-penetration phase of infec-on by *M. grisea* involves a programme of growth and fferentiation triggered at spore germination and regu-ted by multiple signals from the host and surrounding nvironment.

ole of contact sensing. Surface contact was found to be ssential for appressorium induction but not conidium ermination. It is well established that contact of a germ ube with a solid surface is an essential prerequisite for ppressorium formation in many plant pathogens Emmett and Parbery 1975; Hoch and Staples 1991; ead et al. 1992). Our study does not support the conclu-ions of Lee and Dean (1993a) who recently reported for *M. grisea* that contact with a surface induces conidium ermination whilst a high surface hydrophobicity, as ound on a rice leaf, induces appressorium formation. Unfortunately, we cannot comment on their findings re-arding conidium germination because of the lack of ex-erimental details in their paper. These authors did show hat appressoria differentiated readily on substrata with high hydrophobicity (wax paper, polystyrene and olyester) but not on glass and agarose which were more ydrophilic. However, *M. grisea* has been shown to form ppressoria on cellophane (Hashioka 1972; Araki and Miyagi 1977; Uchiyama et al. 1979; Hirooka et al. 1982; Bourett and Howard 1990) and glass (Uchiyama et al. 979; Yaegashi et al. 1987; Uchiyama and Okuyama 990), and our results confirm this.

There is an interesting discrepancy in the literature egarding appressorium formation on glass. Although, as ndicated, a number of papers have shown that appresso-ia of *M. grisea* can develop on this substratum, other vorkers have reported that they do not (Hamer et al. 988, 1989; Howard et al. 1991a; Lee and Dean 1993a). The reason for this inconsistency is not clear but may be ttributable to differences in the type of glass used, strain ariation or instability of certain genes involved in ap-ressorium formation. In relation to the latter point, of ossible relevance is that *M. grisea* is highly mutable at ertain genetic loci (Valent and Chumley 1991). One such ocus is *SMO* and Hamer et al. (1989) found that smo mutants, in contrast to the wild type from which they were isolated, formed significant numbers of appressoria on glass.

The ability of germ tubes to differentiate into appressoria may be related to how they adhere to their substratum – an important aspect of plant-pathogen interactions about which little is known (Nicholson and Epstein 1991). It has been suggested that a hydrophobin-like protein produced by the *MPG1* gene may be important for appressorial adhesion through hydrophobic interactions with the rice leaf (Talbot et al. 1993). However, it seems unlikely that such a mechanism is involved in the adhesion of appressoria to cellophane considering the latter's hydrophilic nature.

Evidence was found for germ tubes, but not conidia, exhibiting contact-sensing. Firstly, a solid surface was required for germ tubes to differentiate. Secondly, a high substratum hydrophobicity (of Teflon or rice leaves) resulted in shorter differentiated germ tubes than on more hydrophilic substrata (glass and cellophane). This may be a result of earlier differentiation, or alternatively slower growth, on the hydrophobic substrata. However, it should be noted that the conidia used in our analysis lacked spore tip mucilage (Hamer et al. 1988) and it is conceivable that this may play a role in conidial contact sensing. This aspect needs to be addressed in a future study.

Role of light. There is a dearth of knowledge on the significance of light in regulating the pre-penetration phase of plant pathogens (Emmett and Parbery 1975). We found on rice leaves and cellophane that the lengths of differentiated germ tubes were, on average, shorter in the light than the dark. A possible explanation of this phenomenon is that light stimulates germ tubes to differentiate earlier after germination than in the dark, but this needs to be confirmed by further analysis. On all substrata, germinated conidia incubated in the light produced consistently more appressoria than those kept in the dark.

The mechanistic basis of how light is perceived by germ tubes is unknown. However, it was interesting to note that the lengths of differentiated germ tubes, but not the number of appressoria formed, were significantly influenced by the photon flux density of the light. Thus the effect on the length of differentiated germ tubes was a graded response to the irradiance, whilst increased appressorium numbers were not. This distinction suggests that these two responses involve different signal transduction pathways.

Increasing light levels usually are associated with higher temperatures in those parts of the world where rice blast is endemic. Our data demonstrated that temperatures above 30° C resulted in reduced appressorium formation. Conidia of *M. grisea* are dispersed mainly at night (Ou 1985). Since it takes several hours after spore deposition for appressoria to be initiated, then this process will sometimes occur in early daylight as temperatures start to rise. The advanced formation of appressoria at this time before temperatures rise too high may be a distinct advantage for *M. grisea*, particularly since appressoria can endure more adverse conditions than germ tubes (Emmett and Parbery 1975).

A 'conducive environment' is required for appressorium initiation. Signalling during the pre-penetration phase of infection by *M. grisea* inevitably involves an extremely complex network of interactions rather than independent, linear pathways of signalling events. Visualizing appressorium initiation in *M. grisea* as being controlled by just one or even a few external factors is probably too simplistic. Instead, a whole network of external and internal signals may exert control but each component to varying extents (e.g. see: Kacser and Porteous 1987; Trewavas 1987). Appressorium initation might be achieved in a variety of ways depending on the precise mixture and balance of signals and signal transduction elements present. Emmett and Parbery (1975) concluded that few plant pathogens require specific external stimuli for appressorium induction but instead, need a *conducive environment* for the process to take place. We suggest that what comprises a conducive environment may vary depending on the signalling capabilities of the germ tube and the environmental factors prevalent.

The germ tube seems to act as a specialised 'sense organ' which grows out from the spore. So what environmental signals, influencing its differentiation into an appressorium, does it sense? We have shown that surface contact, surface hydrophobicity, light, light intensity and temperature are all important. However, other factors are also influential, including water, pH, and signals derived from the host. Free water is required for conidium germination and a high relative humidity is essential for infection (Ou 1985). Germ tubes form most appressoria in the pH range 5.0–6.0 (data not shown). Host-derived signals must also be important because we found that consistently higher numbers of appressoria were formed on rice leaves than on any of the artificial substrata used in our study. Rice leaves consistently provided the most conducive environment for appressorium formation under the different illumination conditions employed. Whether these host-derived signals are chemicals or physical attributes (e.g. microstructure) of the leaf surface, is not clear.

Of signals identified as playing a role in regulating the pre-penetration phase, we can distinguish between those that are essential and those which are not. The essential factors (e.g. surface contact and a high relative humidity) seemed to be passive in effect rather than providing active stimulation of appressorium formation. The passive role of surface contact is indicated by the observation that germ tubes did not differentiate immediately on making contact with a surface but grew to different lengths before forming appressoria. Other factors (e.g. light and the precise physical and chemical make up of the contact surface) may not be indispensible but can play important roles as *modulatory signals* providing the conducive environment for appressorium initiation. It is possible that all of these external signals act in concert to make the germ tube competent to respond to an, as yet unidentified, internal signal (see next section).

Although most fungal leaf pathogens, like *M. grisea*, do not seem to rely on specific external signals for appressorium formation (Emmett and Parbery 1975), some clearly do. In this respect, rusts deserve special mention. A number of rusts respond to well-defined topographic features as primary signals of appressorium inducti (Allen et al. 1991a; Hoch and Staples 1991; Read et 1992). For example, > 90% of germ tubes of the be rust (*Uromyces appendiculatus*), grown on artificial su strata, are optimally induced to differentiate appresso over steps with a height of 0.5 μm (Hoch et al. 1987; All et al. 1991a). This topographical signal was closely cor lated with the guard-cell lip (or ledge) of the host pla *Phaseolus vulgaris* (Hoch et al. 1987; Allen et al. 1991 Terhune et al. 1991). Rusts have evolved this type of ser ing process in order to precisely locate appressoria ov stomata through which they penetrate. *Magnaport grisea* and most other leaf pathogens, however, have requirement for such a mechanism because they direct penetrate through the leaf cuticle and thus do not need form appressoria at specific locations on the leaf surfa

Induction of conidium germination and appressorium d ferentiation. Our work shows that the pre-penetrati phase of *M. grisea* involves a defined programme of c lineage to which the fungus becomes committed at coni ium germination. A similar conclusion was reached Howard et al. (1991b) who described this succession growth and developmental events as representing a *m phogenetic unit.* What triggers germination is not defini ly known. However, since percentage germination was 92% in the light and dark on all substrata and in liqu suspension, this indicates that water is probably impo tant because it was a common, external factor in all the experiments. However, whether spore hydration provid a primary stimulus for germination, or whether wa allows the release from spores of a germination self-i hibitor (Macko 1981), remains to be determined.

As indicated earlier, we found no evidence for an e ternal inductive signal for appressorium differentiatio This suggests that appressorium initation is depende on intracellular signalling. Since the whole of the p penetration phase can occur in water devoid of exter nutrients, starvation may provide this stimulus. In su port of this is the finding that RNA transcripts of t *MPG1* gene, which is differentially expressed at a hi level during appressorium formation, are also elevated cultures starved of a carbon or nitrogen source (Talbot al. 1993). Furthermore, cAMP, which is elevated in sponse to starvation in some eukaryotes (e.g. in *Dicty telium*, Gerisch 1987), also seems to be involved in a pressorium induction in *M. grisea* (Lee and Dean 1993

It is clear from our study that the different artific substrata used did not completely mimic results obtain on the more conducive environment of rice leaves. T indicates a shortcoming of soley using in-vitro systems experimentally analyse the pre-infection phase in *grisea*, and probably other pathogens as well. It emph sizes the need to perform experiments in parallel on t natural host substratum.

We are grateful to the Science and Engineering Research Cou for research studentship to T.C.J., and for financial funding (gr number GR/G 28765) to N.D.R. We thank Mr. Tony Collins, Jim Deacon, Dr. Rick Howard (DuPont Co., Wilmington. D USA) and Prof. Tony Trewavas for helpful comments during pre

tion of this manuscript. Jim Deacon also provided advice on atistical analysis.

References

Allen, E.A., Hazen, B.E., Hoch, H.C., Kwon, Y., Leinhos, G.M.E., Staples, R.C., Stumpf, M.A., Terhune, B.T. (1991a) Appressorium formation in response to topographical signals by 27 rusts. Phytopathology **81**, 323–331

Allen, E.A., Hoch, H.C., Stavely, J.R., Steadman, J.R. (1991b) Uniformity among races of *Uromyces appendiculatus* in response to topographic signaling for appressorium formation. Phytopathology **81**, 883–887

Araki, F., Miyagi, Y. (1977) Effects of fungicides on penetration by *Pyricularia oryzae* as evaluated by an improved cellophane method. Pestic. Sci. **2**, 457–461

Bourett, T.M., Howard, R.J. (1990) *In vitro* development of penetration structures in the rice blast fungus *Magnaporthe grisea*. Can. J. Bot. **68**, 329–342

Chumley, F.G., Valent, B. (1990) Genetic analysis of melanin-deficient, nonpathogenic mutants of *Magnaporthe grisea*. Mol. Plant-Microbe Interact. **3**, 135–143

Dobinson, K.F., Hamer, J.E. (1992) *Magnaporthe grisea*. In: Molecular biology of filamentous fungi, pp. 67–86, Stahl, U., Tudzynski, P., eds. VCH, Weinheim

Emmett, R.W., Parbery, D.G. (1975) Appressoria. Annu. Rev. Phytopathol. **13**, 147–167

Gerisch, G. (1987) Cyclic AMP and other signals controlling cell development and differentiation in *Dictyostelium*. Annu. Rev. Biochem. **56**, 853–879

Hamer, J.E., Howard, R.J., Chumley, F.G., Valent, B. (1988) A mechanism for surface attachement in conidia of a plant pathogenic fungus. Science **239**, 288–290

Hamer, J.E., Valent, B., Chumley, F.G. (1989) Mutations at the SMO genetic locus affect the shape of diverse cell types in the rice blast fungus. Genetics **122**, 351–361

Hashioka, Y. (1972) Fine structure of the rice blast. IX. Scanning electronmicroscopical observations on appressoria of the rice blast fungus and other species of *Pyricularia*. Res. Bull. Fac. Agric Gifu Univ. **33**, 65–73

Hirooka, T., Miyagi, Y., Araki, F., Kunoh, H., Ishizaki, H. (1982) The effect of isoprothiolane on the emergence of infection pegs from appressoria of *Pyricularia oryzae*. Pestic. Sci. **13**, 379–386

Hoagland, D.R., Arnon, D.I. (1950) The water-culture method for growing plants without soil. Univ. Calif. Agric. Exp. Stn. Cir. 347

Hoch, H.C., Staples, R.C. (1991) Signaling for infection structure formation in fungi. In: The fungal spore and disease initiation in plants and animals, pp. 25–46, Cole, G.T., Hoch, H.C., eds. Plenum Press, New York

Hoch, H.C., Staples, R.C., Whitehead, B., Comeau, J., Wolf, E.D. (1987) Signaling for growth orientation and cell differentiation by surface topography by *Uromyces*. Science **253**, 1659–1662

Howard, R.J., Ferrari, M. (1989) Role of melanin in appressorium function. Exp. Mycol. **13**, 403–418

Howard, R.J., Ferrari, M.A., Roach, D.H., Money, N.P. (1991a) Penetration of hard substrates by a fungus employing enormous turgor pressures. Proc. Natl. Acad. Sci. USA **88**, 11281–11284

Howard, R.J., Bourett, T.M., Ferrari, M.A. (1991b) Infection by *Magnaporthe*: an in vitro analysis. In: Electron microscopy of plant pathogens, pp. 251–264, Mendgen, K., Lesemann, D.-E., eds. Springer Verlag, Berlin

Kacser, H., Porteous, J.W. (1987) Control of metabolism: what do we have to measure? TIBS **12**, 4–10

Lee, Y.-H., Dean, R.A. (1993a) cAMP regulates infection structure formation in the plant pathogenic fungus *Magnaporthe grisea*. Plant Cell **5**, 693–700

Lee, Y.-H., Dean, R.A. (1993b) Stage-specific gene expression during appressorium formation of *Magnaporthe grisea*. Exp. Mycol. **17**, 215–222

Macko, V. (1981) Inhibitors and stimulants of spore germination and infection structure formation. In: The fungal spore: morphogenetic controls, pp. 565–584, Turian, G., Hohl, H.R., eds. Academic Press, New York

Nicholson, R.L., Epstein, L. (1991) Adhesion of fungi to the plant surface. Prerequisite for pathogenesis. In: The fungal spore and disease initiation in plants and animals, pp. 3–23, Cole, G.T., Hoch, H.C., eds. Plenum Press, New York

Ou, S.H. (1980) A look at worldwide rice blast disease control. Plant Dis. **64**, 439–445

Ou, S.H. (1985) Rice diseases, 2nd edn. Commonwealth Mycological Institute, Kew, UK

Peng, Y.-L., Shishiyama, J. (1988) Temporal sequence of cytological events in rice leaves infected with *Pyricularia oryzae*. Can J. Bot. **66**, 730–735

Read, N.D., Kellock, L.J., Knight, H., Trewavas, A.J. (1992) Contact sensing during infection by fungal pathogens. In: Perspectives in plant cell recognition, pp. 137–172, Callow, J.A., Green, J.R., eds. Cambridge University Press, Cambridge, UK

Talbot, N.J., Ebbole, D.J., Hamer, J.E. (1993) Identification and characterization of *MPG1*, a gene involved in pathogenicity from the rice blast fungus *Magnaporthe grisea*. Plant Cell **5**, 1575–1590

Terhune, B.T., Allen, E.A., Hoch, H.C., Wergin, W.P., Erbe, E.F. (1991) Stomatal ontogeny and morphology in *Phaseolus vulgaris* in relation to infection structure initiation in *Uromyces appendiculatus*. Can. J. Bot. **69**, 477–484

Trewavas, A.J. (1987) Many a mickle makes a muckle; network maxims may mitigate controversy. BioEssays **7**, 84–86

Uchiyama, T., Okuyama, K. (1990) Participation of *Oryza sativa* leaf wax in appressorium formation by *Pyricularia oryzae*. Phytochemistry **29**, 91–92

Uchiyama, T.N., Ogasawara, Y., Nanba, Y., Ito, H. (1979) Conidial germination and aprressorium formation of the plant pathogenic fungi on the cover-glass or cellophane coated with various lipid components of plant waxes. Agric. Biol. Chem. **43**, 383–384

Valent, B. (1990) Rice blast as a model system for plant pathology. Phytopathology **80**, 33–36

Valent, B., Chumley, F.G. (1991) Molecular genetic analysis of the rice blast fungus, *Magnaporthe grisea*. Annu. Rev. Phytopathol. **29**, 443–467

Valent, B., Farrall, L., Chumley, F.G. (1991) *Magnaporthe grisea* genes for pathogenicity and virulence identified through a series of backcrosses. Genetics **127**, 87–101

Woloshuk, C.P., Sisler, H.D., Tokousbalides, M.C., Dutky, S.R. (1983) Melanin biosynthesis in *Pyricularia oryzae*: site of tricyclazole inhibition and pathogenicity of melanin-deficient mutants. Pestic. Biochem. Physiol. **14**, 256–264

Yaegashi, H., Matsuda, I., Sato, Z. (1987) Production of appressoria at the tips of hyphae of *Pyricularia oryzae*. Ann. Phytopathol. Soc. Japan **53**, 203–209